VIRAL-BACTERIAL INTERACTIONS IN CYSTIC FIBROSIS LUNG DISEASE

by

Matthew Ryan Hendricks

Bachelor of Science, University of Oregon, 2012

Submitted to the Graduate Faculty of

School of Medicine in partial fulfillment

of the requirements for the degree of

Doctor of Philosophy

University of Pittsburgh

2017

UNIVERSITY OF PITTSBURGH

SCHOOL OF MEDICINE, MOLECULAR VIROLOGY & MICROBIOLOGY GRADUATE PROGRAM

This dissertation was presented

by

Matthew Ryan Hendricks

It was defended on

December 1, 2017

and approved by

Jeffrey L. Brodsky, Ph.D., Avinoff Professor, Department of Biological Sciences

Carolyn B. Coyne, Ph.D., Associate Professor, Department of Pediatrics

Saumendra N. Sarkar, Ph.D., Associate Professor, Department of Microbiology and Molecular Genetics

Robert M.Q. Shanks, Ph.D., Associate Professor, Department of Ophthalmology

Dissertation Advisor: **Jennifer M. Bomberger, Ph.D.**, Associate Professor, Department of Microbiology and Molecular Genetics

VIRAL-BACTERIAL INTERACTIONS IN CYSTIC FIBROSIS LUNG DISEASE

Matthew Ryan Hendricks, Ph.D.

University of Pittsburgh, 2017

Pseudomonas aeruginosa is a Gram-negative, opportunistic pathogen that chronically infects approximately 80% of cystic fibrosis (CF) patients by early adulthood, accounting for the majority of morbidity and mortality in these patients. The development of chronic *P. aeruginosa* infections in the CF lung involves the formation of highly recalcitrant biofilm communities. Clinical observations have noted a correlation between respiratory virus infection and the acquisition of chronic *P. aeruginosa* infection by CF patients, but the mechanism underlying this interaction in the CF lung is not understood. In this dissertation, we hypothesized that respiratory viral co-infection promotes *P. aeruginosa* biofilm formation on airway epithelial cells (AECs).

We demonstrate that in the presence of respiratory syncytial virus (RSV) co-infection, *P. aeruginosa* biofilm growth is significantly increased. We observed that RSV infection increased the release of iron-bound transferrin, suggesting that RSV infection disrupts iron homeostasis in the airway epithelium. Iron is an essential nutrient for *P. aeruginosa* biofilm growth, and both iron chelation and depletion of transferrin from apical secretions collected from AECs blocked the biofilm stimulatory effect of RSV co-infection. We also demonstrate that RSV infection promotes the apical release of extracellular vesicles (EVs) from AECs, which increases the availability of iron-loaded transferrin in the apical secretions of AECs. Interestingly, purified EVs stimulate *P. aeruginosa* biofilm growth, suggesting that host-derived EVs interact with a bacterium to promote chronic bacterial infections. Finally, the innate immune response to virus

infection, measured by type I and type III (IFN-β and -λ, respectively) interferon production, peaks at the same time as virus-induced biofilms growth, and treatment of AECs with either IFN replicates the enhanced biofilm growth observed during virus co-infection. Our data suggest a novel mechanism by which the host response to viral infection contributes to the development of chronic pulmonary *P. aeruginosa* infection and provide mechanistic insight into our understanding of nutritional immunity in the lung.

TABLE OF CONTENTS

LIST OF TABLES

LIST OF FIGURES

LIST OF ABBREVIATIONS

Adv	Adenovirus
AECs	Airway Epithelial Cells
Alb	Albumin
ALI	Air-Liquid Interface
AP	Alkaline Protease
ASL	Airway Surface Liquid
BALF	Bronchoalveolar Lavage Fluid
CF	Cystic Fibrosis
CFTR	Cystic Fibrosis Transmembrane Conductance Regulator
CFP	Culture Filtrate Protein
CFU	Colony Forming Unit
CM	Conditioned Media
COPD	Chronic Obstructive Pulmonary Disease
DFO	Deferoxamine
DMT1	Divalent Metal Transporter 1
dpi	Days Postinfection
DSX	Deferasirox
ELISA	Enzyme Linked Immunosorbent Assay

ER	Endoplasmic Reticulum
EV71	Enterovirus 71
FBS	Fetal Bovine Serum
Fe^{2+}	Ferrous Iron
Fe^{3+}	Ferric Iron
FEV_1	Forced Expiratory Volume during 1 second
FPN-1	Ferroportin-1
Ga^{3+}	Gallium
GFP	Green Fluorescent Protein
HAV	Hepatitis A Virus
HBE	Human Bronchial Epithelial
HBV	Hepatitis B Virus
HCV	Hepatitis C Virus
hpi	Hours post-infection
HPIV3	Human Parainfluenza Virus 3
HRP	Horseradish peroxidase
hRV	Human Rhinovirus
IAP	Inhibitor of Apoptosis Protein
ICP-OES	Inductively Coupled Plasma Optical Emission Spectrometry
IFN	Interferon
IFN-β	Interferon-Beta
IFN-λ	Interferon-Lambda
IFNAR	Interferon-Alpha/Beta Receptor

IFNλR	Interferon-Lambda Receptor
ILV	Intraluminal Vesicle
IP	Immunoprecipitation
ISG	Interferon Stimulated Gene
MEM	Minimal Essential Media
MOI	Multiplicity of Infection
MPV	Metapneumovirus
MVB	Multivesicular Body
NK	Natural Killer
NOS2	Nitric Oxide Synthase 2
OAS1	2', 5'-Oligoadenylate Synthetase 1
OMV	Outer Membrane Vesicle
OSBP	Oxysterol-Binding Protein
PA	*Pseudomonas aeruginosa*
PBS	Phosphate Buffer Saline
PI	Phosphatidylinositol
PI4K	Phosphatidylinositol-4 Kinase
PI4P	Phosphatidylinositol-4 phosphate
poly(I:C)	Polyinosine-Polycytidylic Acid
PrpL	Endoprotease
PRR	Pattern Recognition Receptor
PS	Phosphatidylserine
qRT-PCR	Quantitative Reverse Transcriptase-Polymerase Chain Reaction

RIG-I	Retinoic Acid-Inducible Gene I
RSV	Respiratory Syncytial Virus
siRNA	Small Interfering RNA
STAT1	Signal Transducer and Activator of Transcription 1
TEER	Transepithelial Electrical Resistance
TLR	Toll-Like Receptor
Tfn	Transferrin
TfnR	Transferrin Receptor
WCL	Whole Cell Lysate

ACKNOWLEDGEMETS

The journey towards completing a PhD is a challenging road that would not have been possible without the support of my friends, family and colleagues.

First and foremost, I would like to thank my mentor, Dr. Jennifer Bomberger, for her time, and thoughtful guidance over the years. You have shaped my graduate career in many ways and have had a profound impact on my development as a scientist and a person. I am especially grateful for the freedom you gave me to grow as a scientist, develop hypotheses, and pursue ideas that did not always align with your own interests. I have always admired your passion for science and the enthusiasm you bring to lab every day. It has truly been a privilege to work in your lab and I hope to be able to follow the example you have set during the course of my own career.

I would also like to thank my committee members, Jeff, Carolyn, Saumen and Rob. I really appreciate all the time and energy you have put into my committee meetings. Your critiques and suggestions have been helpful in advancing my research. I am very grateful for all your input. You have been a great thesis committee and I am very fortunate to have been able to interact with each of you.

I also want to thank all the members of the Bomberger lab, both past and present. Anna, Angela, Abiola, Becca, Brian, Catherine, Jeff, Jordan, Megan, Lauren, Doug, thank you all for being amazing colleagues in lab. The last five years would not have been nearly as fun and

productive without all of you. I am grateful for all the technical help and scientific discussions you have provided. All of you have been great friends and have provided me with many memories I will always cherish from graduate school from our summer Pirates games to even our “Anything That Floats” boat race.

The work presented in this dissertation has been a collaborative effort that would not have been possible without the help and input of a number of people. I would like to thank Becca, Brian, Jeff, Jordan, Megan, Lauren, and Doug for technical and intellectual help, and for taking care of cells at various times throughout the years. I would also like to thank Katherine Eichinger and Kerry Empey for their assistance with mouse experiments. To JoAnne Flynn, thank you for your time and guidance since I have come to the University of Pittsburgh. I have always enjoyed our discussions and training grant meetings. Your insight has had an incredible impact on my development as a scientist.

Last but not the least, I am thankful for my family for supporting me as I pursued my PhD from so far away. To my brother, Kyle, thank you for always reminding me of how cool my research is when we chat and for keeping life in perspective for me. To my parents, Terry and Debbie, thank you for your love, support and words of encouragement over the years. To my Dad, for fostering my interest in science from a young age. I could not have gotten to this point without you and your sacrifices. I am sure you are proud of me for this achievement and I want to dedicate this dissertation to you.

Finally, to my wife Marayd. You are my world. This journey would not have been possible without you. You chose to follow me to Pittsburgh as I pursued this PhD based on your faith in us, and I think that is part of the reason I was able to accomplish what I have in graduate school. Your endless love and support will never be forgotten.

1.0 INTRODUCTION

A fundamental requirement for the survival of all living organisms, including the microorganisms that constantly engage in pathogenic and symbiotic relationships with their hosts, is the ability to acquire nutrients from the surrounding environment. For example, transition metals are critical to many essential biological processes including replication, transcription and metabolism. As a consequence, hosts and microorganisms are both involved in a continuous struggle to outcompete each other for nutrients. This fosters a dynamic environment in which many complex interactions take place between host and microbial proteins that ultimately dictate whether microbes successfully colonize their hosts and in the case of pathogenic microorganisms, cause disease. Studies at the host-pathogen interface have identified many mechanisms by which the host regulates the availability of essential nutrients to limit microbial growth and prevent infection, a collective process termed “nutritional immunity.” One of the most widely studied nutrients at this interface is iron.

Epithelial cells are present at mucosal sites throughout the body and are constantly exposed to both resident and infectious microorganisms, as well as other environmental factors. The epithelium is responsible for many cellular processes critical to tissue homeostasis and human health including the selective absorption of nutrients, detection of the extracellular environment, secretion of signaling molecules and other products that mediate cell-to-cell communication, and protects underlying tissues from infection by serving as the first line of

defense microbes encounter in the human body. Consequently, epithelial cells contribute to both the physical and biological barriers that are utilized to prevent colonization by pathogenic microorganisms and preserve human health. For example, tight junctions maintain the structural integrity of the epithelial layer, providing a physical barrier, that prevents dissemination of microorganisms into deeper tissues. In addition, epithelial cells secrete antimicrobial factors, such as antimicrobial peptides and secretory IgA, that create an innate biological barrier microorganisms must first circumvent to successfully colonize host tissues. Epithelial cells also play a critical role in bridging the gap between the innate and adaptive immune responses to invading microbes by secreting chemokines and cytokines [1-3]. In addition, the epithelium is involved in additional mechanisms, such as nutrient sequestration, by which hosts limit microbial colonization and growth. Due to these selective pressures, microorganisms have established countermeasures to manipulate their environments and host epithelial cells to limit host immune responses and colonize host tissues. Ultimately, it is these back-and-forth interactions between the host and microbes at mucosal surfaces that determine the fate of infections and disease outcomes.

In this regard, one aspect of the Bomberger lab focuses on nutritional immunity in airway epithelial cells, and how these processes are altered during viral-bacterial coinfections to promote nutrient accessibility and infection in the respiratory tract. Compared to previously identified mechanisms of viral-bacterial interactions, the involvement of nutritional immunity is unique in several aspects that will be explained in this dissertation.

1.1 CYSTIC FIBROSIS PULMONARY INFECTIONS

Cystic fibrosis (CF) is a genetic disease caused by mutations in the cystic fibrosis transmembrane conductance regulator (CFTR). The first description of CF was made in 1938 by Dorothy Andersen, who originally described mucus plugging of the pancreas and pancreatic insufficiency in infants who experience malnutrition and died due to pulmonary infection [4]. At the time, this disease was characterized by mucus plugging of the exocrine glands and patients did not survive past early childhood due to lung infections [4]. In the last 80 years, tremendous progress has been made understanding the basic biology of CF including: (i) the discovery that the sweat of CF patients had an abnormally high salt concentration and development of the "sweat test," which led to the identification of patients with milder CF disease, (ii) identification of chloride transport as the basic physiological defect in CF, and (iii) the identification of the CF gene [4]. There have now been more than 2000 CFTR mutations identified, of which 127 mutations meet clinical and functional criteria for disease [5]. Deletion of phenylalanine at position 508 of CFTR (ΔF508) is the most common mutation in CF patients. It is estimated that 70,000 individuals globally have some form of CF, of which 30,000 individuals are in the United States. Because CFTR is expressed on many cell types, including epithelial cells, CF is a multi-organ disease characterized by disorders of endocrine, gastrointestinal, reproductive and respiratory systems. However, the major determinant of mortality in CF patients is pulmonary disease. Infection with the Gram-negative, opportunistic *Pseudomonas aeruginosa* in the CF lung has been associated with significant morbidity and eventual loss of pulmonary function in patients [6, 7]. *P. aeruginosa* is the most common bacterial species isolated from the respiratory tract of CF patients, where it often establishes chronic infection and persists in the airways of patients for the rest of their lives [6]. The lung environment is a major factor that impacts host-pathogen

interactions and ultimately, a determinant of colonization of the lung by invading pathogens. Loss of function of CFTR is associated with changes in the lung environment, many of which create an environment that is favorable for *P. aeruginosa* colonization and chronic infection.

1.1.1 CFTR Activity and Lung Environment

Airway epithelial cells (AECs) are the first barrier in the respiratory tract encountered by inhaled pathogens and foreign particles. Besides acting as a physical barrier that prevent dissemination of inhaled material, ciliated cells in the airways actively contribute to removal of pathogens and foreign material from the lungs in a process termed mucociliary clearance [8]. This process is dependent upon proper airway surface liquid (ASL) hydration. The ASL consists of a periciliary fluid layer with an overlying mucus layer. The periciliary layer acts as a barrier between the mucus layer and cell surface that creates an optimal depth of ~7 μm, which allows cilia to fully extend and beat in the airways [9, 10]. In the non-CF airways, apical secretion of Cl^- and HCO_3^- by the CFTR anion channel promotes the movement of water into the ASL, which maintains a periciliary layer depth of ~7 μm and reduces the viscosity of the mucus. This removes debris, including bacterial and viral pathogens, that have been trapped in the mucus from the lungs. In the CF lung, significantly reduced CFTR function leads to dehydration of the ASL, resulting in a decrease in the depth of periciliary layer and ability of cilia to beat [9].

In addition to its role in mucociliary transport, the composition of the ASL is very important innate defense mechanism of the airways. For example, antimicrobial peptides are produced by AECs and are important antibacterial components of the ASL [11-13]. Moreover, synergistic and additive killing of bacteria by antimicrobial peptides found in the ASL has been observed [14]. The functional activity of antimicrobial peptides is sensitive to the environment,

as both acidic pH and high salt concentrations decrease the antibacterial activity of antimicrobial peptides [14-16]. In CF, the reduction in CFTR activity has been associated with more acidic ASL [17-19]. In a pig model of CF, the ASL was also found to be more acidic than the ASL from non-CF pigs [18]. Although the concentration of antimicrobial peptides in the ASL of non-CF and CF pigs were similar, decreased killing of *Staphylococcus aureus* in the presence of ASL from the CF pigs was observed [18]. The acidity of the ASL in CF has been associated with decreased HCO_3^- secretion due to reduced CFTR activity, and stimulation of HCO_3^- secretion alkalinized ASL collected from CF bronchial cells [17]. Interestingly, addition of HCO_3^- to ASL from CF pigs increased both the pH of the ASL but also bacterial killing in the presence of the ASL [18], suggesting that correcting the ASL pH defect in CF patients may be a therapeutic target that could increase bacterial killing in the airways of CF patients. In addition, decreased HCO_3^- secretion, lower pH and ASL dehydration have been associated with increased mucus viscosity in the CF lung [20-22]. MUC5AC and MUC5B, the predominant components of airway mucus, are abnormally compact in CF airways, which likely results from a combination of these changes to the ASL composition [22]. Mucus is an important part of innate immunity in the lung that creates a barrier between the airway surface and particulate matter, including infectious microorganisms. Mucociliary transport removes mucus from the airways and in the CF lung this process is impaired due to these mucus abnormalities, thereby creating an environment that is predisposed to bacterial infection.

Iron is essential nutrient for a wide variety of cellular processes, and due to the requirement of iron for microbial growth, the host meticulously regulates iron so that it is inaccessible to pathogens. Despite this regulation, iron levels are increased in the CF lung compared to healthy controls (Table 1) [23-26]. Furthermore, *in vitro* studies have confirmed

that AECs with the ΔF508 CFTR mutation release greater amounts of iron than cells with functional CFTR [27]. Given that increased iron levels are negatively correlated with pulmonary function but positively correlated with bacterial burden, it has been suggested that iron may play an important role in facilitating *P. aeruginosa* infections in the CF lung [25, 28]. Taken together, these results suggest that defects in CFTR function are strongly associated with increased iron in the airways of CF patients, but it is still not understood how defects in CFTR function regulate iron homeostasis in the lung.

In summary, defects in CFTR function have many consequences for innate defenses such as mucus clearance and iron abundance in the airways that impacts the environment in the lungs of CF patients. The combination of all these factors creates a setting that is conducive to bacterial infection in the CF airway, particularly chronic infection with *P. aeruginosa*, highlighting both the importance of all these innate defenses for normal lung function but also the broad effect that CFTR function has on airway physiology. However, the effect respiratory viral infection has on many of these components, such as iron levels, in the CF lung have not been investigated.

Table 1: Total Iron Concentrations in CF Airways

Subject Population	Iron Concentration		Sampling Method	Iron Detection Method	Reference
	Non-CF Controls	CF			
Adults	0 ng/mg protein	242.5 ± 2.1 ng/mg protein	Expectorated Sputum	Colorimetric*	[29]**
Adults	0 μM	7.5 ± 2.1 μM	BALF	Colorimetric*	[26]**
Adults	Not Assessed	63 μM (17 – 134 μM)	Expectorated Sputum	Colorimetric*	[23]***
Adults	0 μM (0 – 13.2 μM)	Acute: 44.4 μM (17.0 – 128.7 μM) Stable: 33.3 (0 – 111.2 μM)	Expectorated Sputum	Colorimetric*	[24]***
Adults	0 μM (0 – 15.8 μM)	Acute: 46.6 μM (10.0 – 200.0 μM) Stable: 34.0 μM (2.4 – 78.0 μM)	Expectorated Sputum	Colorimetric*	[25]***
Adults	13.5 μg/L (8.6 – 21.5 μg/L)	56.9 μg/L (24.3 – 115.3 μg/L)	Expectorated Sputum	ICP-OES	[30]****
Pediatric	Not Assessed	32 μM (Range: 3.7 – 118.5 μM)	BALF	Colorimetric*	[28]****

*Total iron measured by colorimetric iron detection kits. Assay kits based on reaction of Fe^{2+} with chromogen to form colorimetric product. Iron is released from complexes (i.e. iron-binding proteins) by acidic buffer, and Fe^{3+} is reduced to Fe^{2+} by reducing agent to measure total iron in reaction. **Data presented as mean ± standard deviation. ***Data presented as median (range).

Iron concentration reported for CF patients during an acute exacerbation and clinically stable CF patients. [****]Data presented as median (range).

1.1.2 Chronic Infection and Biofilm Formation of *Pseudomonas aeruginosa* in the Cystic Fibrosis Airway

Environmental isolates of *P. aeruginosa* are responsible for initial infections in CF patients and occur in infancy or early adulthood. Infections are often aggressively treated and cleared by antibiotics, but recurrent intermittent infections commonly follow. *P. aeruginosa* undergoes genetic adaption over time to the lung environment during waves of antibiotic treatment and the constant pressure imposed by the host immune system. It is hypothesized that the sinuses provide a protected niche that allows for the genetic adaptation of *P. aeruginosa* occur, and bacteria from the sinuses can recolonize the lungs following antibiotic eradication of *P. aeruginosa* in the airways [31]. The time over which genetic adaptations occur is variable between patients and bacterial isolates, but eventually clonal selection of a dominate strain occurs and establishes a chronic infection [7, 31].

The development of chronic *P. aeruginosa* infections in the CF lung involves the formation of highly recalcitrant biofilm communities. Biofilms are surface-associated communities of bacteria, which are characterized by upregulation of antibiotic resistance genes and polymeric matrix production that serve to protect bacteria from the antibiotic- and host immune system-mediated clearance in the CF airways [32]. Biofilms in the environment perform a similar function whereby they protect bacterial communities from stress such as heavy metal intoxication and antibacterial compounds [33, 34]. Biofilm development occurs in a well-coordinated manner in response to environmental cues, such as nutrient availability. Biofilm

development has been described as a temporal process involving the transition through different stages that begin with bacterial attachment to a surface. Attached bacteria multiply on the surface, form microcolonies and then ultimately mature into biofilm structures. The final step in biofilm development is the dispersal of bacteria from the biofilm, which can seed new sites for infection and colonization [32, 35, 36]. Many factors are involved in the development of *P. aeruginosa* biofilm growth, including the initiation of biofilm formation by increased production of the second messenger cyclic-di-GMP (c-di-GMP), QS systems, production of exopolysaccharides Pel and Psl, and the availability of environmental factors, such as extracellular DNA (eDNA) and iron [34]. Iron is required for *P. aeruginosa* growth and biofilm formation [37]. In addition, QS systems are a form of intercellular communication based on cell density and the accumulation of small diffusible molecules produced by neighboring bacteria in the environment. These systems have been shown to regulate virulence factor production, some of which could be important for nutrient acquisition, and are important for biofilm production in *P. aeruginosa* [38-41]. For example, a mutation in the *P. aeruginosa las* system (one of the QS systems in *P. aeruginosa*) formed shorter, flat biofilms compared to the biofilms formed by wild type bacteria, suggesting that mature biofilm formation requires intact QS systems [42]. Furthermore, QS regulates iron limitation-induced twitching motility. Mutations in the *rhl* QS system in *P. aeruginosa* increased biofilm growth in iron-limited conditions, which was linked with decreased twitching motility under these conditions [43]. The sputum of CF patients has increased abundance of *P. aeruginosa* QS signals, N-(3oxododecanoyl)-L-homoserine lactone (3OC12-HSL) and N-butyryl-L-homoserine lactone (C4-HSL), produced by the *las* and *rhl* QS systems, respectively [44]. This was suggestive that *P. aeruginosa* grows in biofilms in CF airways, which had been hypothesized based on the observation that *P. aeruginosa* was highly

resistant to antibiotics in the CF lung [32]. In addition, microscopic examination of the explanted lungs from CF patients has long demonstrated the intraluminal presence of alginate-positive *P. aeruginosa* microcolonies in the lungs of CF patients, and more recently, the use of fluorescence in situ hybridization peptide nucleic acid probes have also shown *P. aeruginosa* biofilm architecture in the airways of CF patients [44-46].

The development of treatments that either inhibit biofilm growth or promote dissociation of the biofilms in CF airways have been of great interest because biofilms contribute to persistence of *P. aeruginosa* infections and the corresponding tissue-damaging inflammation in patients. In this regard, DNase treatment is known to reduce *P. aeruginosa* biofilm formation and bacterial colonization has been reduced in patient airways when treated with the therapeutic Pulmozyme (rhDNase I) [47, 48]. In addition, iron chelation has been shown to impair *P. aeruginosa* biofilm growth and the use of iron chelation compounds increases the efficacy of biofilm disruption with antibiotics [27, 49].

1.2 RESPIRATORY VIRAL INFECTIONS IN PATIENTS WITH CYSTIC FIBROSIS AND OTHER CHRONIC LUNG DISEASES

Portions of this section are adapted from the published manuscript:

Matthew R. Hendricks[a] and Jennifer M. Bomberger[a]

Digging through the Obstruction: Insight into the Epithelial Cell Response to Respiratory Virus Infection in Patients with Cystic Fibrosis. *Journal of Virology*, 2016. **90** (9): 4258-4261

[a]Department of Microbiology and Molecular Genetics, University of Pittsburgh School of Medicine, Pittsburgh, PA 15219

Respiratory virus infections are common but generally self-limiting infections in healthy individuals. In patients with chronic lung diseases, such as CF and chronic obstructive pulmonary disease (COPD), respiratory viral infections are associated with acute exacerbations, which generally involve acute episodes of increased respiratory symptoms (i.e. cough, fever, increased sputum production, etc.) and decreased lung function (as measured by decline in FEV_1), that promote disease progression [50-64]. Importantly, acute exacerbations not only contribute to progressive declines in lung function but also lead to decreases in quality of life for these patients, including psychosocial health [65-69]. This highlights the important point that besides the physical toll that respiratory viral infections have on patients with chronic lung disease, there is also a psychological burden that patients and their families must confront, some aspects of which are measurable and others not.

Early clinical studies reported low detection rates of viruses in patients with chronic lung diseases. For example, in CF patients respiratory viral infections were associated with up to approximately 40 to 50% of pulmonary exacerbations [51, 52, 54, 70-72]. However, these values likely underestimated the true impact of respiratory viral infections on disease progression because they are based on insufficiently sensitive detection methods, such as cell culture and serology. The development of molecular diagnostics techniques by polymerase chain reaction (PCR) has led to (i) an increased detection rate of respiratory virus infections in patients with chronic lung diseases, (ii) a greater diversity of respiratory viruses identified in patients, including picornaviruses and human metapneumovirus [53, 55], and (iii) an increased

recognition that respiratory virus infections are associated with morbidity and acute exacerbations in these patients. The more recently reported rates of detection of respiratory viral infection during periods of pulmonary exacerbations in CF patients are now greater than 50% [53, 55-58, 61]. RNA viruses influenza A virus, human rhinovirus (hRV), and respiratory syncytial virus (RSV) are the most common viral infections detected in CF patients, with RSV promoting early respiratory tract morbidity and hRV being the most common causative viral agent in pulmonary exacerbation. Similarly high detection rates of respiratory virus infections are observed in asthma (up to 80%) and COPD (up to 60%) exacerbations as well, with influenza virus, hRV and RSV also being the most commonly identified viruses [62-64, 73-75]. Although the incidence of viral infections is not greater in patients with CF than in healthy controls, the severity and length of viral infections were amplified in patients with CF [55, 76]. In addition, respiratory viral infections in CF patients are associated with increased antibiotic use [51, 53], deterioration of pulmonary function [50, 51, 53, 54], and longer durations of hospitalizations [54, 71, 77]. RSV is reported to be account for 9-58% of all reported viral infections CF patients, with a higher incidence in young children than adults [78]. Besides the association between respiratory viral infections and morbidity, clinical studies have linked respiratory viral infections with the development of chronic infections with the Gram-negative bacterium *P. aeruginosa* in CF patients [53, 72, 79]. The mechanisms underlying the increased severity of respiratory viral infections and the interactions between respiratory viruses and chronic bacterial infections in patients with CF and other chronic lung diseases remains poorly understood despite the fact that these observations have been made in the clinic for the past 30 years. Interestingly, an emerging body of literature is beginning to suggest that the innate immune response to respiratory viral infection likely plays a critical role in viral pathogenesis in chronic lung diseases. Moreover, it is

now appreciated in the field that the protective antiviral immune response to viral infection also has consequences for secondary bacterial infections by making the airway more permissive for bacteria, suggesting that the viral-bacterial interactions are not simply direct interactions between viruses and bacteria but are also facilitated by intricate relationships with host cells the airway.

In this regard, the Bomberger laboratory focuses on understanding the relationship between respiratory viral infections and the development of chronic *P. aeruginosa* infections in the CF lung and how the respiratory epithelium contributes to this interaction. As will be described in this thesis, the mechanisms that contribute to the development of chronic bacterial infections in the context of respiratory viral infections provide a unique perspective on viral-bacterial interactions in the lung, as compared with previous reports that have described synergy between viruses and bacteria in the respiratory tract.

1.2.1 Respiratory Syncytial Virus (RSV)

Respiratory syncytial virus (RSV) is an enveloped, negative-sense RNA virus that belongs to the O*rthopneumovirus* genus within the *Pneumoviridae* family of viruses. The single-stranded RSV genome has 10 genes organized as 3'-NS1-NS2-N-P-M-SH-G-F-M2-L-5' that are transcribed into separate mRNA encoding single viral proteins [80]. One notable exception is the M2 mRNA, which contains two overlapping open reading frames (ORFs) for two distinct proteins, M2-1 and M2-2. Translation of M2-2 is dependent upon re-initiation by ribosomes at a start codon that overlaps the M2-1 ORF [81, 82]. The M2-1 and M2-2 proteins are important for regulating RSV genome transcription and the balance between genome transcription and replication, respectively [83, 84]. The nucleoprotein (N), phosphoprotein (P), and RNA-dependent RNA polymerase (L) encapsulate the RSV genome to form the ribonucleoprotein

(RNP) complex. In addition, the RSV genome encodes three glycoproteins that are present in the viral envelope: the glycoprotein (G), the fusion protein (F), and small hydrophobic protein (SH). The G protein is important for viral attachment to host cells, whereas the F protein is important for fusion of the viral envelope with host membranes for release of RSV RNP complexes into cells [85]. Although multiple cell surface proteins, including CX3CR1, have been shown to interact with the G protein, recent studies identified CX3CR1 as a cellular receptor that mediates RSV entry in primary, well-differentiated human bronchial epithelial cells [86, 87]. The F protein has also been shown to interact with host proteins such as nucleolin and TLR4, albeit only in immortalized cell lines, and may play some role in viral attachment [88, 89]. In addition, studies have shown that inhibition of clathrin- and dynamin-dependent endocytosis does not inhibit RSV entry into host cells and that RSV can infect cells via macropinocytosis [90]. Together these studies suggest that RSV potentially has overlapping mechanisms by which it can enter host cells. Following attachment and fusion, the RSV RNP complex is released into the cytoplasm, where viral genomes are transcribed and replicated. Inclusion bodies are hypothesized to be the location of viral transcription and replication due to the accumulation of RNP complex proteins and viral RNA at these sites [91-93]. Progeny virions assemble and bud from the surface of infected cells, and these processes are dependent upon the viral F and M proteins [94-96]. Budding of RSV virions from the cell surface requires intact apical recycling endosome sorting pathways, which involves Rab11 family interacting protein 2 (FIP2), but interestingly, is vacuolar protein sorting-associated protein 4 (Vps4)-independent, suggesting that RSV release is not dependent upon endosomal sorting complexes required for transporter (ESCRT) proteins [97, 98]. In addition, cholesterol rich microdomains (i.e. lipid rafts) have been implicated in both RSV entry and release in host cells [99, 100]. However, the exact molecular

details of RSV replication, assembly and budding in host cells, and particularly the host factors that are needed for these processes, remain to be fully elucidated.

1.2.2 Human Rhinovirus (hRV)

Human rhinoviruses (hRVs) are non-enveloped, positive-sense RNA viruses that belong to the *Enterovirus* genus within the *Picornaviridae* family of viruses. They are grouped into three species: hRV-A, hRV-B and hRV-C. Depending on the type, hRVs use intercellular adhesion molecule 1 (ICAM-1), low-density lipoprotein receptor (LDLR) family members or cadherin-related family member 3 (CDHR3) for entry [101-103]. Upon internalization, virions undergo conformational changes due to cues from receptor-binding and the lower pH in endosomes and release viral RNA into the cytoplasm of cells [104]. The single-stranded hRV genomes are translated into a precursor polyprotein that is processed by viral proteases into 11 proteins, four of which are capsid proteins. The remaining seven nonstructural proteins mediate viral replication, and like with other picornaviruses, cellular membranes are remodeled to form replication compartments, also referred to as replication organelles, at the endoplasmic reticulum (ER)-Golgi interface during hRV replication [105]. The formation of replication compartments during picornavirus infection is dependent upon both viral and host factors [105]. It was recently demonstrated during hRV infection that phosphatidylinositol-4 phosphate (PI4P) and cholesterol are highly enriched at replication compartments [106]. There are two classes of phosphatidylinositol-4 kinases (PI4K) that are responsible for producing PI4P from phosphatidylinositol (PI), and interestingly, depending on the strain of hRV, different subsets of PI4Ks are important for hRV replication. For example, hRV-A1A is less sensitive to PI4K3β inhibition but is more sensitive to PI4K2α inhibition than hRV14, hRV16 and hRV37 [106].

Similarly, multiple mechanisms are utilized by diverse strains of hRVs to promote cholesterol accumulation in replication compartments [106]. Of particular note, oxysterol-binding protein (OSBP)-like proteins are intracellular proteins important for cholesterol transport and are involved in hRV replication. For example, inhibition of OSBP-1, which drives PI4P-cholesterol exchange between the ER and Golgi, broadly suppresses replication of many hRV strains, demonstrating lipid flow in replication compartments is required for efficient hRV replication [106]. Newly, synthesized hRV RNA is encapsidated by capsid proteins to form new virions, which according to classical dogma are released from host cells by lysis [105]. However, recent studies have suggested that hRV egress can occur by additional mechanisms, including non-lytic release of virions packaged within phosphatidylserine lipid-enriched vesicles [107]. Other picornaviruses, including coxsackievirus B and hepatitis A virus (HAV), can also be released in membrane-enclosed vesicles, suggesting this may be a release mechanism broadly utilized by picornaviruses and potentially other non-enveloped viruses [108, 109].

1.2.3 Antiviral Innate Immune Response to Respiratory Virus in Airway Epithelial Cells

The respiratory epithelium is a critical component of the innate immune system and the primary site of host-pathogen interactions in the lung [110]. In addition, the airway epithelium is the primary site of virus replication during respiratory virus infection, including RSV infections, and plays a critical role in viral pathogenesis [111, 112]. When microbial ligands engage various families of pattern recognition receptors (PRRs), distinct signaling cascades are activated within AECs that coordinate the host's response to the invading microbe. In the context of respiratory viral infection, the most relevant PRRs are Toll-like receptors and retinoic acid-inducible gene I-like receptors (RIG-I like), which detect double-stranded RNA (dsRNA), a by-product of virus

replication. Detection of dsRNA by these receptors activates signaling cascades that culminate in the induction of antiviral molecules called interferons (IFN). Type I and type III IFNs are the major IFNs produced by AECs in response to respiratory viral infection, including RSV [113-115]. IFNs act in an autocrine and paracrine manner to induce the production of IFN-stimulated genes (ISGs), which establish an antiviral state within AECs.

1.2.4 *In Vitro* Models of Airway Epithelial Cells from Patients with Chronic Lung Disease

The respiratory epithelium forms a critical mucosal barrier at which the body is constantly exposed to the external environment. Consequently, AECs are equipped with many complex functions that play critical roles in surveying, responding and clearing environmental factors, such as infectious agents. To better mechanistically understand many of these functions, investigators have commonly used cell culture models of the respiratory epithelium, including primary human bronchial epithelial (HBE) cells cultured on porous supports at air-liquid interface (ALI) [9, 116, 117]. These models are beneficial to investigators in that they allow the specific study of epithelial function in the absence of other cell types, control of experimental conditions, and because primary HBE cultures are originally obtained from explanted lungs, they closely resemble *in vivo* physiology when cultured at ALI. In addition to primary HBE cells, and driven mostly by the intermittent availability of primary HBE cells, many immortalized cell lines have been developed for the study of the respiratory epithelium in chronic lung diseases, including CF [118]. Both primary HBE and immortalized cell lines have been critical to our understanding of many of the biochemical, genetic, immunological and physiological mechanisms that occur at the respiratory epithelium in chronic lung diseases. For example, investigators compared primary CF cell cultures to non-CF cells and observed airway surface

liquid (ASL) height was decreased in primary CF cells, resulting in reduced reduce mucus transport, which is now considered a hallmark of CF lung disease [9].

1.2.5 Impaired Antiviral Immune Response Contributes to Respiratory Virus-Induced CF Exacerbations

Respiratory viruses cause significant morbidity in patients with chronic lung diseases, but the underlying mechanism to explain this clinical observation has not yet been elucidated. Because viral load is greater in patients with chronic lung diseases than control patients, the majority of studies have focused on mechanisms that contribute to increased viral replication in the respiratory epithelium. Although some studies suggest that alterations in interferon (IFN) signaling and IFN stimulated gene (ISG) induction may play a role in increased viral replication in the CF lung, a clear consensus on this topic has not been reached. Studies using primary AECs have shown that primary CF AECs produce reduced levels of antiviral mediators downstream of IFN signaling, specifically, nitric oxide synthase 2 (NOS2), 2' ,5'-oligoadenylate synthetase 1 (OAS1), and signal transducer and activator of transcription 1 (STAT1), in response to human parainfluenza virus 3 (HPIV3) [119]. This results in greater release of infectious virus from CF AECs compared to non-CF AECs [119]. Interestingly, similar levels of other known ISGs, such as MxA and PKR, were produced in both CF and non-CF cells in response to HPIV3 challenge [119]. In addition, a recent clinical study has demonstrated that the lower airway hRV burden is greater in patients with CF than in healthy controls and that the greater hRV load in CF patients is negatively associated with type I IFN levels in BAL fluid of the patients [120]. These studies raise the question of whether CF AECs are inefficient at responding to virus infection and IFN induction, have a blunted response to IFN and cannot signal efficiently, or respond to IFN

stimulation but do not produce certain ISGs. Recent work has demonstrated that CF AECs produce levels of type I and III IFNs similar to those of non-CF AECs in response to either virus infection or treatment with the dsRNA analog polyinosine-polycytidylic acid [poly(I:C)] [121-124]. Although the majority of ISGs that have been investigated thus far are similarly expressed in both CF and non-CF cells in response to virus infection, a few notable ISGs have been observed to be differentially expressed in CF versus non-CF cells, including MxA, PKR, and viperin [119, 121, 124, 125]. So far, these studies have only measured a select subset of ISGs and an extensive study comparing the full antiviral response in CF and non-CF AECs has not been described yet, leaving open the possibility that many more ISGs are potentially dysregulated between CF and non-CF AECs. Viral infections, and the PAMPs produced during viral infection, are not the only triggers that induce the production of IFN in AECs. Recently, it was shown that bacterial infections and LPS treatment also induced type I and III IFN production in AECs and the airways of mice [122, 126, 127]. Although the ability to produce IFNs is similar between CF and non-CF AECs during virus infection, induction of type I IFN was reduced in CF cell lines compared to non-CF cell lines either infected with *P. aeruginosa* or treated with LPS [122]. One explanation for this defect is that TLR4 surface expression is reduced in CF AECs [128]. Thus, defects in the IFN response to stimulus may be attributed to both impaired IFN induction and/or reduced expression of a subset of ISGs, but it appears that IFN induction is dependent upon the stimulating ligand and signaling pathway triggered in CF AECs. In the context of respiratory viral infection, IFN induction appears fully intact, suggesting no defect in dsRNA PRRs or the associated signaling pathways.

It is important to point out that inflammatory cytokine secretion is similar in CF and non-CF AECs during respiratory viral infection [129]. Thus, the inflammatory response induced by

virus infection in CF patients does not contribute to increased morbidity in these patients. Because of the negative correlation between virus-induced cytotoxicity and inflammatory cytokine production in CF AECs [129, 130], a possible explanation for the lack of an exaggerated inflammatory response during viral infection could be the increased virus-induced death of AECs in CF. Taken together, these studies suggest that reduced antiviral responses to respiratory viral infections result in uncontrolled viral replication and increased viral burden, but not exaggerated inflammation, in the CF lung. It appears that ISG induction plays a critical role in determining viral burden in the CF lung, which likely has implications for virally-induced exacerbations in CF, although a link between the two has not yet been established *in vivo*. Further research will be needed to clearly define what defects exist in antiviral signaling pathways in the CF airway. Whether there is an opportunity to design specific therapeutics that target these pathways to limit virus infections and can be used to treat virus-induced exacerbations in CF patients remains to be seen.

As in CF patients, the virus loads in asthma and COPD patients are higher following respiratory viral infection than in healthy controls [131, 132]. Interestingly, studies with primary HBE cultures have demonstrated that the antiviral innate immune response to respiratory virus infection is impaired in these patients as well. For example, type I and III IFN induction is reduced in primary HBE cells from asthmatics compared to non-asthmatic cells in response to hRV infection, and consequently, hRV replication is increased in asthmatic cells [133, 134]. Moreover, the levels of IFN that are measured in the airways of asthmatic patients are inversely correlated with viral loads and exacerbation severity [134]. In contrast, it was recently reported that there is no significant difference in hRV replication or type I or III IFN production between primary HBE cells from asthmatic patients and healthy controls [135]. One potential explanation

for this contradictory result is that primary HBE cells were isolated from patients with well controlled asthma in this study, and the authors postulated that defective IFN induction in response to respiratory viral infections in asthmatic patients may be a feature of more severe, less well controlled disease [135]. Recently, it was shown that suppressor of cytokine signaling 1 (SOCS1), a negative regulator of the IFN response to respiratory viruses, is upregulated in primary HBEs from asthmatic patients, suggesting a potential mechanism for the deficient antiviral responses observed during respiratory viral infections in asthma patients [136]. In addition, the production of inflammatory mediators and increased neutrophil influx during respiratory viral infections in asthma and COPD patients has been reported and likely contributes to the pulmonary damage patients experience during viral infections [131, 132].

1.2.6 Bacterial Coinfection During Respiratory Viral Infections in Chronic Lung Disease Patients

Beyond the morbidity linked to respiratory viral infections alone, clinical studies have linked respiratory viral infections with the development of chronic infections with the Gram-negative bacterium *P. aeruginosa* in CF patients. *P. aeruginosa* is the most common bacterial pathogen in patients with CF and is well known to have deleterious effects on lung function. Seasonal trends have been noted in which the majority of patients with CF were initially infected with *P. aeruginosa* during respiratory viral seasons [79]. In addition, up to 85% of new *P. aeruginosa* colonization in CF patients occurred within 3 weeks following a respiratory viral infection [53]. In children hospitalized for severe respiratory symptoms in which a respiratory virus was identified, 25% of patients were later infected with *P. aeruginosa* [71]. Overall, 35% of patients who were hospitalized for severe respiratory symptoms were colonized with *P. aeruginosa* with

12-60 months, and although in the majority of these patients a respiratory virus was not detected, this study did not rely on PCR-based detection methods and likely underestimated the burden of respiratory virus infection [71]. In addition, it has been observed that a rise in antipseudomonal antibodies is preceded by a viral infection [72]. Although many viruses have been isolated from CF patients, RSV has been reported to be the most common respiratory virus associated with the development of chronic *P. aeruginosa* infections in CF patients [72]. However, the mechanisms underlying how respiratory viruses enhance the development of chronic infections by *P. aeruginosa* in CF patients remains poorly understood.

An association between respiratory viral infections and bacterial coinfection has also been observed in asthma and COPD patients. Respiratory viral infection (only hRV infections were included in analysis) increased the likelihood of bacterial detection, and thus, bacterial burden in the upper respiratory tract in children with asthma [137]. Interestingly, both the likelihood of bacterial coinfection and bacterial infection within one week following hRV infection were increased in this study [137]. In clinical studies of COPD patients, it has been observed that up to 60% of patients with a viral infection also have a bacterial coinfection and that the presence of a viral infection increases bacterial burden of bacteria already in the lower airway [74, 75, 138]. Moreover, in a cohort of COPD patients with hRV-positive exacerbations who were negative for bacteria at presentation, 73% became positive for bacteria by day 14 post-presentation [139]. The relationship between respiratory viral infection and subsequent bacterial infections has been further established in studies with experimental hRV infection in patients with COPD. In one study, it was shown that hRV infection increased secondary bacterial infection in 60% of virally-infected patients whose sputum tested negative for bacterial culture at the beginning of the study [140]. Bacteria investigated in this study were *Streptococcus*

penumoniae, *Haemophilus influenzae*, *Moraxella catarrhalis*, *S. aureus*, and *Haemophilus parainfluenzae*. In further studies with this model, it has been observed that hRV infection alters the respiratory microbiota in patients with COPD and that these changes are evident up to 42 days post-hRV infection [141]. This suggests that respiratory viral infection potentially not only alters the abundance of what are thought of as traditionally pathogenic bacteria but also the overall microbial composition in the airways of COPD patients. Other studies have also made similar observations, showing that respiratory viral infection and the resulting antiviral immune response can alter the microbiome of the upper respiratory tract [142]. Interestingly, observations in asthma, COPD, and CF patients have similarly noted that bacterial acquisition can occur following peaks in respiratory virus infection [71, 137, 139]. This suggests that respiratory viral infections not only have short-term consequences that predispose patients to secondary bacterial infection at the time of viral infection, but also can have long-term consequences on airway physiology that makes the airway more permissive for secondary bacterial pathogen after the virus has been cleared. Again, very little is understood about the mechanisms underlying how respiratory viruses alter airway physiology to promote a more permissive environment for secondary bacterial infection.

1.3 VIRAL-BACTERIAL COINFECTION IN THE RESPIRATORY TRACT

Studies of viral-bacterial interactions in the respiratory tract have revealed many mechanisms by which a preceding virus infection promotes secondary bacterial infection. Many studies have focused on the interactions between influenza virus and secondary bacterial infections caused by commensal organisms of the upper respiratory tract, namely *S. pneumoniae* and *S. aureus*.

However, as our understanding of viral-bacterial co-infections continues to grow, it is now recognized that respiratory viral infections are associated with severe secondary bacterial infections in both acute, such as bacterial pneumonias, as well as chronic, such as CF, pulmonary disease settings. Moreover, the field of viral-bacterial co-infections has expanded to investigate interactions between diverse viral and bacterial pathogens. Although many mechanisms have been described by which viruses predispose the airways to secondary bacterial infection, they can be broadly categorized as: (i) the virus augmenting bacterial adherence to the respiratory epithelium or (ii) dysregulation of antibacterial immune responses due to viral infection. In this dissertation, we focus on the interaction between RSV and *P. aeruginosa*. Our data provides evidence that respiratory viral infection dysregulates nutritional immunity in the airways to promote *P. aeruginosa* biofilm growth, which represents an emerging mechanism by which viruses are observed to predispose the airways to secondary bacterial infection.

1.3.1 Viral Infection Enhances Bacterial Adherence to Airway Epithelial Cells

Viral infections have been described to increase bacterial attachment to respiratory epithelial cells through many distinct mechanisms that may play a role in establishing bacterial infections. Moreover, increased binding of bacteria to virus-infected cells does not appear to be dependent on any single respiratory virus infection and multiple combinations of bacterial and viral pathogens have been described. Respiratory viral infections are known to target ciliated cells and damage the respiratory epithelium [143, 144]. This benefits bacterial attachment by (i) impairing mucociliary clearance, which increases airway obstruction [145], and (ii) exposing basal cells and basement membrane, which provide additional sites where bacteria may readily adhere [146, 147]. Moreover, RSV infection reduces the periciliary layer depth below the optima height of 7

μm required for cilia to beat, which would result in impaired mucociliary transport [10]. Viral infection can upregulate the expression of bacterial receptors on host AECs, such as intercellular adhesion molecule 1 (ICAM-1), platelet activating factor receptor (PAFR), and α5 integrin [148-150]. For example, it was shown that influenza virus infection increased TGF-β signaling, which was required for augmented surface expression of α5 integrin and bacterial adherence to AECs during viral infection, demonstrating that the immune response to respiratory viral infection may play a role in upregulation of bacterial receptors on host AECs and bacterial coinfection in the respiratory tract [150]. Bacteria can also directly bind to viruses or viral structures on virally-infected cells, which act as coupling agents to increase bacterial interaction with the respiratory epithelium [151-153]. In the case of RSV, the *S. pneumoniae* penicillin binding protein 1a binds to the RSV G proteins, which leads to increased attachment of *S. penumoniae* to AECs and increased virulence *in vivo* [154]. The magnitude of these effects have been reported to be dependent upon cell type and the strain of the viral or bacterial pathogens investigated [148, 155]. In terms of *in vivo* infection, the likely explanation for the decreased bacterial clearance observed during coinfection in the respiratory tract is due to a combination of all these effects.

1.3.2 Immunological Alterations in Antibacterial Immunity at the Respiratory Epithelium during Respiratory Viral Infection

The respiratory epithelium is the primary site of viral replication and PRR-mediated detection of viral infection results in the production of type I and III IFNs that mediate the antiviral immune response. The release of IFNs has been observed to subvert many antibacterial response in the airways, and although this response is crucial for viral immunity and clearance, it creates an

environment that is unable to control bacterial growth and is predisposed to secondary bacterial infection. In a mouse model of influenza infection, type I IFN signaling was shown to be responsible for impaired phagocytic chemoattractant production in the airways and as a result, decreased macrophage and neutrophil responses during secondary bacterial infection [156, 157]. Conversely, in other studies, influenza infection did not lead to decreased neutrophil or macrophage recruitment to the airways during bacterial coinfection [158, 159], suggesting that mechanisms besides inflammatory cell recruitment likely contribute to diminished bacterial clearance. Type I IFN signaling in response to influenza infection was also shown to diminish Th17 immunity, including IL-17 and IL-22 production in the airways, resulting in decreased production of antimicrobial peptides and increased susceptibility of mice to bacterial infection in response to influenza infection [158-160]. Impaired antimicrobial peptide production has also been observed in the airway of chinchillas following RSV infection [161]. Interestingly, respiratory viral infection increases susceptibility to both Gram-negative (i.e. *Escherichia coli* and *P. aeruginosa*) and Gram-positive (*S. pneumoniae* and *S. aureus*) bacterial pathogens [156, 159]. As a proof of principle that impairment of bacterial clearance in the airways is due to an antiviral immune response, independent of virally-mediated tissue injury or some other alteration in host physiology facilitated by viral proteins, it was demonstrated that intranasal administration of poly(I:C) was sufficient to induce type I IFNs in the airways and impair bacterial clearance from the lungs of animals [162]. Type III IFN production has also been shown to contribute to reduced clearance of *P. aeruginosa* from the airways [127], although the mechanism(s) by which type III IFN contributes to inhibition of bacterial clearance during viral-bacterial coinfection are even less well understood than those discussed for type I IFNs.

Besides inducing the production of type I and III IFNs, the pathways activated by the PRRs that sense respiratory viruses also culminate in the expression of pro-inflammatory chemokines and cytokines [163]. For example, RSV and hRV infections increase the release of the pro-inflammatory cytokine IL-6 and IL-8 from AECs [164, 165]. These signaling pathways must be tightly regulated to minimize over-activation and immune-mediated pathology. Consequently, these regulatory mechanisms may delay the response to secondary infections in the context of coinfections when cells continuously encounter multiple pathogens. In a mouse model of influenza infection, it was shown that macrophage and neutrophil recruitment to the airways was impaired during secondary *S. pneumoniae* infection [166]. Interestingly, macrophages isolated from influenza-infected mice were hypo-responsive to bacterial ligands in this study, but the authors did not provide a mechanism for TLR desensitization and postulated that the signaling molecules downstream of TLRs were either downregulated or functionally augmented as a result of viral infection [166]. Defects in phagocyte recruitment and function in response to respiratory viral infection have also been reported to lead to decreased bacterial clearance during coinfection in models of RSV, hRV and other models of influenza infection [167-169]. In regards to neutrophils, myeloperoxidase activity was the only functional impairment observed in neutrophils during viral-bacterial co-infections in these studies. In another study of influenza-*S. pneumoniae* co-infection, it was observed that there was an increased release of the anti-inflammatory cytokine IL-10 into the airways of animals and neutralization of IL-10 reduced bacterial burden and lethality [170]. Because the anti-inflammatory properties of IL-10 can influence the function of various immune cells, it was proposed that IL-10 augments the function of phagocytes and create an immunosuppressive state in the airways that is permissive to secondary bacterial infection [170]. However, macrophages

and neutrophil recruitment to the airways was not impaired during coinfection with influenza and *S. aureus*, and the cells isolated from mice did not demonstrate a defect in phagocytosis [160]. Taken together, these studies suggest that respiratory viral infection may delay or impair the innate immune response to bacterial infection, creating a permissive environment that can be colonized, but the molecular details underlying these observations are still poorly understood and further work will be required to understand the intricacies of these interactions that contribute to differences observed between studies and models.

Bacterial infections are also capable of modulating secondary viral infection in the respiratory tract. The attachment of hRV is enhanced on cells pretreated with *H. influenzae* due to increased expression of ICAM-1, the cellular receptor for hRV [171, 172]. In addition, preceding bacterial infections may augment the immune response to secondary viral infections. For example, antigen presentation is an important process that is needed for an effective adaptive immune response to respiratory viral infection and it has been shown that *P. aeruginosa* can disrupt antigen presentation in AECs by altering the trafficking of TAP1 and promoting TAP1 degradation, resulting in reduced cell surface expression and antigen availability to major histocompatibility complex (MHC) class I at the plasma membrane [173]. In addition, AECs infected with *P. aeruginosa* and hRV were observed to have decreased production of type I and III IFNs compared to cells infected with hRV alone [121]. Secondary viral infection has also been shown to induce dispersion of bacteria from established biofilms [174, 175]. This has important implications for our understanding of bacterial transmission in the respiratory tract and how bacterial biofilms are established *in vivo*, but the mechanisms underlying the relationship between bacteria and secondary viral infections remain poorly understood and require further attention. It is likely that the respiratory epithelium will be critical to these interactions as well.

1.4 NUTRITIONAL IMMUNITY

During the course of infection, the host-pathogen interface is a dynamic environment where the multiple interactions ultimately determine whether the host clears or is colonized by the invading microorganism. One such interaction is the competition for nutrients. Bacterial pathogens must have mechanisms to facilitate their acquisition of nutrients, such as iron, from the environment to successfully colonize a host, establish a replicative niche, and survive during the course of infection. Conversely, host cells strongly oppose these bacterial processes by restricting nutrient accessibility for many different nutrients. Over four decades ago, nutritional immunity was originally coined to describe the restriction of iron by the host [176, 177] . At that time, it was known from animal models of bacterial infection that exogenous iron supplementation increased bacterial growth and virulence. For example, in a mouse model of *Yersinia pestis*, mice treated with 40 μg of ferrous iron were more susceptible to infection and had decreased survival [178]. Similar results were subsequently found in models of *Listeria monocytogenes*, *E. coli* and *P. aeruginosa* infections [179-181]. Since then, however, extensive studies have begun to identify the host mechanisms for limiting iron availability as well as address how microorganisms circumvent these mechanisms of nutrient limitation to colonize their hosts and cause disease in a number of disease settings [182]. In the field of viral-bacterial co-infections, an emerging body of literature demonstrates that an additional mechanism by which virus predispose to secondary bacterial infection is by viral subversion of nutritional immunity in the respiratory tract.

1.4.1 Host Mechanisms for Withholding Iron

Iron is essential for numerous physiological processes, including DNA replication, gene expression, and energy generation. The utility of iron in many diverse biological processes is due to its role as a redox catalyst, where it can cycle between ferrous (Fe^{2+}) or ferric (Fe^{3+}) oxidation states. However, the redox potential of iron also makes it conducive to catalyzing the Fenton reaction in the presence of reactive oxygen intermediates and generating hydroxyl radicals that damage cells. Thus, it is critical that the host not only regulate the quantity and location of iron to restrict pathogen accessibility of iron but also limit cellular damage. There are many distinct mechanisms by which hosts limit free iron and maintain iron homeostasis.

Dietary iron uptake is regulated in response to infection or high total body iron levels to systemically lower iron levels. Dietary iron is absorbed through enterocytes in the duodenum by the iron importer, divalent metal ion transporter (DMT1), after Fe^{3+} has been converted to Fe^{2+} by ferric reductases present at the apical membrane of enterocytes [182]. DMT1 is also localized to the membrane of phagocytes and pumps iron out of the phagosomal compartment to restrict access of iron to intracellular pathogens [182]. Once in enterocytes, the iron can either enter the labile iron pool, where it is either stored in the iron storage protein ferritin or used for cellular processes, or the iron is exported from the cells as Fe^{2+} into plasma by the iron exporter, ferroportin-1 (FPN-1), localized at the basolateral membrane of enterocytes. Ferrioxidases convert all Fe^{2+} released by enterocytes to Fe^{3+}, which is then bound by transferrin and transported throughout the body. Hepcidin is a peptide produced in the liver that binds FPN-1 and promotes its degradation in the lysosome [183]. This results in a loss of basolateral FPN-1 in enterocytes, a decrease in overall iron flux into plasma, and a reduction in dietary iron-absorption [184]. Because hepcidin is expressed in response to high iron levels in the body or infection, this

mechanism of iron limitation results in a hypoferremic response that lowers iron levels throughout the host. In addition, hepcidin reduces the levels of cell surface ferroportin and promotes iron retention in macrophages [185]. Hepcidin is also produced by neutrophils and macrophages in response to infection, suggesting that hepcidin-mediated control of ferroportin levels on phagocytes is also regulated in the local environment of an infection [186].

The majority of human iron is bound to hemoproteins either inside host cells or extracellularly. For example, most of the iron in circulation is complexed with heme and heme is complexed within hemoglobin inside erythrocytes. Although some pathogens have evolved mechanisms to lyse erythrocytes, the host proteins haptoglobin and hemopexin bind free hemoglobin and heme, respectively [187]. In addition to its sequestration in erythrocytes, iron is stored in ferritin in other cell types, such as AECs. The availability of extracellular iron is extremely limited by iron-binding proteins in the extracellular environment, such as members of the transferrin family of iron-binding proteins. Typically, transferrin iron saturation is less than 50%, and as transferrin saturation increases, the ability of transferrin to sequester iron and inhibit bacterial growth decreases. Interestingly, in CF patients, transferrin iron saturation is less than 20% in the majority of patients [23, 188], but the clinical significance of this observation is unknown.

1.4.2 Transferrin

The transferrin family of iron-binding proteins consist of serum transferrin, lactoferrin and ovotransferrin. Due to their ability to sequester iron at the sites of infection, transferrin family members have been appreciated to have antimicrobial activity for nearly 7 decades [189]. Serum transferrin is a serum glycoprotein that plays a central role in iron metabolism by regulating the

transport and delivery of iron to tissues throughout the body. Lactoferrin was originally isolated from human milk but has since been found in a wide-range of mucosal secretions [190]. In addition to its iron-binding capabilities, lactoferrin has additional antimicrobial properties that are derived from the cationic properties of its N-terminus. In particular, lactoferricin and lactoferrampin are peptide fragments released from the N-terminus of lactoferrin by proteolytic cleavage that exhibit broad antimicrobial activity [191, 192]. Finally, ovotransferrin is the major component of egg white and was the first transferrin family protein discovered in 1944 after it was recognized a protein component of raw egg white was capable of binding iron and inhibiting bacterial growth [193].

Transferrin is an approximately 76 kDa serum glycoprotein with a high affinity for iron (K_d ~10^{-22} M) [194]. Each molecule of transferrin is organized into two lobes (termed C- and N-lobes), each with an Fe^{3+}-binding sites. Because each molecule of transferrin binds two atoms of Fe^{3+}, up to four different species of transferrin may be present at any one time [195]. Transferrin is present in mucosal secretions and due to its high affinity for iron, transferrin is very effective at binding extracellular iron. This property serves many purposes in the host including: (i) sequestration of iron from pathogens, (ii) keeping Fe^{3+} in an inert redox state to limit free radical production, (iii) maintaining Fe^{3+} in a soluble form in the body (Fe^{3+} is normally not soluble under physiologic conditions), and (iv) facilitating iron transport throughout body. Iron is delivered to target cells through a series of steps that are initiated when iron-loaded transferrin binds to the transferrin receptor (TfnR) on the plasma membrane of target cells with nanomolar affinity (**Figure 1**) [196]. In polarized epithelial cells, such as AECs, this initial binding event takes place at the basolateral membrane. The transferrin-TfnR complex is endocytosed in clathrin-coated pits and the pH of the endosome decreases as the endosome matures through the

action of ATP-dependent H^+ pumps. As the pH decreases, the affinity of transferrin for Fe^{3+} decreases and ultimately Fe^{3+} is released at the significantly lower pH. Through the action of ferric reductases (Steap proteins), Fe^{3+} is converted to Fe^{2+} and transported into the cell by DMT1 to be stored in ferritin or used for cellular processes. In the acidic environment of the endosome, iron-free transferrin (apo-transferrin) remains bound to TfR with high affinity. The complex is recycled back to the basolateral membrane and apo-transferrin is released back into the serum, likely through a combination of the low (micromolar) affinity of apo-transferrin for the TfnR at physiological pH and the competition from iron-loaded transferrin in the serum.

Due to the presence of transferrin in mucosal secretions and its importance in iron trafficking in the host, transferrin represents a potentially significant source of iron for invading microorganisms. Consequently, pathogens have evolved mechanisms by which they use transferrin as an iron source for growth [197-200]. For the majority of pathogens, the principal mechanism by which they acquire iron from transferrin is via the production of siderophores, which will be discussed further in the next section in regards to *P. aeruginosa* iron acquisition. Additionally, some pathogens have evolved transferrin uptake systems that are based on receptors that directly bind transferrin, including *Neisseria meningitidis* [201], Recently, it was demonstrated that transferrin has undergone rapid evolution in the C-lobe, in sites that overlap with the binding site of bacterial transferrin receptors [202]. This indicates that transferrin is involved in the evolutionary arms race between host iron sequestration and microbial iron acquisition, which has implications for bacterial (and likely other pathogens) colonization, virulence, and competition within communities. Furthermore, it has been demonstrated that pathogens have the ability to alter host cell physiology, without causing cellular lysis, to increase transferrin abundance at the site of infection. For example, in the context of *Helicobacter pylori*

infection of gastrointestinal epithelial cells, the bacteria promoted mislocalization of transferrin receptor from the basolateral to apical membrane of cells [203]. As a result, *H. pylori* increased transcytosis and apical secretion of transferrin, which can be utilized by the bacterium for growth [199, 203]. However, it is currently unknown how virus infections, including respiratory viral infections, alter transferrin localization at the site of an infection.

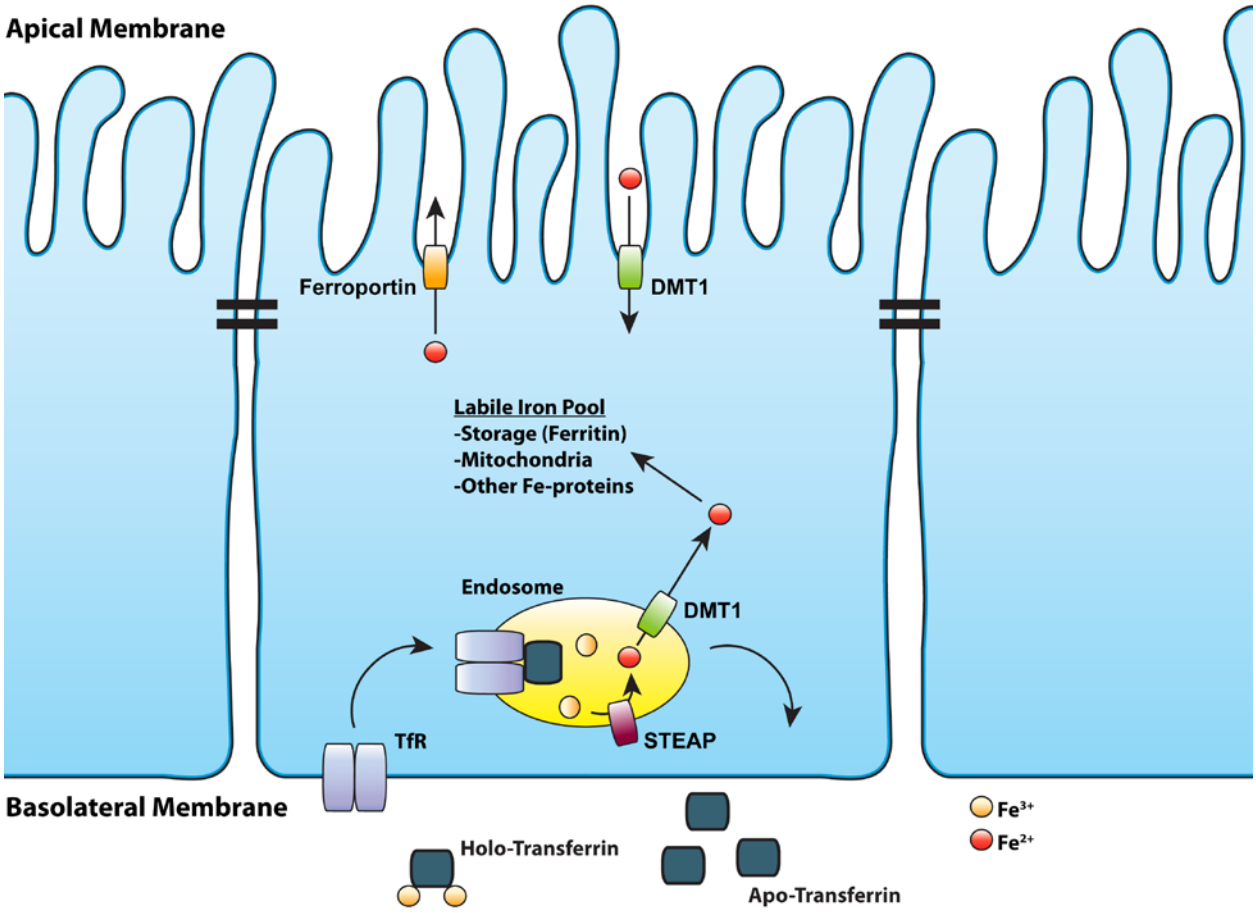

Figure 1: Iron Trafficking in Airway Epithelial Cells

Transferrin binds to ferric iron (Fe^{3+}) and delivers iron to cells throughout the body, including epithelial cells. Iron-bound transferrin (holo-transferrin) binds to transferrin receptor (TfnR) on the basolateral cell surface and is taken up by epithelial cells by clathrin-mediated endocytosis. The resulting acidification of the endosome facilitates decreased binding affinity of transferrin for Fe^{3+}. Iron-free transferrin (apo-transferrin) remains bound to its receptor at this low pH. Released Fe^{3+} is reduced to ferrous iron (Fe^{2+}) and transported into the cytosol by DMT1. Apo-transferrin is recycled back to the basolateral membrane. The low binding affinity of TfnR for apo-transferrin at physiological pH releases apo-transferrin into the extracellular environment, where it may bind more Fe^{3+}. Iron is then utilized based on the metabolic needs of the cell. Iron can enter the mitochondria where it is incorporated into iron-sulfur clusters for use in DNA replication, protein synthesis, redox enzymes involved in metabolism, etc. Excess iron not immediately required for use is stored in the intracellular iron-binding protein ferritin. Fe^{2+} uptake and release at the plasma membrane is facilitated by the iron transporters DMT1 and ferroportin, respectively.

1.4.3 *Pseudomonas aeruginosa* Iron Acquisition

The ability to acquire iron from the environment is essential for *P. aeruginosa* biofilm growth. When *P. aeruginosa* is grown under iron-limited environments or iron is limited with iron-chelation molecules, biofilm growth is significantly impaired [27, 37, 43, 204]. Although the host innate immune system restricts iron availability to invading microorganisms, *P. aeruginosa* can overcome host-mediated iron limitation and acquire iron, from either heme or nonheme sources, through several diverse mechanisms (**Figure 2**). These strategies can generally be categorized as siderophore, heme, and free Fe^{2+} iron acquisition systems [187].

In the natural environment heme is an uncommon iron source and under aerobic conditions, such as the airways, iron is oxidized to insoluble Fe^{3+}. In healthy humans, Fe^{3+} is bound to host proteins and has limited bioavailability. Consequently, *P. aeruginosa* other bacteria, and fungi, produce high-affinity Fe^{3+} binding proteins called siderophores that facilitate Fe^{3+} acquisition and are important for colonization [205]. *P. aeruginosa* produces two siderophores, pyoverdine and pyochelin in response to low-iron. When bound to iron, ferripyoverdine and ferripyochelin are first imported into the periplasm of *P. aeruginosa* by the TonB-dependent receptors FpvA and FptA, respectively (**Figure 2**). ATP-binding cassette (ABC) transporters then mediate the transfer the iron across the inner membrane (**Figure 2**). Pyoverdine has an extremely high affinity for iron, higher even than host-iron binding proteins, such that it is capable of displacing iron from transferrin [206]. The importance of pyoverdine to *P. aeruginosa* biofilm formation has previously been established; in bacteria unable to produce pyoverdine, *P. aeruginosa* biofilm growth was significantly decreased compared to pyoverdine-producing bacteria [204]. Pyochelin has a lower affinity for iron than both pyoverdine and transferrin, and its appears to be less essential for *P. aeruginosa* biofilm growth than pyoverdine

[204]. *P. aeruginosa* also has the ability to utilize siderophores from other bacterial species, known as xenosiderophores, [205]. The use of these xenosiderophore-based iron uptake strategies may be beneficial in the context of multispecies communities where *P. aeruginosa* could steal ferrisiderophores from other bacterial species, but may be detrimental for chelation therapies that are based on siderophores produced by bacteria, such as deferoxamine (DSX).

Although siderophores are critical to iron acquisition, siderophores also play important roles as signaling molecules [207]. For example, binding of FpvA by ferripyoverdine simultaneously initiates ferripyoverdine uptake and a signaling cascade through the anti-sigma factor FpvR, which controls the sigma factor PvdS. Besides the requirement of PvdS for expression of pyoverdine biosynthesis genes, PvdS also controls the expression of two secreted proteases, endoprotease (PrpL) and alkaline protease (AP) [205, 207]. Both PrpL and AP have been shown to degrade transferrin *in vitro* (**Figure 2**) [208, 209]. Importantly, transferrin and lactoferrin degradation products have been detected in the sputum of CF patients infected with *P. aeruginosa*, indicating that degradation of these host iron-binding proteins may have a role in iron acquisition *in vivo* [210]. It cannot be ruled out that other secreted *P. aeruginosa* proteases or host-derived proteases contributed to the increase in transferrin and lactoferrin degradation products in these patients; LasB is another protease secreted by *P. aeruginosa* that has been shown to cleave transferrin *in vitro* (**Figure 2**) [211].

The majority of iron in the human body is bound to hemoproteins, such as hemoglobin or hemopexin, where the iron is incorporated into heme. Although the concentration of free heme is low, *P. aeruginosa* has the capacity to acquire heme via two systems, the Has and Phu systems (**Figure 2**) [205]. In the Has system, a secreted heme-binding protein (HasA) captures heme from host-hemoproteins. The heme-HasA protein complex is recognized by the TonB-dependent

receptor HasR and the heme is transported into the bacterial periplasm. Conversely, heme is directly transported into the periplasm by the TonB-dependent receptor PhuR in the Phu system. ABC transporters mediate the transfer of heme from the periplasm to the cytoplasm of *P. aeruginosa*. The Has and Phu systems likely play a minimal role in iron acquisition during initial colonization of the CF lung when lung function is still relatively high and lung damage has not significantly accumulated. However, later in infection when lung damage has significantly accumulated in CF patients, these systems could play an important role in iron acquisition, as the sources of iron are likely changing. In support of this hypothesis, longitudinal analyses of different CF *P. aeruginosa* clinical isolates recently demonstrated that pyoverdine production decreases in clinical isolates over time, and heme utilization as the sole iron source is more efficient by later clinical isolates compared to earlier isolates [212, 213].

Although Fe^{2+} iron abundance is relatively low in aerobic environments, Fe^{2+} is soluble and more likely to be present in anaerobic conditions. Recently, it was demonstrated that Fe^{2+} is abundant in the sputum of CF patients, and negatively correlates with disease severity in patients [28], suggesting Fe^{2+} may be a relevant iron source for bacteria in the CF lung. Soluble Fe^{2+} is acquired by *P. aeruginosa* by the cytoplasmic membrane Fe^{2+} transporter FeoB (**Figure 2**) [205]. In addition, *P. aeruginosa* produces redox-cycling compounds called phenazines that can convert Fe^{3+} to Fe^{2+} (**Figure 2**) [205]. It has been shown that phenazines are present in CF patient sputum, and similarly to Fe^{2+} levels, are negatively correlated with lung function, suggesting the importance of phenazines *in vivo* [214]. Phenazines have been shown to promote biofilm growth by a siderophore-deficient (*ΔpvdAΔpchE*) strain of *P. aeruginosa* in the presence of Fe^{3+}, as well as in the presence of an iron-binding proteins [215]. This last observation is of particular relevance as it suggests that phenazines may provide one mechanism by which *P. aeruginosa*

circumvents iron chelation, which has implications for the design and use of chelation-based therapeutics in CF patients to treat *P. aeruginosa* infections.

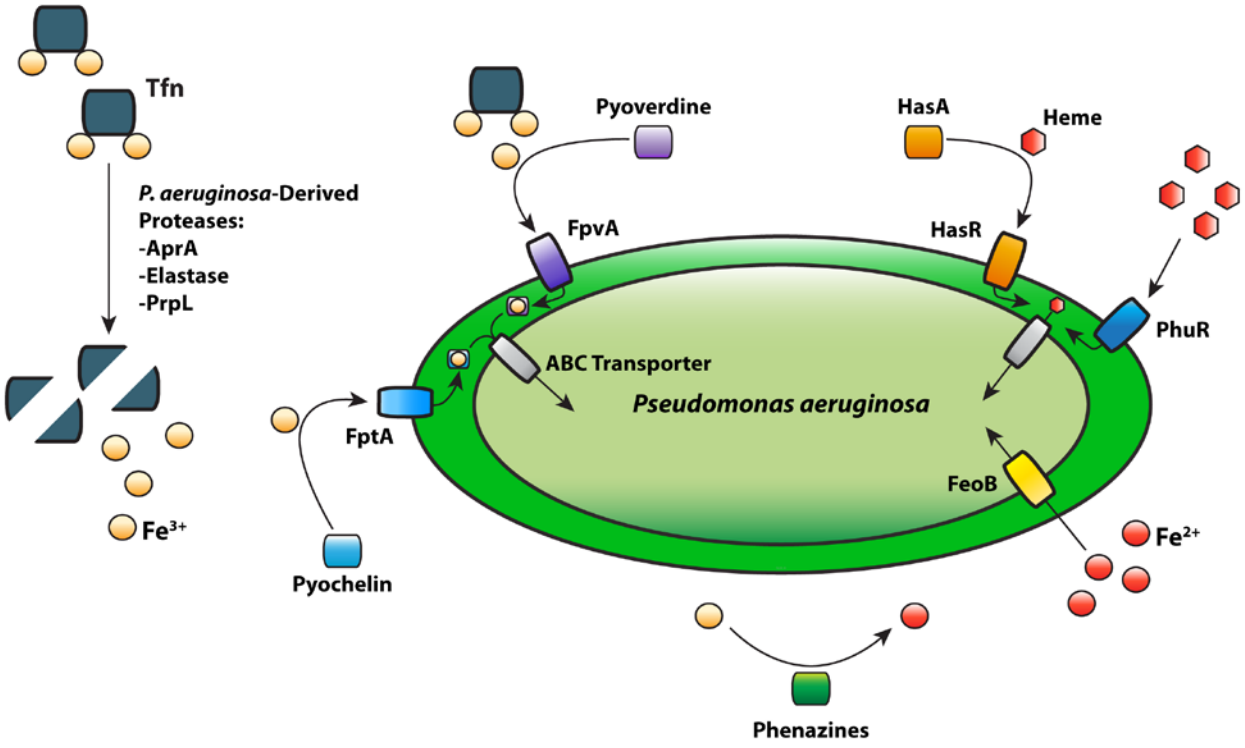

Figure 2: Iron Acquisition Systems in Pseudomonas aeruginosa

P. aeruginosa produces two siderophores, pyoverdine and pyochelin, that bind to ferric iron (Fe^{3+}). Ferripyoverdine and ferripyochelin are imported into the periplasm of the bacterium by the TonB-dependent receptors FpvA and FptA, respectively. Pyoverdine has a higher affinity for iron than the host-iron binding protein transferrin (Tfn), and thus, can directly outcompete Tfn for Fe^{3+}. Pyochelin has a lower affinity for Fe^{3+} than Tfn, and does not have this ability. *P. aeruginosa* produces multiple proteases that can cleave Tfn including: AprA, Elastase, PrpL. Cleavage of Tfn releases free Fe^{3+} into the environment to be taken up by either siderophore system. Phenazines produced by *P. aeruginosa* can reduce Fe^{3+} to ferrous iron (Fe^{2+}), which can be taken up by the *P. aeruginosa* cytoplasmic membrane Fe^{2+} transporter FeoB. *P. aeruginosa* can acquire heme-bound iron via two systems, the Has and Phu systems. The Has system produces a secreted heme-binding protein (HasA) that captures heme, and is imported into the periplasm by the TonB-dependent receptor HasR. The Phu system directly transports heme into the periplasm by the TonB-dependent receptor PhuR. ABC transporters are responsible for transporting iron from the periplasm to the cytoplasm of *P. aeruginosa*.

1.5 EXTRACELLULAR VESICLES IN VIRAL AND BACTERIAL INFECTIONS

Cell-to-cell communication is a critical component of cellular physiology that regulates appropriate and quick responses to cellular damage and infection, among other functions. Extracellular vesicles (EVs) are a form of intercellular communication that have been increasingly studied in the context of infectious diseases. EVs are released from most cells and are composed of cytosolic proteins and RNA surrounded by a lipid bilayer containing transmembrane proteins from the cells that release them. The protective nature of the lipid bilayer allows the transfer of functional proteins and RNAs between cells that can change the physiology of recipient cells. For example, EVs have been shown to transfer ISGs between hepatocytes that protected recipient cells against hepatitis B virus infection [216]. In addition, mRNA and microRNA is packaged into EVs, and although the mRNAs can be translated into proteins, the majority of studies have focused on the identification of microRNAs and their functions in recipient cells [217-219]. Bioactive lipids are also transferred in EVs to recipient cells and mediate signaling that alters target cells [220]. For example, prostaglandin E2 containing EVs were shown to promote natural killer (NK) T cell anergy [221]. Thus, EVs are ubiquitously produced messengers, potentially containing numerous bioactive molecules that may contribute to host defense or promote pathogenesis during the course of an infection.

EVs released during an infection can either be host-derived or pathogen-derived. For example, Gram-negative bacteria produced outer membrane vesicles (OMVs) that impact both bacteria-bacteria and bacteria-host interactions [222]. Recently, Gram-positive bacteria membrane vesicles have also been described [223]. In addition, parasites release EVs that mediate parasite-parasite and parasite-host interactions [224, 225]. During viral infections, EVs are generated by host cells and are thought to have an important role in virus infection, but owing

to the biophysical similarities between viruses and EVs, the line between host-derived EV and virions is often blurry [217, 226].

EVs derived from cells during infection are divided into three categrories: exosomes, and microvesicles or ectosomes, and apoptotic-bodies. Originally, EVs were first described during studies following the trafficking of TfnR in the context of maturing reticulocytes. The distinguishing trait of these EVs were that they originated within endosomal compartments referred to as multivesicular endosomes or multivesicular bodies (MVBs) and were subsequently released into the extracellular environment following fusion of the MVB with the plasma membrane [227, 228]. Because reticulocytes lose TfnR as they mature and TfnR was present on these vesicles, it was believed that this was an alternative mechanism by which cells could downregulate receptors and dispose of components no longer needed. The term exosome was coined a few years following this observation to refer to this population of EVs, which generally have a size that is equivalent to that of the vesicles that accumulate in MVBs (less than 150 nm) [229]. In the mid-1990's, however, it was found that these vesicles might have functions important for intercellular communication. In one study, it was demonstrated that exosomes isolated from B-cells contained major histocompatibility complex (MHC) class II molecules and were able to induce T cell proliferation and IL-2 secretion from hybridomas [230]. Additionally, it was demonstrated that exosomes isolated from DCs pulsed with tumor peptide could be added to mice and reduce the growth of established tumors *in vivo* [231]. Membrane-derived vesicles were also described and suggested to also have a function in intercellular communication around the same time [232-235]. Microvesicles or ectosomes are vesicles that bud off the plasma membrane with sizes that range from 100 nM to 1 μM [236, 237]. Both microvesices and exosomes have similar buoyant density and contain cytoplasmic and membrane-bound molecules

(i.e. proteins and RNAs), but there are generally additional protein markers associated with exosomes [238, 239]. Apoptotic bodies are larger vesicles up to 4 μM in size, and unlike other extracellular vesicles, they contain nuclear fractions (i.e. DNA) and are annexin V-positive [238, 239]. Because of the overlapping sizes and biophysical characteristics, EVs are defined by their cellular origin. Since traditional EV purification methods co-isolate different subtypes of EVs, the general term EVs should be used when the intracellular origin of the vesicles has not been determined, and functional activity should be attributed to the general vesicle population and not to a single subtype of vesicle.

1.5.1 EV Biogenesis

Multiple mechanisms have been proposed as essential for EV biogenesis and release. Although both exosomes and plasma membrane-derived EVs have been described for approximately the same amount of time in the literature, much more is known about the formation of exosomes and the topic has been extensively reviewed recently [240, 241]. In all cases, it's likely that a number of key events must take place for EV formation to occur. Notably, mechanisms that regulate lipid curvature are essential for budding and release of EVs from membranes. In addition, the proteins and other cellular components that are loaded into EVs appear to be regulated, at least at a certain level. In the case of an infection, signals that regulate EV formation, either by increasing or reducing EV biogenesis and release, are also important to consider. In the case of exosomes, many of these pathways have been described, while release of membrane-derived EVs is less well understood.

Endocytic compartments are highly dynamic and regulate the internalization and subsequent degradation and/or recycling of transmembrane proteins, such as receptor-ligand

complexes, within cells. As endosomes mature to late endosomes, they accumulate intraluminal vesicles (ILVs) that are formed as a result of the inward budding of the endosome membrane and form MVBs [242]. Fusion of the MVB with the plasma membrane releases these ILVs as exosomes. Alternatively, MVBs may fuse with the lysosome, leading to the degradation of the ILVs and their components. Both endosomal sorting complex required for transport (ESCRT)-dependent and ESCRT-independent mechanisms of ILV formation and thus, exosome biogenesis have been described [243-245]. ESCRT proteins also play an important role in plasma membrane-derived EV release [236], and ESCRT-independent pathways are also beginning to be described for membrane-derived EV release [240, 241]. In addition, Rab proteins are regulators of vesicular transport between endocytic compartments and the plasma membrane within cells. Thus, Rab proteins play an essential role in the decision in whether MVBs are directed to the plasma membrane or lysosome, and thus, exosome release. Rab proteins implicated in controlling exosome release include Rab11a, Rab27a, Rab27b and Rab35 [246-248].

Although many mechanisms have been implicated in EV biogenesis and release, a complete understanding of EV formation still has been elusive and it appears that the mechanisms thus far described for EV biogenesis may be cell type specific. For example, exosome release was reduced from MCF7 breast cancer cells following ALIX (an ESCRT-associated protein) depletion but not in HeLa cells [243, 249]. Moreover, knockdown of some ESCRT components but not others decreases exosome release from cells [243]. The same observation has been made when Rab proteins have been examined in EV biogenesis [247]. Another paradox of the field is that complete inhibition of EV release from cells is never observed in studies when only single (ESCRT -dependent or -independent) pathways are inhibited [216, 250]. This suggests that the mechanisms of EV formation are not independent and

there is likely overlap in the previously described mechanisms of EV release, and that compensatory mechanisms likely exist. Because cellular physiology is altered during the course of infections, generally as a result of the pathogen actively manipulating host processes, further studies are needed to examine EVs are formed before we can fully understand the importance of EVs in the context of an infection and whether EVs are more beneficial to the host or the pathogen.

1.5.2 The Role of EVs in Virus Infections

EVs share many functional and structural features with viruses that make them extremely difficult to separate from viruses, including: (i) the size of the majority of EVs is about the size of many RNA viruses (<300 nm), (ii) EVs have a similar buoyant density to some RNA viruses, (iii) at least in the case of enveloped viruses, both EVs and viruses contain protein and RNA enclosed by a lipid bilayer, (iv) EVs and viruses form at the plasma membrane or at endocytic compartments, (v) EVs can bind to receptors on recipient cells and enter via endocytosis, (vi) EVs can also fuse with recipient cells, and (vii) EVs can deliver genetic material and other functional molecules that can change the physiology of recipient cells [217, 226]. It is likely that a population of diverse vesicles are released by cells during a virus infection, and that in the absence of techniques that sufficiently separate these vesicles, phenotypes assigned to EVs should be attributed to the overall population and not a specific subset of vesicles [226]. Because of the similarities outlined above, current techniques make it difficult to separate EVs consisting entirely of host cell components, on one extreme, from EVs that carry viral proteins or genomic elements but do not consist of all the virus-specific molecules required for infectivity on the other extreme [226]. This is different for nonenveloped viruses because they can be separated

from EV-enclosed virions and EVs with neutralizing antibodies, but it is likely that a heterogeneous population of EVs is still released by cells infected with noneveloped viruses. The release of EVs by virus-infected cells has been reported to play various roles in the pathogenesis of viral infections that can be categorized as either pro- or antiviral. It is currently unknown if the functions described for EVs produced during virus infection can be attributed to any single subpopulation of EV within the total EV population. Rather, it is likely that the functional characteristics reported thus far in the literature are the net effects of the total EV population.

1.5.2.1 EV Facilitation of Viral Infection

Numerous mechanisms have been described whereby EVs contribute to viral infection, but the potential pro-viral effects of EVs can be broadly broken into two categories: (i) host evasion or (ii) expansion of viral tropism.

EVs isolated from cells infected with hepatitis C virus (HCV) replicons that do not produce structural viral proteins have been shown to contain HCV RNA [251]. In these studies, it was demonstrated that HCV RNA is transferred in EVs to naïve cells, where a new infection was induced [251, 252]. Because HCV RNA was spread to uninfected cells in these studies and was partially resistant to neutralizing antibodies [251-254], it strongly suggests that HCV spread in EVs is an immune evasion strategy utilized by the virus that promotes viral spread. This is likely a common mechanism by which viruses evade immune recognition and antibody neutralization, as others have found that hepatitis A virus (HAV), coxsackievirus B, poliovirus, and enterovirus 71 (EV71) are also released in EVs [107-109, 250]. Notably, it has been found that enteroviruses are released in phosphatidylserine (PS)-positive EVs originating from the autophagosome [107]. PS lipids are well known to be anti-inflammatory and inhibit the production of pro-inflammatory cytokine production in macrophages [255, 256]. As a

consequence, it has been proposed that PS-positive vesicles containing virus may actively attenuate the immune response in macrophages [257]. In addition, viral proteins can be packaged into EVs and transferred to uninfected immune cells, where the proteins can modulate the host immune responses to virus [217].

Besides promoting the spread of virus by protecting viral genomes from immune recognition during transmission from an infected cell to an uninfected cell, the packaging of viral RNA into EVs may have other biological implications. For example, the packaging of viral RNA into EVs may help expand viral tropism and induce viral infection in tissues that would otherwise not normally be infected by free virus particles. This was recently demonstrated with EV71. Mice were injected with either free-EV71 virions or EVs containing EV71 RNA (EV-EV71) [250]. The mice that were injected with free EV71 had increased accumulation of viral RNA in the brain and intestines, whereas EV71 RNA was significantly more enriched in the liver and spleen of animals injected with EV-EV71 [250]. Moreover, EV-EV71 promoted the infection in a receptor-independent manner, since EV-EV71 could induce a productive infection in a non-permissive cell line that lacked the EV71 receptor [250]. Taken together, these observations demonstrate that the accumulation of viral RNA in tissues, and hence overall viral tropism, may be expanded when viral RNA is packaged in EVs. While this might suggest that viral association with EVs reduces the necessity of viral receptors on host cells for infection, this may not always be true and instead may be specific for the subpopulation of EV that is hijacked. For example, PS-positive EVs containing poliovirus were highly infective when added to naïve cells [107]. However, infection could be inhibited by either addition of a CD155 (poliovirus receptor) neutralizing antibody or by masking the PS lipids with Annexin V prior to infection

[107]. In the case of EV71, the authors' data suggested that exosomes and not PS-positive EVs were the hijacked vesicle subpopulation [250].

Despite extensive studies on the role of EVs during viral infections, very little is known about the composition and function of EVs to respiratory viral infections. Recently, rhinovirus infection was shown to alter the microRNA profile of EVs isolated from the nasal secretions of patients [258]. Analysis of the RSV secretome revealed that approximately one third of the total proteins secreted from AECs during RSV infection were secreted on EVs [259]. The functional consequences of respiratory viral infection on EVs released from AECs is still poorly defined. However, it is likely that many of the pro- and antiviral functions previously described for EVs will be broadly applicable to EV biology during respiratory viral infection.

1.5.2.2 Suppression of Viral Infection by EVs

As previously discussed, studies have shown that HCV RNA can be transferred from infected to uninfected cells via EVs [251]. However, the presence of viral genomes in EVs likely represents a double-edged sword that, while beneficial to the virus and viral spread, also has been shown to prime the immune system to viral infection. For example, it has been shown that EVs can shuttle HCV RNA between neighboring cells that triggers IFN-α production in neighboring dendritic cells (DCs) [260]. Importantly, the authors observed similar results using subgenomic replicon cells that replicate HCV RNA but do not produce infectious virus particles [260]. The presence of viral RNAs in EVs has also been reported to stimulate the innate immune response in uninfected cells for infections with other viruses, including Epstein-Barr virus (EBV), human immunodeficiency virus (HIV), and hepatitis B virus (HBV) [261-263]. For example, EVs released by HBV-infected hepatocytes induced NKG2D ligand expression in macrophages [263]. NKG2D is an immunoreceptor found on NK cells, and ligation of the receptor by NKG2D

ligands, including those expressed on macrophages, are known to activate NK cells and induce NK cell-mediated IFN-γ production, which mediates antiviral immunity [264, 265]. Studies also suggest that EVs prime the innate immune response to viral infection by other mechanisms that do not require transferring viral RNA between cells. Virus-resistant cells have been shown to produce EVs containing host miRNA. Delivery of the vesicle-associated miRNAs conferred viral resistance to recipient cells, making them resistant to a number of viral infections [266]. In addition, it was demonstrated that EVs produced by macrophages treated with type I IFN contained antiviral molecules that were transferred to hepatocytes and restricted subsequent HBV infection in these cells [216]. These studies imply that antiviral immunity can be transferred between cells by two distinct mechanisms: (i) soluble proteins (i.e. IFNs) that rely on receptor-mediated signaling to establish an antiviral state within cells, and (ii) the intercellular transfer of antiviral molecules to recipient cells via EVs.

1.5.3 The Role of EVs in Bacterial Infections

The role of host-derived EVs in bacterial infections is less well understood than with other infections. Still, it is now beginning to be appreciated that bacterial infection influences the content and function of EVs produced by the host. Although the majority of these studies have specifically focused on how mycobacterial infection alters the physiology of EVs produced by infected cells, new studies have shown that many similar concepts likely apply to the role of EVs in other bacterial infections.

1.5.3.1 Compositional and Functional Differences of EVs Isolated during Mycobacterial Infections

Host-derived EVs have the potential to transfer bacterial proteins between mammalian cells, much like EVs-derived from virally infected cells. For example, during *Mycobacterium tuberculosis* infection, mycobacterial lipids and proteins are released from the phagosome and traffic to late endosomes in macrophages, where they can be loaded on EVs and released into the extracellular environment [267, 268]. In addition, EVs isolated from the serum of tuberculosis patients were shown to contain mycobacterial proteins, and thus, likely play some role in the pathogenesis of *M. tuberculosis* [269]. In some cases, the transfer of bacterial components leads to the stimulation of certain immune responses. For example, EVs isolated from macrophages infected with *Mycobacterium bovis* contain the mycobacterial components lipoarabinomannan (LAM) and 19-kDa lipoprotein [270]. Moreover, EVs isolated from the bronchoalveolar lavage fluid (BALF) of mice infected with *M. bovis* also contained LAM and 19-kDa lipoprotein [270]. LAM and 19-kDa lipoprotein are components of the mycobacterial cell wall that are well known mycobacterial PAMPs, and consequently, have immunomodulatory functions [271-276]. For example, it has also been shown that uninfected macrophages secrete pro-inflammatory cytokines and chemokines in response to EVs isolated from *M. tuberculosis*-infected macrophages [277]. In addition, uninfected macrophages treated with EVs isolated from *M-tuberculosis*-infected macrophages *in vitro* or from BALF of infected mice induced a pro-inflammatory response in uninfected macrophages, measured by TNF-α production [270]. This response is primarily driven by the presence of 19-kDa lipoprotein, as extracellular vesicles isolated from macrophages infected with a knockout strain of *M. tuberculosis* that lacks 19-kDa lipoprotein fails to induce such responses [278].

Proteomic analysis has also identified many other mycobacterial proteins on EVs isolated from monocytes infected with *M. tuberculosis*, as well as changes in the composition of host proteins on EVs isolated from these infected monocytes [279, 280]. These changes may also play roles in the immune responses generated by EVs isolated from monocytes, but this has not yet been investigated. It is important to note that many of the EV purification methods will isolate both host-derived, as well as bacterial-derived membrane vesicles during bacterial infection. Hence, many of the observations that report changes in EV composition or function during bacterial infection could be the net result of a mixed population of host- and bacterial-derived EVs. In support of this hypothesis, it was recently shown that *M. tuberculosis*-infected macrophages release two distinct EV populations; one population contains host proteins classically used to identify EVs, while the other population contains *M. tuberculosis* molecules [281]. It was the vesicle population that contains molecules from the bacteria that elicit an immune response in uninfected macrophages [281], suggesting that bacterial-derived and not host-derived EVs transport mycobacterial proteins between cells to drive immune response in uninfected cells. However, it has been observed that EVs isolated from macrophages treated with *M. tuberculosis* culture filtrate proteins (CFP) contained mycobacterial proteins, namely 19-kDa lipoprotein, and induced a more predominate T_h1 response in mice treated with the EVs compared to BCG treated mice, as measured by flow cytometry [282]. This provided evidence that mycobacterial proteins can be loaded onto host-derived EVs, even in the absence of bacterial infection in the EV-producing cell, and that host-derived EVs can stimulate immune responses. Conversely, EVs isolated from *M. tuberculosis*-infected macrophages did not activate T_h1 $CD4^+$ T cells *in vitro* [283]. Because both host-derived and bacterial-derived EVs are released from *M. tuberculosis*-infected macrophages, these observations suggest that the bacterial-derived vesicles

contain molecules that that inhibit T cell responses. Taken together, these studies suggest that at least two distinct subpopulations of EVs are produced during *M. tuberculosis* infection, which promote disparate immune responses.

As has previously been described here, Rab27a may play an important role in EV biogenesis. Recently, it has been demonstrated that EVs isolated by *M. tuberculosis*-infected Rab27a-deficient macrophages produced less vesicles than wild type macrophages [284]. EVs isolated from Rab27a-deficient macrophages infected with *M. tuberculosis* induced a decreased pro-inflammatory response in uninfected cells compared to the response induced by EVs from wild type macrophages [284]. Ag85A has previously been identified on EVs produced by macrophages infected with *M. tuberculosis* [279]. Both Rab27a-deficient and wild type mice were infected with *M. bovis* expressing a DsRed-Ag85A conjugate and the number of DsRed-specific T cells were measured. Interestingly, T cells from Rab27a-deficient animals produced less INF-γ in response to *ex vivo* stimulation with DsRed compared to T cells from WT animals [284]. One interpretation of this result is that host-derived EVs are important for inducing a pro-inflammatory response and activating T cells during *M. tuberculosis* infection and that depletion of EVs impairs one mechanism by which antigens are presented to the immune system. However, in light of the other studies presented here, another possible interpretation of this observation is that the balance between pro-inflammatory host-derived EVs and immune-dampening bacterial vesicles has been skewed, and bacterial-derived EVs have a greater influence on the immune system than host-derived EVs. Whether this is the case is unknown, but further highlights a challenge of the field moving forward will be to discriminate between host- and bacterial-derived EVs. In the case of *M. tuberculosis* infection this could have important

implications, namely do variations in EV production and EV-mediated antigen presentation predict disease outcome (i.e. latent versus active disease).

1.5.3.2 The Role of EVs in Other Bacterial Infections

Host-derived EVs have been shown to also be secreted from cells during the course of infection by a number of other bacterial pathogens besides mycobacteria. For example, *Neisseria gonorrhoeae* increases the secretion of cIAP2 on EVs derived from endocervical epithelial cells [285]. cIAP2 is an inhibitor of apoptosis protein (IAP) with E3 ubiquitin ligase function that regulates apoptosis, necroptosis, and RIPK1 signaling [286, 287], and the importance of cIAP2 secretion on EVs has not been established. It is known that deletion of cIAP2 results in increased cell death in the context of both bacterial and viral infections [288, 289]. Because cIAP2 release on EVs corresponded to depletion of intracellular cIAp2 and cell death during *N. gonorrhoeae* infection, it has been speculated this is a host defense mechanism by which cells promote cell death during bacterial infection. However, this may also be a process co-opted by *N. gonorrhoeae* to transfer cIAP2 between cells to prevent highly inflammatory cell death during bacterial infection. Additionally, EVs isolated from *Legionella pneumophila*-infected macrophages stimulate a robust pro-inflammatory response in uninfected macrophages [290]. Interestingly, when host-derived EVs were depleted, either by blocking their release with neutral sphingomyelinase (SMase) inhibitor GW4869 or by depletion using CD63 immunoprecipitation, uninfected macrophages still responded to EVs [290]. Taken together, these results also suggest that host-derived and bacterial-derived EVs may contribute to the host response to bacterial infection, as was discussed during mycobacterial infection.

In the case of some bacterial infections, EVs released by host cells during the course of infection have not been shown to interact with the immune system, but have other roles that

contribute to bacterial pathogenesis. One example is the ability of EVs to transfer bacterial toxins between host cells. Anthrax lethal toxin is an A-B toxin and a virulence factor produced by *Bacillus anthracis*, composed of three protein subunits know as protective antigen (PA), lethal factor 9LF) and edema factor (EF). The PA subunit is involved in cell binding, while the other two protein subunits contain enzymatic activity of the toxin. LF is a protease that targets MAPK kinases [291]. It has been shown that PA is found on ILVs and interestingly, disruption of ILV formation via ALIX knockdown by RNA interference (RNAi) resulted in increased association of LF with endosomes and delayed cleavage of MAPK kinases in cells treated with PA and LF [292]. Because MAPK kinase cleavage is also dependent upon transport of LF to late endosomes, it was hypothesized that LF could be loaded into ILVs. This hypothesis was recently confirmed and extended to show that EVs released from host cells deliver LF into naïve cells [293]. In addition, it has been shown that EVs released from cells treated with *Clostridium perfringens* enterotoxin (CPE) or *S. aureus* α-toxin contain these toxins, but it was not observed that the toxins were transferred to mammalian cells [294, 295]. Importantly, all these studies were performed with purified toxin, in the absence of live bacteria, suggesting that the EVs being studied were purely host-derived. This excluded the possibility that toxin-loaded bacterial EVs "contaminated" the EV populations being investigated and therefore, did not contribute to the observations. Overall, the loading of bacterial toxins onto host-derived EVs could be a common phenomenon during bacterial infections, but further investigation will be required to understand the significance of this observation and whether this is beneficial to the bacterial infection or host.

1.5.4 Bacterial-Derived Outer Membrane Vesicles

Both Gram-negative and Gram-positive bacteria have been described to release vesicles into the extracellular environment [222, 223]. As discussed above, these bacterial-derived vesicles are potentially co-purified with host-derived EVs. Thus, further studies will be essential to determine the relative contribution of host EVs and bacterial EVs to many of the functions described above. Because these vesicles contain bioactive proteins, many of which are virulence factors, they have many functions that are critical to bacteria-bacteria and bacteria-host interactions. For example, OMVs produced by *P. aeruginosa* have been shown to contain many bacterial toxins, including CFTR inhibitory factor (Cif) [296]. Studies have shown that OMVs fuse with host cells, delivering Cif to the cytoplasm of host cells and induces the degradation of CFTR as well as TAP1 [173, 296, 297]. TAP1 plays a key role in antigen presentation, and therefore, degradation of TAP1 has important implications for adaptive immunity. It has been proposed that OMVs are a source of iron that can be utilized by bacteria for growth [298, 299], although it is unknown if OMVs produced by one bacterial species can be utilized by a second bacterial species. Additionally, data suggest that OMVs also contribute to bacterial defense by acting as decoys for antimicrobial peptides and bacteriophages, thereby promoting bacterial survival in the presence of potential antibacterial factors that target the outer membrane of Gram-negative bacteria [300]. Thus, OMVs and other bacterial-derived vesicles have many functions that affect host physiology and promote bacterial survival. Whether these vesicles will be useful for vaccines or other therapeutics because of the many potential antigens and PAMPs associated with them is an area that will require future investigation.

1.6 SUMMARY

Although our fundamental understanding of viral-bacterial interactions in the airways is rapidly increasing, there is still very little understood about the underlying mechanisms for the clinical observation that respiratory viral infections are associated with *P. aeruginosa* colonization in the CF lung. In this dissertation, I report that RSV infection stimulates *P. aeruginosa* biofilm growth through the release of iron and the host-iron binding protein transferrin. Iron levels are increased in the CF airway, and this is the first study to directly demonstrate that respiratory viral infection is one mechanism by which iron levels are increased in the CF lung. In addition, I extend these studies to show that EVs released by AECs during RSV infection promote *P. aeruginosa* biofilm formation, and that iron-loaded transferrin is bound to the outside of EVs were it may be utilized by *P. aeruginosa* as an iron source. Taken together, the findings in this dissertation have greatly improved our understanding of viral-bacterial co-infections in the respiratory tract, providing evidence that nutritional immunity is at the interface of viral-bacterial interactions in the airways, as well as increasing our understanding for how the host contributes to chronic bacterial infections in the lung.

2.0 MATERIALS AND METHODS

2.1 MATERIALS

2.1.1 Cell Culture and Reagents

The immortalized human CF bronchial epithelial cell line CFBE41o- (herein referred to as "CFBEs"), derived from a ΔF508 homozygous CF patient, were generously provided by Dr. J.P. Clancy (University of Cincinnati). CFBE cells were cultured in MEM (Thermo Fisher, Catalog number: 11095098) supplemented with 10% fetal bovine serum (FBS; Gemini Bio-Products, Catalog number: 100-106), 2 mM L-glutamine (Fisher Scientific, Catalog number: MT2500Cl) and 5 U/mL penicillin-5 μg/mL streptomycin (Sigma Aldrich, Catalog number: P0781) and 0.5 μg/mL Plasmocin prophylactic (InvivoGen, Catalog number: ant-mpp). Cells were seeded as monolayers onto transwell inserts with 0.4 μM pore size (Corning Life Sciences), coated with collagen and fibronectin, at the densities listed in Table 2 and grown at air-liquid interface (ALI) at 37°C and 5% CO_2 for 7-10 days to allow cell polarization before assays were performed. In all experiments where apical secretions (referred to as conditioned media) were collected, MEM was added to the apical compartment of CFBE41o- cells at the volumes indicated in Table 2.

Table 2: Properties of Transwell Inserts

Insert Diameter (mm)	Insert Membrane Growth Area (cm^2)	Density of CFBE41o- Seeded (cells/insert)	Volume Apical Compartment (mL)
6.5	0.33	7.5×10^4	0.1
12	1.12	2.5×10^5	0.5
24	4.67	1×10^6	1
75	44	4×10^6	5

In biotic biofilm imaging experiments, CFBEs were seeded onto 40 mm glass coverslips (Bioptechs) at a density of 3×10^6 cell per coverslip and cultured for 7-10 days prior to use.

Primary CF and non-CF human bronchial epithelial cells (HBEs) were obtained from the explanted lungs of CF and non-CF patients in accordance with protocols approved by the Institutional Review Board (IRB) of the University of Pittsburgh. Primary HBE cells were seeded on 6.5 mm transwell inserts with 0.4 μM pore size (Corning Life Sciences) at 2.5×10^5 cells per filter and cultured for 4-6 weeks at air-liquid interface at 37°C and 5% CO_2, prior to use to allow for differentiation.

2.1.2 Bacterial and Viral Strains

Pseudomonas aeruginosa strain PAO1 carrying the pSMC21 plasmid that constitutively expresses green fluorescent protein (GFP; kind gift from Dr. George O'Toole, Geisel School of Medicine at Dartmouth) was used for these studies.

The following viruses were studied: respiratory syncytial virus (RSV) line A2, human rhinovirus serotype 14 (hRV14), human adenovirus serotype 5 (Ad5) and human metapneumovirus subgroup A2 (hMPV). hRV14 and Ad5 were kind gifts from Dr. Carolyn

Coyne (University of Pittsburgh) and hMPV was generously provided by Dr. John Williams (University of Pittsburgh School of Medicine).

2.1.3 Quantitative Reverse Transcriptase PCR Primers

Primers used in qPCR assays were purchased from Sigma Aldrich and are listed in Table 3.

Table 3: qPCR Primers

Gene	Primer Sequence (5'-3')	
Adv5	Forward	CAG CGT AGC CCC GAT GTA A
	Reverse	TTT TTG AGC AGC ACC TTG CA
G3PDH	Forward	CGA CCA CTT TGT CAA GCT CA
	Reverse	AGG GGA GAT TCA GTG TGG TG
hRV14	Forward	GGC GCC ATA TCC AAT GGT GT
	Reverse	TCC ACC TGA TCG AAC GTC CA
IFN-β	Forward	GAG CTA CAA CTT GCT TGG ATT CC
	Reverse	CAA GCC TCC CAT TCA ATT GC
IFN-λ1	Forward	CGC CTT GGA AGA GTC ACT CA
	Reverse	GAA GCC TCA GGT CCC AAT TC
ISG56	Forward	TTC GGA GAA AGG CAT TAG A
	Reverse	TCC AGG GCT TCA TTC ATA T
RSV	Forward	GCT CTT AGC AAA GTC AAG TTG AAT GA
	Reverse	TGC TCC GTT GGA TGG TGT ATT

2.1.4 Antibodies

The primary antibodies used for western blot analysis are listed in Table 4. Secondary antibodies used included goat anti-mouse HRP conjugate (Bio-Rad, Catalog number: 172-1011), goat anti-rabbit HRP conjugate (Bio-Rad, Catalog number: 172-1019) and donkey anti-goat HRP conjugate.

Table 4: Primary Antibodies

Protein of Interest	Company	Catalog Number	Dilution
Actin	BD Biosciences	612656	1:500
Albumin (Mouse)	GeneTex	GTX77024	1:1000
ALIX	EMD Millipore	ABC40	1:500
Calnexin	Santa Cruz Biotechnology	sc-70481	1:100
CD81	Thermo Fisher	PA5-13582	1:250
DMT1	EMD Millipore	ABS983	1:500
Ezrin	BD Biosciences	610603	1:100
Ferritin	Abcam	ab75972	1:500
Ferroportin-1	EMD Millipore	ABS1021	1:500
Flotillin-1	BD Bioscience	610820	1:500
GM130	BD Biosciences	610822	1:100
Hsp90	Enzo Life Sciences	ADI-SPA-830	1:500
IL-28Rα	GeneTex	GTX46261	1:500
Lactoferrin	Santa Cruz Biotechnology	sc-25622	1:500
MHC Class I	LifeSpan Biosciences	LS-C107394	1:1000
RSV	Meridian Life Science, Inc.	B65840G	1:1000
Transferrin (Human)	Santa Cruz Biotechnology	sc-52256	1:250
Transferrin (Mouse)	GeneTex	GTX77131	1:500
Transferrin Receptor	BD Biosciences	612125	1:500

Tsg101	GeneTex	GTX70255	1:500

The antibodies used for immunoprecipitation experiments were: rabbit anti-transferrin (Abcam, Catalog number: ab1223) and rabbit anti-GFP (Santa Cruz Biotechnology, Catalog number: sc-8334).

2.1.5 Cytokines

Human IFN-β was acquired from PBL Assay Science (Catalog number: 11415-1). Human IFN-λ1 (IL-29) was purchased from R&D Systems (Catalog number: 1598-IL-25) and reconstituted in PBS containing carrier protein (0.1% BSA).

2.1.6 Small Interfering RNA (siRNA)

FlexiTube siRNA targeting IL-28Rα was acquired from Qiagen and MISSION siRNA universal negative control (negative control) was acquired from Sigma Aldrich. The siRNAs were used at a final concentration of 15 nM following dilution in HiPerfect transfection reagent (Qiagen, Catalog number: 301705) and 1x OptiMEM Reduced Serum Media + GlutaMAX supplement (Thermo Fisher, Catalog number: 51985034).

Table 5: Commercial siRNAs

Gene Symbol	Organism	Catalog Number
IL-28Rα	Human	SI03076521
Universal Negative Control	Human, Mouse, Rat	SIC001

2.2 METHODS

2.2.1 Virus Infections

For all virus infections, the apical and basolateral compartments of CFBE cells or primary CF and non-CF HBEs were washed in MEM supplemented with 2 mM L-glutamine two times. The media in the basolateral chamber of the transwell was replaced with MEM supplemented with 10% FBS and 2 mM L-glutamine (antibiotic-free growth media).

Stocks of RSV were prepared from and virus titers were determined by plaque assay on NY3.2 cells, an immortalized murine fibroblast cell line from $STAT1^{-/-}$ mice [301, 302]. For virus infection, CFBE or primary CF and non-CF HBE cells were inoculated with RSV [multiplicity of infection (MOI) of seeded cells = 1, unless otherwise noted] diluted in MEM, no phenol red (Thermo Fisher, Catalog number: 51200038), supplemented with 2 mM L-glutamine. Cells were placed at 37°C, 5% CO_2 for 2 hours before the apical media was removed and cells were maintained at ALI. Infections were allowed to proceed for 72 hours. After 72 hours monolayer integrity was compromised.

Stocks of Ad5 and hRV14 were obtained from Dr. Carolyn Coyne, where viruses where expanded and tittered in HeLa cells. For virus infections, CFBE cells were washed and inoculated with Ad5 (MOI=1) or hRV (MOI=1, unless otherwise noted) diluted in MEM supplemented with 2 mM L-glutamine. Virus was prebound to cells for 2 hours at 4°C and any unattached virus was washed away. Infections were allowed to proceed for 24 hours before cellular monolayers were disrupted.

Stocks of hMPV was acquired from Dr. John Williams, where stocks were prepared and tittered in LLC-MK2 cells [303]. For virus infections, CFBE cells were inoculated with hMPV (MOI=1) diluted in MEM supplemented with 2 mM L-glutamine. As with RSV, cells were placed at 37°C, 5% CO_2 for 2 hours before the apical media was removed and cells were cultured for 72 hours.

2.2.2 *Pseudomonas aeruginosa* Culture

For all bacterial infections, overnight cultures of *P. aeruginosa* were grown at 37°C in Lysogeny Broth (LB) with continuous agitation.

2.2.3 Biotic Biofilm Imaging

Live cell imaging was used as previously described to image bacterial biofilm growth on epithelial cells in the presence or absence of virus infection (**Figure 3**) [27, 304, 305]. Briefly, CFBE cells were seeded onto 40 mm glass coverslips (Bioptechs) as described in Section 2.1.1 and infected with RSV for 24 hours before epithelial cell nuclei were stained with Hoechst 33342 (Thermo Fisher, Catalog number: H3570). Immediately after Hoechst staining, cells were

transferred into a FCS2 closed system, live-cell micro-observation chamber (Bioptechs), assembled according to the manufacturer's instructions, and mounted on the stage of a Nikon Ti-inverted microscope (Figure 2.1). In this system, MEM (no phenol red) supplemented with 2 mM L-glutamine maintained at 37°C, 5% CO_2 is continuously perfused at a flow rate of 50 mL/hour across cells using a peristaltic pump, to simulate mucociliary movement in the airways. For bacterial infections, cells were infected with GFP expressing PAO1 (MOI=25, PAO1-GFP) via injection of PAO1-GFP into the chamber through a two-way valve. Bacteria were allowed to attach for 2 hours in the absence of media perfusion. Biofilms were then grown for 4 hours in the presence of perfusion. After a total of 6 hour PAO1-GFP infections, z-stack images of 6-10 random fields from each flow chamber were acquired and bacterial biofilm biomass was quantified using COMSTAT image analysis software, as described previously [305].

For attachment assays, *P. aeruginosa* attachment on CFBE cells was imaged after 1 hour of bacterial infection with PAO1-GFP in the absence of perfusion. Bacterial counts were normalized to the number of epithelial cells per field by counting cell nuclei.

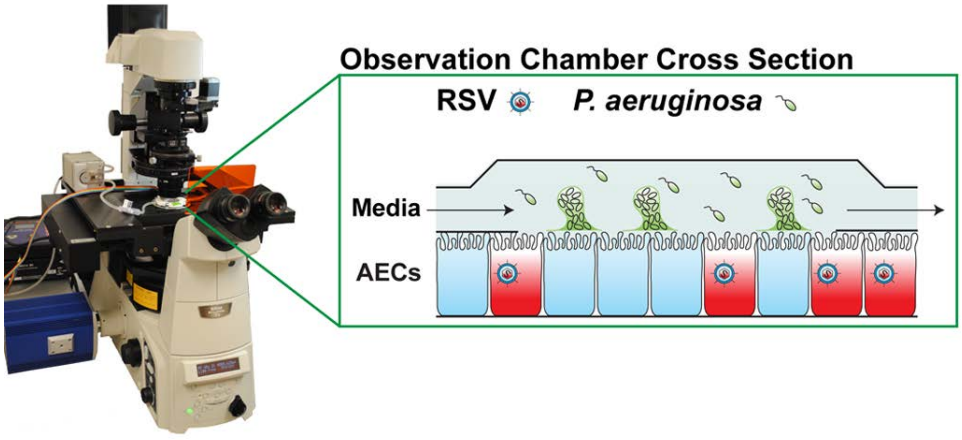

Figure 3: The setup for live-cell biotic biofilm imaging.

A FCS2 closed system, live-cell micro-observation chamber is placed on the stage of a Nikon Ti-inverted microscope. Enlargement: Cross-sectional view of the micro-observation chamber indicating the location of airway epithelial cells (AECs) in relation to PAO1-GFP biofilm growth and media perfusion within chamber.

2.2.4 Static Co-culture Biotic Biofilm Assay

For static co-culture biotic biofilm infection experiments, CFBE or primary CF and non-CF cells were infected with viruses as described in Section 2.2.1. Overnight cultures of *P. aeruginosa* were washed twice in MEM supplemented with 2 mM L-glutamine and the optical density at 600 nm (OD_{600}) was measured using a SpectraMax M2 Microplate Reader (Molecular Devices) and normalized to OD_{600} = 0.5 in MEM supplemented with 2 mM L-glutamine. For bacterial infections, cells were inoculated with OD_{600} normalized *P. aeruginosa* diluted in MEM supplemented with 2 mM L-glutamine. The total volume of media added to the apical compartment of cells is listed in Table 2 and the volume of OD_{600} normalized *P. aeruginosa* is listed in Table 6 for different transwell insert sizes used. These inoculation volumes correspond to a MOI of 25 on the respective transwell insert sizes. Bacteria were allowed to attach for 1

hour, after which unattached bacteria were removed and the apical media was replaced with MEM supplemented with 2 mM L-glutamine and 0.4% L-arginine. Biofilms were then grown for an additional 5 hours. After a total of 6 hour *P. aeruginosa* infections, apical media was discarded and cells were washed twice with MEM supplemented with 2 mM L-glutamine to remove unattached bacteria. Biofilms were disrupted and collected in MEM supplemented with 2 mM L-glutamine and 0.1% Trition X-100 (Bio-Rad, Catalog number: 1610407). Colony-forming units (CFU) were determined by plating serial dilutions of bacteria on LB agar plates. The plating was carried out by plating 10 μL aliquots of these dilutions using the track-dilution method [306, 307]. These plates were incubated overnight at 37°C and then counted. CFU counts were divided by insert membrane growth area listed in Table 2 to normalize bacterial counts between transwell insert.

Table 6: Properties of Transwell Inserts for Static Co-culture Biotic Biofilm Assays

Insert Diameter (mm)	Density of CFBE41o- Seeded (cells/insert)	Volume of OD_{600} Normalized (OD_{600} = 0.5) *P. aeruginosa* Used (μL)
6.5	7.5×10^4	2
12	2.5×10^5	7
24	1×10^6	28

2.2.5 Conditioned Media Collection

CFBE or primary CF and non-CF cells were infected with RSV as described in Section 2.2.1. At 48 hours post-infection (hpi), MEM (no phenol red) supplemented with 2 mM L-gluatamine

were added to the apical compartment for the final 24 hours of virus infection to collect apical secretions from cells. The volume of MEM added to the apical compartment is listed in Table 2. At the end of 72 hour virus infection, apical airway surface liquid [herein referred to as "condition media" (CM)] was collected and centrifuged at 1,400 x g for 3 minutes to remove cell debris.

2.2.6 Extracellular Vesicle Isolation

For experiments with extracellular vesicles, CFBE cells were seeded onto 75 mm transwell inserts at a density of 4 x 10^6 cells/insert and infected with viruses as described in Section 2.2.1 and cultured in MEM supplemented with 10% exosome-depleted FBS (Systems Biosciences, Catalog number: EXO-FBS-250A-1) and 2 mM L-glutamine added to the basolateral compartment of the transwell insert. Extracellular vesicles were isolated from conditioned media of CFBE cells using differential ultracentrifugation, as described previously (Figure 4) [308-311]. Briefly, CM collected from CFBE cells was centrifuged at 1,400 x g for 3 minutes to pellet cells. Supernatants were centrifuged at 10,000 x g for 30 minutes, transferred to new tubes and filtered through syringe filter unit, 0.22 μm pore size (Millipore, Catalog number: SLGV033RS). The filtrate was centrifuged for 90 minutes at 100,000 x g in a Optima L-90k Ultracentrifuge with a SW-60Ti rotor (Beckman Coulter). All pellets were resuspended in 1 mL MEM, no phenol red, supplemented with 2 mM L-glutamine.

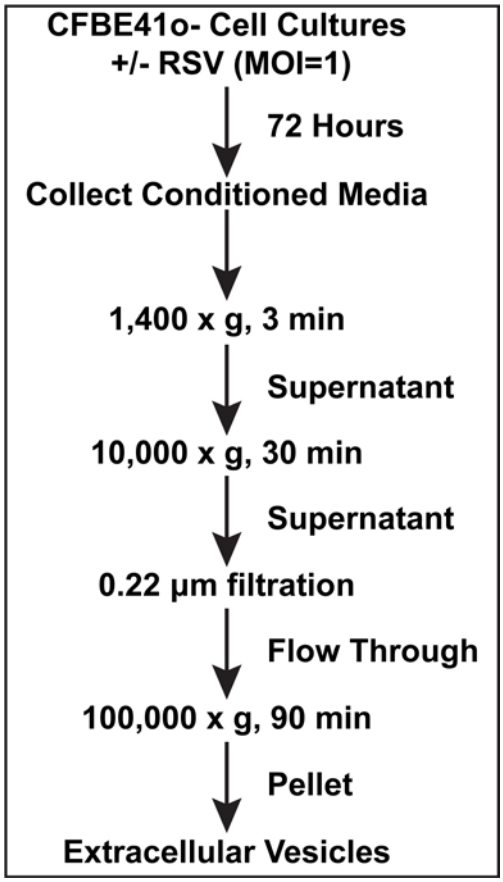

Figure 4: Flow chart for extracellular vesicle isolation from CFBE cells.

The length and speed of each centrifuge spin are indicated. Pellets from the first spins are discarded and the supernatants are kept for the next step. In the last spin, supernatants are discarded and pellets are kept.

2.2.7 Static Abiotic Biofilm Assay

For static abiotic biofilm assays, CM or extracellular vesicles were isolated as described in the sections 2.2.4 and 2.2.5. Overnight cultures of *P. aeruginosa* expressing GFP (PAO1-GFP) were washed twice in MEM supplemented with 2 mM L-glutamine and the optical density at 600 nm (OD_{600}) was measured using a SpectraMax M2 Microplate Reader (Molecular Devices). Cultures were normalized to OD_{600} = 0.5 and added to CM or extracellular vesicles supplemented with

0.4% L-arginine in a volume of 7 μL. Biofilms were grown for 6 hours on 35 mm uncoated glass-bottom dishes (MatTek Corporation, Catalog number: P35G-1.0-14-C) at 37°C, 5% CO_2. After 6 h hours, biofilms were fixed in 2.5% glutaraldehyde overnight at 4°C and washed one time in phosphate buffered saline (PBS) the next morning. Z-stacks images of at least 10 random images were taken for each dish using a Nikon Ti-inverted microscope. Nikon Elements Imaging Software version 4.11 was used to measure biofilm volume and substratum area. Biofilm biomass was calculated as the biofilm volume divided by substratum area.

For attachment assays in static conditions, *P. aeruginosa* attachment on glass was imaged 1 hour following the addition of OD_{600} normalized PAO1-GFP to extracellular vesicles in glass-bottom dishes. Bacterial counts were measured using Nikon Elements Imaging Software version 4.11.

2.2.8 96-Well Microtiter Biofilm Assay

Biofilm growth on plastic microtiter dishes was performed as previously described [312, 313], with minor modifications. Briefly, biofilms were grown in 96-well round bottom plates (Corning, Catalog number: 2797) after the addition of approximately 10^8 CFU *P. aeruginosa* into the indicated growth conditions for 24 hours at 37°C, 5% CO_2. Biofilm growth was quantified by crystal violet staining as measured by absorbance at 550 nm. Absorbance readings were measured by a SpectraMax M2 Microplate Reader (Molecular Devices).

2.2.9 IFN Treatment

Cells were washed twice with MEM supplemented with 2 mM L-glutamine. IFN-β or IFN-λ were diluted in MEM supplemented with 2 mM L-glutamine to a final concentration of 1000 U/mL or 100 ng/mL, respectively. Unless otherwise specified, IFN-β was added to the basolateral compartment of cells for 18 hours and IFN-λ was added to the apical compartment of cells for 12 hours.

2.2.10 mRNA Extraction and qPCR

Total RNA from cells was extracted using the RNeasy Mini Kit (Qiagen), according to the manufacturer's instructions. RNA concentration was measured using a nanodrop. Complementary DNA (cDNA) synthesis was performed with iScript cDNA Synthesis Kit (Bio-Rad). Gene expression was evaluated using quantitative real-time PCR (qPCR) with iQ SYBR Green Supermix (Bio-Rad). PCR reactions were performed on a StepOne Real-Time PCR System (ThermoFisher). The abundance of mRNAs of interest (Primers listed in Table 3) were normalized to GAPDH.

2.2.11 ELISA

To measure apical secretion of IFN-β and IFN-λ, CM was collected from CFBE cells infected with RSV as outlined in Section 2.2.5 and frozen at -80°C until analyzed. IFN-β and IFN-λ (IL-29/IL-28B) concentrations were measured using the Human IFN-β ELISA Kit (R&D Systems,

Catalog number: 41410-1) and Human IL-29/IL-28B DuoSet ELISA Kit (R&D Systems, Catalog number: DY1598B), according to the manufacturer's instructions.

2.2.12 Western Blot Analysis (Immunoblot)

Total protein concentration of all samples was determined using the Pierce 660 nm Protein Assay Kit (Thermo Fisher, Catalog number: 22662). Equal amounts of protein were loaded for analysis on Mini-PROTEAN TGX Precast Gels (Bio-Rad). Protein was transferred onto PVDF membranes using a Trans-Blot Turbo Transfer System (Bio-Rad, Catalog number: 1704150) and Trans-Blot Turbo PVDF Transfer Packs (Bio-Rad, Catalog number: 1704157). Antibodies used are listed in Table 3. Antibodies were diluted in PBS supplemented with 0.1% bovine serum albumin Fraction V (ThermoFisher, Catalog number: 15260037) at the concentration indicated in Table 3. Western Lightning ECL Pro (PerkinElmer, Catalog number: NEL122001EA) was used to develop blots. ImageJ software was used for densitometry on scanned blots.

2.2.13 siRNA Transfection

FlexiTube siRNA targeting IL-28Rα was used to selectively reduce protein expression of IL-28Rα, by methods described previously [297]. Briefly, MISSION siRNA universal negative control served as negative control for siRNA experiments. For siRNA transfection, CFBE cells were seeded on 24 mm transwell inserts at a density of 1 x 10^5 cells/insert. On day 3, post-seeding, cells were transfected with 15 nM siRNAs using HiPerfect transfection reagent (Qiagen), according to the manufacturer's protocol. 1x OptiMEM Reduced Serum Media + GlutaMAX supplement was used as culture media during transfections. After 24 hours, apical

and basolateral media were removed and cells were cultured at ALI at 37°C and 5% CO_2 in MEM supplemented with 10% FBS, 2 mM L-glutamine, 5 U/mL penicillin-5 μg/mL streptomycin and 0.5 μg/mL Plasmocin prophylactic. Cells were treated with IFN-λ for biofilm assays 4 days after transfection. The efficiency of IL-28Rα knockdown was assessed by western blot analysis.

2.2.14 Divalent Metal Analysis

To measure release of divalent metals in CM during 72 hour RSV infection of CFBE or primary CF and non-CF cells, MEM (no phenol red) supplemented with 2 mM L-gluatamine was added to the apical compartment at the beginning of virus infection and removed 72 hpi. Extracellular vesicles were isolated as outlined in section 2.2.5. Total amounts of copper, iron and zinc were measured using the QuantiChrom Copper Assay Kit (BioAssay Systems, Catalog number: DICU-250), QuantiChrom Iron Assay Kit (BioAssay Systems, Catalog number: DIFE-250) and QuantiChrom Zinc Assay Kit (BioAssay Systems, Catalog number: DIZN-250), respectively.

2.2.15 Immunoprecipitation

For transferrin depletion experiments, transferrin was immunoprecipitated from CM or extracellular vesicles. 5 μg Rabbit anti-human transferrin or rabbit anti-GFP was bound directly to 50 μL Protein G Agarose Beads (Thermo Fisher, Catalog number: 20398) overnight at 4°C. CM or extracellular vesicles was incubated with antibody-Protein G complexes for 2 hours at 4°C with continuous rotation. Supernatants were collected and used directly in static abiotic

biofilm assays. Transferrin abundance bound to antibody-Protein G complexes and in supernatants was analyzed by western blot analysis.

2.2.16 Plaque Assays

Viral titers were determined by plaque assay on NY3.2 cells, as described previously [301, 302], with minor modifications. Briefly, NY3.2 cells were seeded in 24-well polystyrene tissue culture plates (Fisher Scientific, Catalog number: 08-772-1) at a density of 4 x 10^5 cells per well. To measure release of infectious viral particles from CFBE cells, CM or extracellular vesicles were collected as described in Section 2.2.5 and Section 2.2.6, respectively, and serially diluted in DMEM + GlutaMAX (Thermo Fisher, Catalog number: 10567-014) supplemented with 1% FBS and 25 mM HEPES acid. Serial dilutions were added to plated NY3.2 cells and incubated for 2 hours at 37°C, 5% CO_2, after which cells were overlaid with Methyl Cellulose-Polyethylene Glycol solution for 48 hours. Goat anti-RSV antibody (Meridian Life Science, Catalog number: B6580G), donkey anti-goat alkaline phosphatase conjugated antibody (Santa Cruz Biotechnology, Catalong number: 2355) and SigmaFast BCIP/NBT tablets (Sigma Aldrich, Catalog number: B5655) were used to detect plaque forming units (PFU).

2.2.17 Bacterial Growth Curves

Extracellular vesicles were isolated from CFBE cells as outline in Section 2.2.6. Overnight cultures of *P. aeruginosa* were washed twice in MEM supplemented with 2 mM L-glutamine and the optical density at 600 nm (OD_{600}) was measured using a SpectraMax M2 Microplate Reader (Molecular Devices). Washed bacteria were added to extracellular vesicles to a final

concentration of OD_{600} = 0.05 and added to 96-well polystyrene tissue culture plates (Fisher Scientific, Catalog number: 08-772-1), covered with breathable optically clear seal (Sigma Aldrich, Catalog number: Z380059). Plates were placed in SpectraMax M2 Microplate Reader, prewarmed to 37°C, and OD_{600} was measured every 20 minutes.

2.2.18 Transferrin Transcytosis

Transferrin transcytosis was assessed as described previously with minor modifications [203, 314]. Briefly, CFBE were infected with RSV for 48 hours as described in Section 2.2.1. After this time, the media in the transwell basolateral chamber was replaced with antibiotic-free growth media supplemented with 25 μg/mL transferrin biotin-XX-conjugate (Thermo Fisher, Catalog number: T23363). MEM (no phenol red) supplemented with 2 mM L-gluatamine was added to the apical compartment to collect apical secretions from cells. After 24 hour incubation at 37°C, 5% CO_2, the media from the apical compartment was collected and centrifuged at 1,400 x g for 3 minutes. Supernatants were added to Streptavidin Agarose Resin (Thermo Fisher, Catalog number: 20349) and incubated overnight at 4°C with continuous rotation. Resin was washed twice in MEM supplemented with 2 mM L-glutamine, once in high salt solution (200 mM NaCl, 400 mM NaOAc, pH 7.4) and once more in MEM supplemented with 2 mM L-glutamine. Affinity-purified proteins were eluted by incubation at 95°C for 5 minutes in 2X Laemmli Sample Buffer supplemented with 0.1 M Dithiothreitol (DTT) and analyzed by western blot analysis for transferrin.

2.2.19 Extracellular Vesicle Association with *P. aeruginosa* Plate Reader Assay

AECs were infected with RSV as outlined in section 2.2.1. AECs were stained with CellTracker Deep Red (Thermo Fisher, Catalog number: C34565) 48 hpi, and extracellular vesicles were isolated from CFBE cells as outline in Section 2.2.6 24 hours later. Overnight cultures of *P. aeruginosa* were washed twice in MEM supplemented with 2 mM L-glutamine. The optical density at 600 nm (OD_{600}) was measured using a SpectraMax M2 Microplate Reader (Molecular Devices). Washed bacteria were added to extracellular vesicles to a final concentration of OD_{600} = 0.15 and grown at 37°C. At the indicated times, bacteria were washed twice in MEM supplemented with 2 mM L-glutamine. After final wash, bacteria were resuspended in 200 μL and CellTracker Deep Red fluorescence was measured using a SpectraMax M2 Microplate Reader [Molecular Devices); excitation: 630 nm, emission: 650 nm].

2.2.20 *In vivo* RSV Infection Model

For *in vivo* RSV infection studies, pathogen-free breeder BALB/cJ mice were purchased from The Jackson Laboratory at 6-7 weeks of age. For the duration of breeding and pregnancy, mice were maintained in pathogen-free facilities at the University of Pittsburgh Division of Laboratory Animal Resources as described previously [315]. Animal protocols were carried out in accordance with the guidelines in the NIH Guide for the Care and Use of Laboratory Animals and approved by the University of Pittsburgh Institutional Animal Care and Use Committee (IACUC, Protocol number: 14023340).

The neonatal mice (pups) from the resulting pregnancies were intranasally inoculated with 5 x 10^5 PFU/gram of body weight with RSV line 19 (kindly provided by Dr. Martin Moore,

Emory University, Atlanta, GA) or PBS for negative controls. Stocks of RSV line 19 were propagated in HEp-2 cells and titred in HEp-2 cells, as described previously [315-317]. At the indicated time points, bronchoalveolar lavage fluid (BALF) was harvested for analysis by iron assay and western blot analysis for albumin and transferrin abundance or used in static abiotic biofilm assays. HBSS containing 3 mM EDTA was used to obtain BALF. Viral titers at the indicated time points were previously assessed by plaque assay [315].

For histological analysis, mice were infected with RSV line 19 and lungs were harvested 7 days post-infection, fixed in 4% paraformaldehyde and embedded in paraffin blocks. Tissues sections were stained with H&E, as described previously [315].

2.2.21 Statistics

GraphPad Prism Software version 6.0 was used for all statistical analysis. Means were compared using Student's t test, or for multiple comparisons, one-way analysis of variance (ANOVA) with Tukey's post hoc test to evaluate statistical significance. All data are shown as mean ± SD of biological replicates within individual experiments. $P < 0.05$ was considered statistically significant. All experiments were repeated a minimum of two times.

3.0 RESPIRATORY SYNCYTIAL VIRUS INFECTION ENHANCES *PSEUDOMONAS AERUGINOSA* BIOFILM GROWTH THROUGH DYSREGULATION OF NUTRITIONAL IMMUNITY

This chapter is adapted from the published manuscript:

Matthew R. Hendricks[a], Lauren P. Lashua[a], Douglas K. Fischer[a], Becca A. Flitter[a], Katherin M. Eichinger[b], Joan E. Durbin[c], Saumendra N. Sarkar[a,d], Carolyn B. Coyne[a], Kerry M. Empey[b], and Jennifer M. Bomberger[a]

Respiratory syncytial virus infection enhances *Pseudomonas aeruginosa* biofilm growth through dysregulation of nutritional immunity. *Proceedings of the National Academy of Sciences of the United States of America*, 2016. **113** (6): 1642-1647 (© 2016 National Academy of Sciences).

[a]Department of Microbiology and Molecular Genetics, University of Pittsburgh School of Medicine, Pittsburgh, PA 15219

[b]Department of Pharmacy and Therapeutics, University of Pittsburgh School of Pharmacy, Pittsburgh, PA 15261

[c]Department of Pathology and Laboratory Medicine, Rutgers-New Jersey Medical School, Newark, NJ 07101

[d]Cancer Virology Program, University of Pittsburgh Cancer Institute, University of Pittsburgh School of Medicine, Pittsburgh, PA 15213

Unless otherwise specified, all data presented in this chapter is published in the *Proceedings of the National Academy of Sciences of the United States of America*. Specific author contributions are listed in the figure legend. Figure 19B and C was not published in this article. Data for figure 19B and C was provided by Dr. Jeffrey A. Melvin, a post-doc in the Bomberger Lab, and is indicated in the figure legend.

3.1 INTRODUCTION

Viral-bacterial interactions impact the development and evolution of chronic infections at many mucosal surfaces, including in the airways [318-320]. In cystic fibrosis (CF) lung disease, viral infections are linked to pulmonary function decline, increased antibiotic use, prolonged hospitalizations and increased respiratory symptoms [78]. Respiratory syncytial virus (RSV) is one of the most common viral pathogens identified in CF patients and leads to disease progression, promoting early respiratory tract morbidity and reductions in lung function [54, 56, 71]. Beyond the morbidity associated with virus infection alone, RSV is one of the most common viral pathogens identified in cases of coinfection in CF. In clinical studies, RSV, and other respiratory viruses, have been linked to the development of *Pseudomonas aeruginosa* coinfections and to the conversion to chronic *P. aeruginosa* colonization in CF patients [51, 53, 71, 72, 321]. Although clinical associations between viral infection and the acquisition of *P. aeruginosa* is clear, the basic biology underlying this interaction is not well understood.

The transition of acute bacterial infections to chronic infections often involves the development of bacterial aggregates, or biofilms. The combination of an up-regulation of

antibiotic resistance genes and the production of a polymeric matrix surrounding the biofilm serves to protect bacteria from the hostile environment in the host [322]. The development of biofilm in human disease has been studied intensely for its involvement in disease progression in CF. Biofilm development at a mucosal surface requires initial attachment of bacteria to a surface, followed by the formation and growth of microcolonies, resulting in the development of bacterial biofilms, which can undergo regulated dispersal and ultimately seed new surfaces [32, 36]. Our present understanding of bacterial biofilm development is largely limited to single-organism infections. Although we have long known of polymicrobial communities colonizing human tissues, there is a surprising gap in our understanding of how these communities develop, how they impact human disease and hot how defense mechanisms influence the relationship between microorganisms in polymicrobial infections. Because our current antimicrobial approaches have limited success for chronic infections, elucidating the mechanism by which biofilms develop during polymicrobial infections may identify new therapeutic targets to combat biofilm persistence.

Many environmental cues have been described as contributing to the conversion of *P. aeruginosa* to biofilm mode of growth. For example, iron is known to be one such cue, as the lack of iron in the environment prevents the formation of *P. aeruginosa* biofilms [27, 37]. Nutrient iron is tightly regulated in the host through complex interactions among uptake, storage and use in host cells. Nutritional immunity postulates that, because iron is required for microbial growth, respiration and metabolism, the host employs many regulatory pathways to sequester iron [182, 187]. In CF, elevated levels of iron in the airways of infections patients are correlated with frequency of exacerbation and have been proposed to play a role in airway colonization [24, 323]. In addition, the sputum of CF patients contains elevated levels of ferrous iron, and these

levels correlate with disease severity [28]. Although increased iron in sputum is associated with CF lung disease severity, it is still unknown how iron homeostasis is altered in CF and how this alteration relates to airway infection (bacterial, fungal or viral).

Using CF lung disease as a model to understand viral-bacterial interactions at a mucosal surface, we use a co-culture system for bacterial biofilm development in association with the airway epithelium. In this study, we use RSV to demonstrate that virus coinfection dramatically enhanced *P. aeruginosa* biofilm growth in association with airway epithelial cells. In addition, we show that virus infection impairs nutritional immunity, allowing the apical release of transferrin and thus, increasing bioavailability of iron to promote the growth of *P. aeruginosa* biofilms. These findings offer new insight into the complex interaction among two pathogens and the host during polymicrobial infections, and suggest a mechanism by which nutritional immunity plays a critical role in regulating bacterial persistence in the airways.

3.2 RESULTS

3.2.1 Respiratory virus infections promote *P. aeruginosa* biofilm growth on airway epithelial cells

To determine if respiratory virus infections promote *P. aeruginosa* biofilm growth on airway epithelial cells (AECs), human ΔF508/ΔF508 cystic fibrosis bronchial epithelial cells (CFBE41o-, hereafter referred to as “AECs”) were grown as polarized monolayers and infected with RSV followed by infection with GFP-tagged *P. aeruginosa* (strain PAO1) in a flow chamber (**Figure 3**). Biofilm growth was then analyzed by live-cell microscopy, as described

previously [27, 305]. We observed that RSV coinfection significantly enhanced *P. aeruginosa* biofilm growth on the surface of AECs (**Figure 5A**). Surprisingly, RSV coinfection increased *P. aeruginosa* biofilm growth in a time-dependent manner, with maximal biofilm growth peaking at 72 hours post-RSV infection (**Figure 5B**), as measured in a static co-culture biofilm model [305]. We also found that RSV infection induced biofilm growth on primary CF bronchial epithelial (HBE) cells (**Figure 5C**) and increased biofilm growth of three CF clinical isolate strains of *P. aeruginosa* (**Figure 6**).

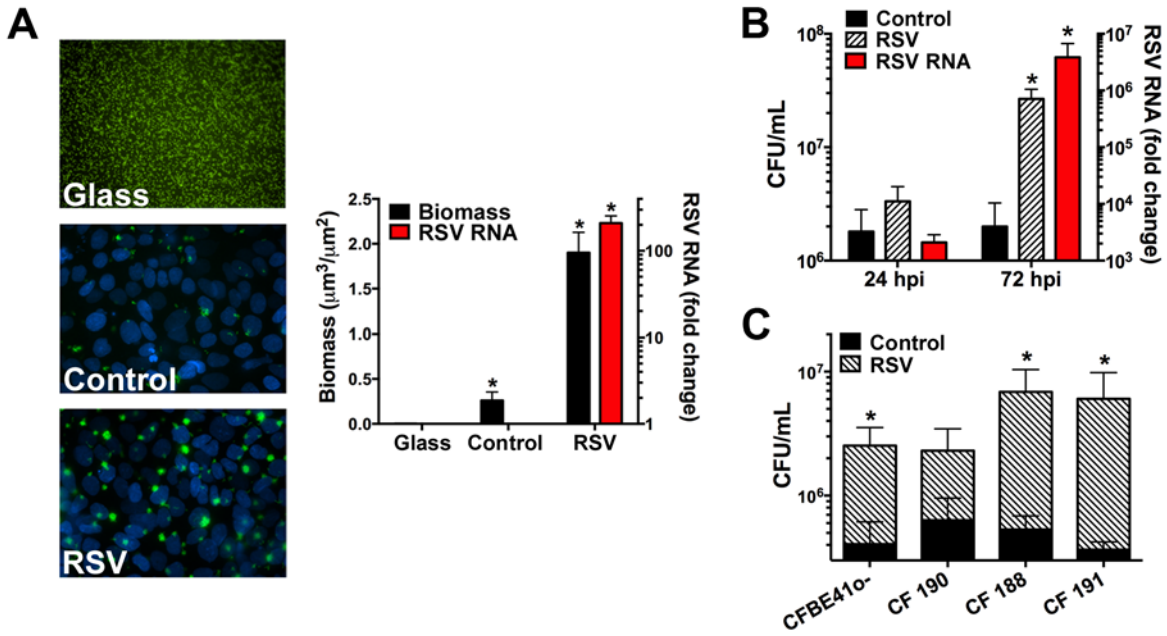

Figure 5: Respiratory viral infection promotes the growth of *P. aeruginosa* biofilm on AECs.

(A, *Left*) *P. aeruginosa* (GFP) biofilms imaged by live-cell microscopy after 6 hr of growth. AEC cell nuclei are shown with Hoechst (blue) staining. (*Right*) Biofilm biomass was quantified using COMSTAT (black bars, left y axis). RSV RNA was measured by quantitative RT-PCR (qRT-PCR) to assess RSV infection (red bar, right y axis). (B) RSV-enhanced biofilm growth is time dependent. In a static coculture biofilm assay, AECs were infected with RSV (striped bar) or were mock infected [Eagle's minimal essential media (MEM) control; black bars] for the indicated times followed by *P. aeruginosa* infection. *P. aeruginosa* biofilm was assessed by colony-forming units (CFU) enumeration (left y axis). RSV RNA was measured by qRT-PCR to assess RSV infection (red bars, right y axis). (C) RSV stimulates the growth of *P. aeruginosa* biofilm on well-differentiated CF HBEs. *P. aeruginosa* biofilms were grown on primary CF HBEs using the static coculture biofilm assay and were quantified by CFU enumeration. RSV, RSV-infected AECs. For all experiments n ≥ 3. Data are presented as mean ± SD; **P* < 0.05 versus control. Data provided by L.P.L., D.K.F., and J.M.B.

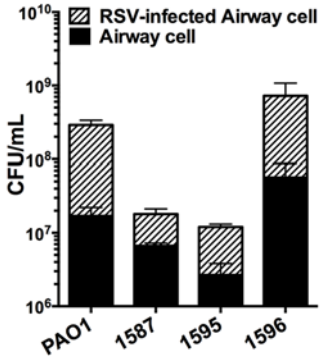

Figure 6: RSV-enhanced growth of *P. aeruginosa* biofilms with CF clinical isolates.

RSV infection promotes biofilm formation by CF P. aeruginosa clinical isolates in a static coculture biofilm assay. In a static coculture biofilm assay, AECs were infected with RSV (striped bars) or were mock-infected (MEM control; black bars) for 72 hr and then were infected with the indicated clinical isolates of P. aeruginosa. Biofilms were quantified by CFU enumeration. Data provided by L.P.L., D.K.F., and J.M.B.

Patients with other chronic lung diseases, such as chronic obstructive pulmonary disease (COPD), are also susceptible to both acute and persistent infections by *P. aeruginosa* [324]. This suggests that *P. aeruginosa* can form biofilms on AECs independent of the mutations in the cystic fibrosis transmembrane conductance regulator (CFTR) ion channel, which are the underlying cause of CF and CF lung disease [325]. In agreement with this hypothesis, we found that RSV infection increased *P. aeruginosa* biofilm growth on primary non-CF HBE cells in a static co-culture biofilm assay (**Figure 7**).

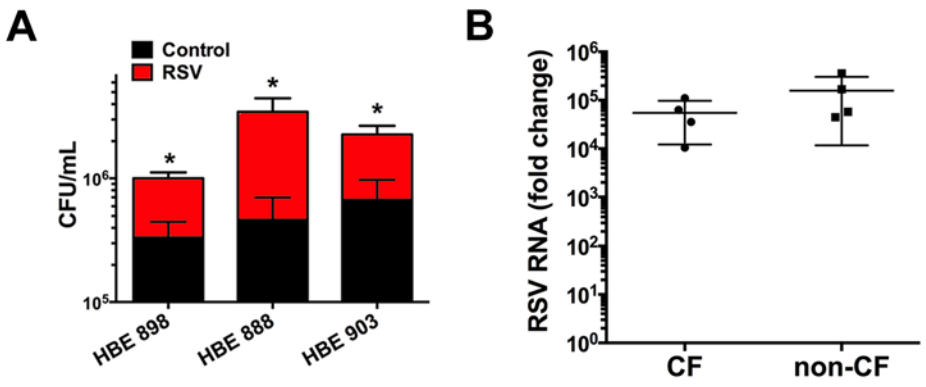

Figure 7: RSV enhances *P. aeruginosa* biofilm on well-differentiated non-CF HBEs.

(A) *P. aeruginosa* biofilms were grown on non-CF HBEs in a static coculture biofilm assay following 72 hr RSV infection and were quantified by CFU enumeration. (B) RSV RNA was measured by qRT-PCR to assess RSV infection, which is equivalent in CF and non-CF HBE cells. RSV, RSV-infected AECs. For all experiments n ≥ 3. Data are presented as mean ± SD; **P* < 0.05 versus control. Data provided by L.P.L., D.K.F., and J.M.B.

3.2.2 Stimulation of bacterial biofilm formation is induced by infection of AECs by disparate viruses

To examine whether virus-enhanced *P. aeruginosa* biofilm formation was specific for RSV coinfection, we infected AECs with human rhinovirus-14 (hRV14) or adenovirus-5 (Ad5), two additional respiratory viral pathogens commonly found in CF patients [78], before bacterial infection. Coinfection with hRV14 or Ad5 also increased the growth of *P. aeruginosa* biofilms on AECs in static co-culture biofilm assays (**Figure 8**). Taken together, these results indicate that several respiratory viruses relevant to CF lung disease can stimulate the growth of *P. aeruginosa* biofilms on AECs.

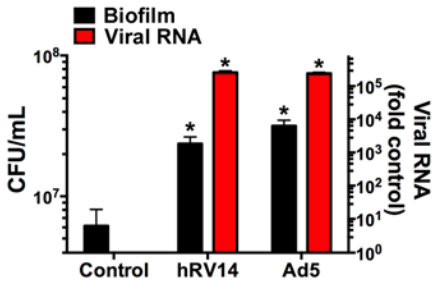

Figure 8: Other respiratory viruses enhance the growth of *P. aeruginosa* biofilm on AECs.

P. aeruginosa biofilms were grown in a static coculture biofilm assay on AECs infected with hRV or AdV or were mock-infected (MEM control). Biofilms were quantified by CFU enumeration (black bars, left y axis). Viral RNA was measured by qRT-PCR to assess virus infection (red bars, right y axis). hRV14, hRV14-infected AECs. Ad5, Ad5-infected AECs. For all experiments n ≥ 3. Data are presented as mean ± SD; **P* < 0.05 versus control. Data provided by L.P.L., D.K.F., and J.M.B.

3.2.3 Viral-stimulated bacterial biofilm formation is not caused by direct virus-*P. aeruginosa* interaction

Using an abiotic biofilm growth assay in a 96-well microtiter dish [312], we found no difference in biofilm formation in *P. aeruginosa* biofilms grown in the presence or absence of RSV (**Figure 9A**). In addition, although bacterial attachment was increased when cells were infected simultaneously with RSV and *P. aeruginosa* (**Figure 9B**), as has been shown previously reported [152], *P. aeruginosa* attachment was not increased on cells infected with RSV (for 72 hours) prior to bacterial infection (**Figure 9B**). Although we observed increased attachment of *P. aeruginosa* to AECs that were simultaneously infected with *P. aeruginosa* and RSV, biofilm growth was only moderately increased compared to *P. aeruginosa* biofilm formation on cells not infected with RSV (**Figure 9C**). Whereas, on cells infected with RSV prior to bacterial infection,

biofilm formation was greatly and much more robustly increased (**Figure 9C**). Moreover, biofilm growth on the apical surface of AECs infected with RFP-tagged RSV (RSV-RGP) showed a random distribution (**Figure 9D**, Person correlation coefficient of 0.072 +/- 0.021), demonstrating that biofilms did not specifically form on virus-infected cells.

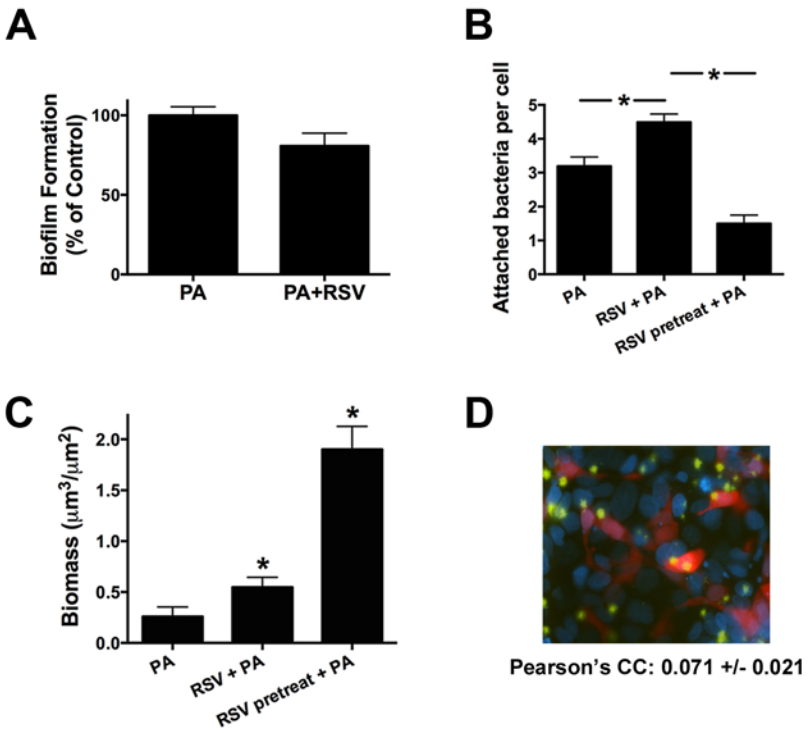

Figure 9: RSV-stimulated biofilm growth is not caused by direct viral-*P. aeruginosa* interaction.

(A) *P. aeruginosa* biofilms were grown in MEM ± RSV for 24 hr in the 96-well microtiter biofilm assay. Biofilms were quantified by crystal violet staining and were measured as absorbance at 550 nm. Biofilms growth is presented as the percentage of growth in MEM alone. (B) *P. aeruginosa* attachment is reduced on AECs with preceding RSV infection. AECs were infected with *P. aeruginosa* (PA), simultaneously with RSV and *P. aeruginosa* (RSV + PA), or with RSV before infection with *P. aeruginosa* (RSV pretreat + PA). *P. aeruginosa* (GFP) adherence on AECs was imaged by live-cell microscopy after 1 hr of bacterial infection. Bacterial counts were normalized to the number of epithelial cells per field by counting nuclei (10 fields were counted per treatment, repeated three times). (C) The growth of *P. aeruginosa* biofilm is enhanced only on AECs with preceding RSV infection. *P. aeruginosa* biofilms were imaged by live-cell microscopy after 6 hr of growth on AECs, and biofilm biomass was quantified by COMSTAT. AECs were infected and are labeled along the x axis as in B. (D) *P. aeruginosa* biofilms are randomly distributed on AECs infected with RSV. Cells were infected with RSV-RFP for 24 hr followed by PAO1-GFP infection, and biofilm growth (green) was imaged after 5 hr by live-cell microscopy. Hoechst (blue) staining shows

epithelial cell nuclei. For all experiments n ≥ 3. Data are presented as mean ± SD; *$P < 0.05$ versus control. Data provided by L.P.L., D.K.F., and J.M.B.

Previous studies have shown that viral infection can increase bacterial attachment by inducing damage to the respiratory epithelium, which increases bacterial access to basal cells and basement membrane [146, 147]. Although we did not observe increased adherence of bacteria to AECs infected with RSV for 72 hours prior to bacterial infection, this does raise an interesting point about whether viral infection increases cellular cytotoxicity. Previously, it has been described that RSV infection increases damage to bronchial epithelial cell cultures by increasing cell death and loss of cilia [112]. However, in our study, cytotoxicity was not detected during RSV infection, as measured by lactate dehydrogenase release (**Figure 10A**) and transepithelial electrical resistance, a measure of epithelial barrier integrity (**Figure 10B**). Together, these results suggest that RSV infection promotes the formation of *P. aeruginosa* biofilm growth on AECs via a mechanism independent of increased adherence of bacteria to cells.

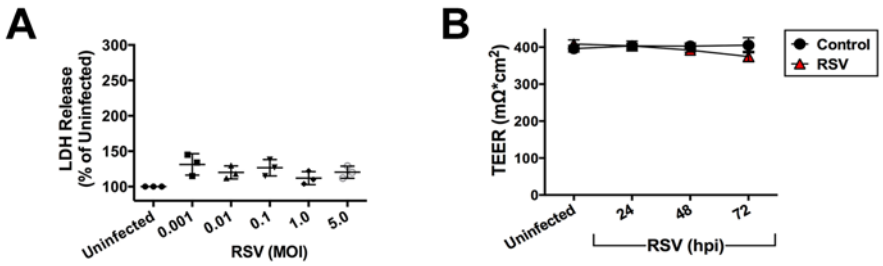

Figure 10: The AEC monolayer is intact during RSV infection.

(A) Epithelial integrity was assessed by the lactate dehydrogenase release assay at 72 hpi for various doses of RSV [Multiplicity of infection (MOI) = 0.001-5] Means are not significantly different from the uninfected control. (B) Transepithelial electrical resistance measurements were used to assess epithelial integrity over the course of 72-hr

RSV infection. AECs were infected with RSV (red triangles) or were mock-infected (MEM control, black circles) for the indicated times. Data provided by L.P.L. and J.M.B.

3.2.4 Antiviral IFN signaling increases the growth of *P. aeruginosa* biofilms on AECs

Host cells, including AECs, commonly respond to viral infections and establish an innate immune response against the virus through the inductions of antiviral IFNs. Because we observed enhanced biofilm growth by diverse respiratory viruses (**Figure 8**), we wanted to determine if the innate antiviral immune response to respiratory viral infection had a role in increased *P. aeruginosa* biofilm growth during respiratory virus infections. To do so, we first measured type I (IFN-β) and type III IFN (IFN-λ) production following RSV infection. We observed that IFN-β and IFN-λ levels in the apical airway surface liquid increased during the course of RSV infection, peaking at 72 hours post-RSV infection (**Figure 11**). Although both IFN-β and IFN-λ were produced by AECs in response to RSV infection, IFN-β was produced to a lesser extent than IFN-λ. This suggests a poor type I IFN response to RSV infection by AECs in our model, which is consistent with previous reports showing low type I IFN responses in other *in vitro* models of RSV infection, such as primary pediatric bronchial epithelium cell cultures and nasal epithelial cells [112, 113, 115]. Additionally, this reflects the low type I IFN levels measured in infants following RSV infection [114, 115, 326, 327]. Interestingly, *P. aeruginosa* biofilm growth also peaked at 72 hours post-respiratory viral infection (**Figure 5**), suggesting that a temporal association between IFN-β and IFN-λ production and increased *P. aeruginosa* biofilm development exists during respiratory viral infection.

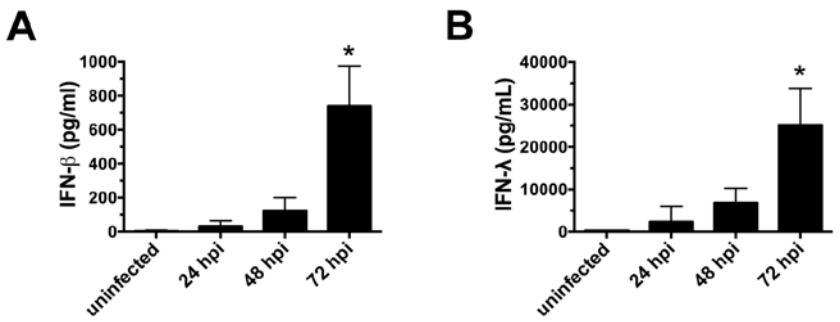

Figure 11: IFN-β and IFN-λ secretion from AECs during RSV infection.

Cells were infected with RSV for the indicated number of hours (hpi), and (A) IFN-β and (B) IFN-λ1/3 (IL-29/IL-28B) release was measured by ELISA. For all experiments n ≥ 3. Data are presented as mean ± SD; **P* < 0.05 versus control. ELISA measurements performed by B.A.F.

We next sought to determine if IFN signaling was sufficient to enhance *P. aeruginosa* biofilm growth in the absence of respiratory viral infection due to the temporal association between peak IFN production and *P. aeruginosa* biofilm formation during RSV infection. Due to the relatively robust IFN-λ response (compared to IFN-β) to RSV infection we and others have observed in AECs [112, 113, 115], we first focused on the role IFN-λ signaling may play in *P. aeruginosa* biofilm growth. Treatment of AECs with purified IFN-λ1 (IL-29, 100 ng/mL) increased the growth of *P. aeruginosa* biofilm on the surface of AECs in both our biotic biofilm imaging and static co-culture biotic biofilm assays (**Figure 12A-B**). We measured ISG56 expression to confirm that IFN-λ treatment led to increased ISG expression in AECs (**Figure 12B**). The IFN-λ receptor is a heterodimer composed of IL-28Rα and IL-10Rβ. To confirm that signaling through IFN-λ receptor was required for IFN-λ-stimulated *P. aeruginosa* biofilm growth, we used RNA interference (RNAi) to selectively knockdown IL-28Rα in AECs and therefore, disrupt IFN-λ receptor signaling. In cells treated with siIL-28Rα, IFN-λ-stimulated biofilm formation was reduced (**Figure 12C**). This suggests that IFN-λ must signal through the

IFN-λ receptor to enhance *P. aeruginosa* biofilm growth. Knockdown of IL-28Rα was confirmed by western blot of whole cell lysate samples (**Figure 12D**). Together these results suggest that IFN-λ signaling is sufficient to stimulate *P. aeruginosa* biofilm growth in the absence of respiratory viral infection.

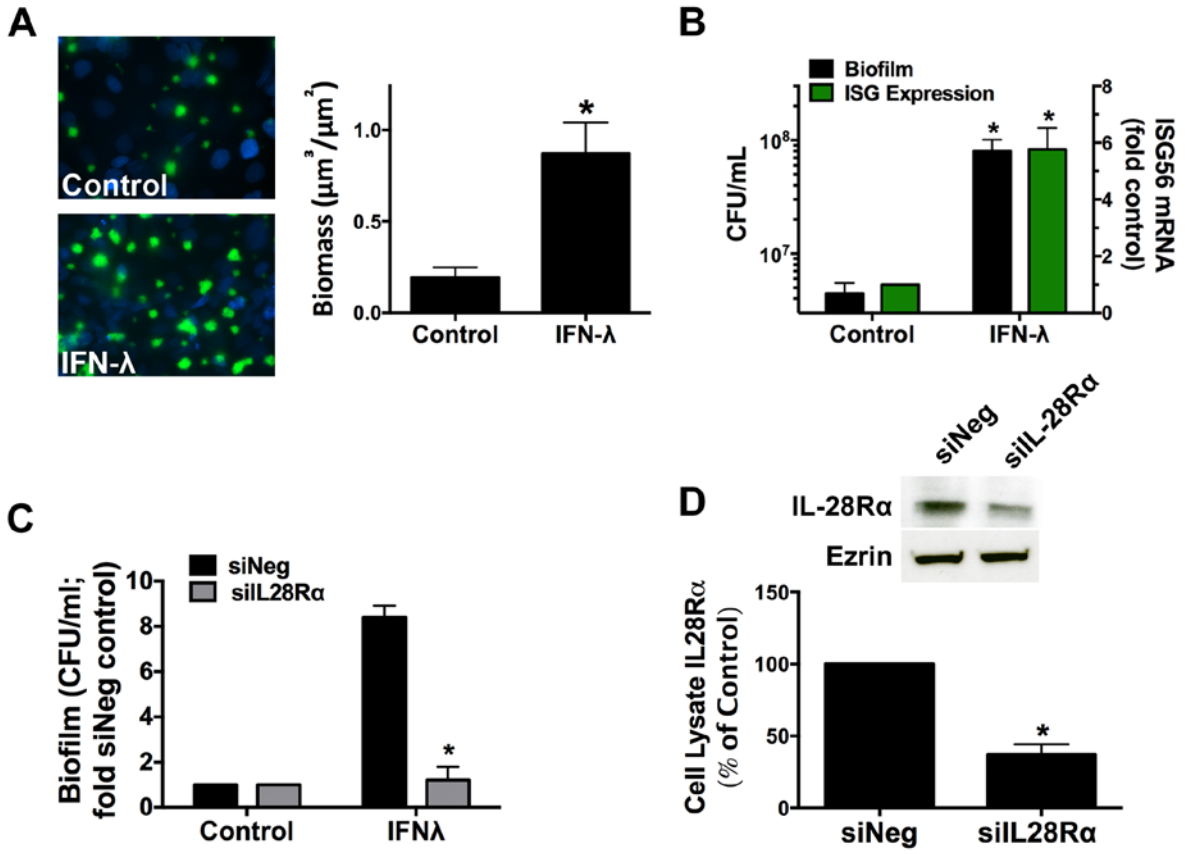

Figure 12: Type III IFN (IFN-λ) signaling stimulates the growth of *P. aeruginosa* biofilm.

(A and B) IFN-λ treatment stimulates the growth of *P. aeruginosa* biofilm on AECs. *P. aeruginosa* biofilm growth increased on AECs treated for 12 hr with IFN-λ1 (100 ng/mL, as assessed by live-cell microscopy (A) or in static coculture biofilm assay (B). (A) Epithelial cell nuclei are shown with Hoechst (blue) staining. The *P. aeruginosa* biofilm (GFP, green) biomass was calculated for each condition using COMSTAT. (B) *P. aeruginosa* biofilm was assessed by CFU enumeration (black bars, left y axis). IFN-λ1 signaling was confirmed with ISG56 induction by qRT-PCR (green bars, right y axis). (C) Signaling via IL-28Rα is required for biofilm growth during IFNλ

treatment. AECs were transfected with scrambled siRNA (siNeg) or siRNA targeting IL-28Rα (siIL28Rα) and were treated with IFN-λ1 (100 ng/mL) for 12 hr, and *P. aeruginosa* biofilms were grown in a static coculture biofilm assay. *P. aeruginosa* biofilm growth was quantified by CFU enumeration and displayed as fold change compared with siNeg-transfected cells. (D) siRNA-mediated knockdown of IL-28Rα was assessed by measuring protein abundance for each condition by Western blot and is displayed as the percent of IL-28Rα in cells transfected with siNeg (control). For all experiments $n \geq 3$. Data are presented as mean ± SD; $*P < 0.05$ versus control. Data provided by L.P.L. and J.M.B.

In addition to antiviral defense, the IFN response to respiratory viral infection has been shown to be necessary for the increase in bacterial growth in the lungs of animals during respiratory viral co-infection [156-158]. In these studies, targeted deletion of IFN receptors decreased bacterial burdens in animals co-infected with a respiratory virus to levels observed in PBS control animals that did not have a viral infection [157, 158]. To test whether IFN-λ signaling was necessary for the increase in *P. aeruginosa* biofilm growth observed during RSV co-infection, we treated cells with a neutralizing antibody against IL-10Rβ during RSV infection to inhibit IFN-λ signaling. This antibody has previously been shown to inhibit IL-10Rβ signaling in relation to IFN-λ treatment [328, 329]. In the presence of the IL-10Rβ neutralizing antibody, we observed reduced *P. aeruginosa* biofilm growth during RSV infection (**Figure 13**). It is worth noting that the decrease in *P. aeruginosa* biofilm growth we observed was not a complete reduction to biofilm formation measured on control cells. This result suggests that IFN-λ signaling is required for full induction of *P. aeruginosa* biofilm growth during RSV co-infection.

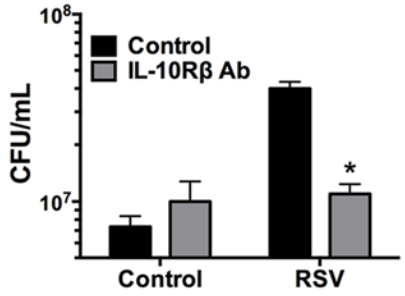

Figure 13: IFN-λ signaling is required for the growth of virus-stimulated *P. aeruginosa* biofilm.

Cells were infected with RSV or were mock-infected (MEM control) for 72 hr and were treated with IL-10Rβ-neutralizing antibody (IL-10Rβ antibody; 10 μg/mL) (gray bars) or were left untreated (black bars). *P. aeruginosa* biofilms were grown in static coculture biofilm assays. The growth of *P. aeruginosa* biofilms was quantified by CFU enumeration. RSV, RSV-infected AECs. For all experiments $n \geq 3$. Data are presented as mean ± SD; $^*P < 0.05$ versus control. Data provided by L.P.L. and J.M.B.

We also investigated the role IFN-β may play in *P. aeruginosa* biofilm induction during respiratory viral infection. Similar to INF-λ treatment, we observed that IFN-β treatment increased *P. aeruginosa* biofilm growth on AECs in our biotic biofilm imaging and static co-culture biotic biofilm assays (**Figure 14A-B**). We observed a reduction in IFN-β-mediated *P. aeruginosa* biofilm formation on AECs that were treated a neutralizing antibody targeting IFNAR (to inhibit IFN-β-mediated signaling in cells treated with IFN-β) (**Figure 14C**). Finally, we also observed a decrease in *P. aeruginosa* biofilm growth on AECs during RSV co-infection in the presence of IFNAR neutralizing antibody (**Figure 14D**). The decrease in *P. aeruginosa* biofilm growth was not a complete abrogation of biofilm formation in response to respiratory viral infection. This is similar to what we observed in experiments using a IL-10Rβ neutralizing antibody to block IFN-λ signaling during RSV co-infection. Taken together, these data support

the conclusion that IFN signaling in response to respiratory viral infection and necessary and sufficient to enhance the growth of *P. aeruginosa* biofilms. Additionally, these data suggest that a common target(s) of both IFN-β and IFN-λ signaling are responsible for increased *P. aeruginosa* biofilm growth during respiratory viral infection.

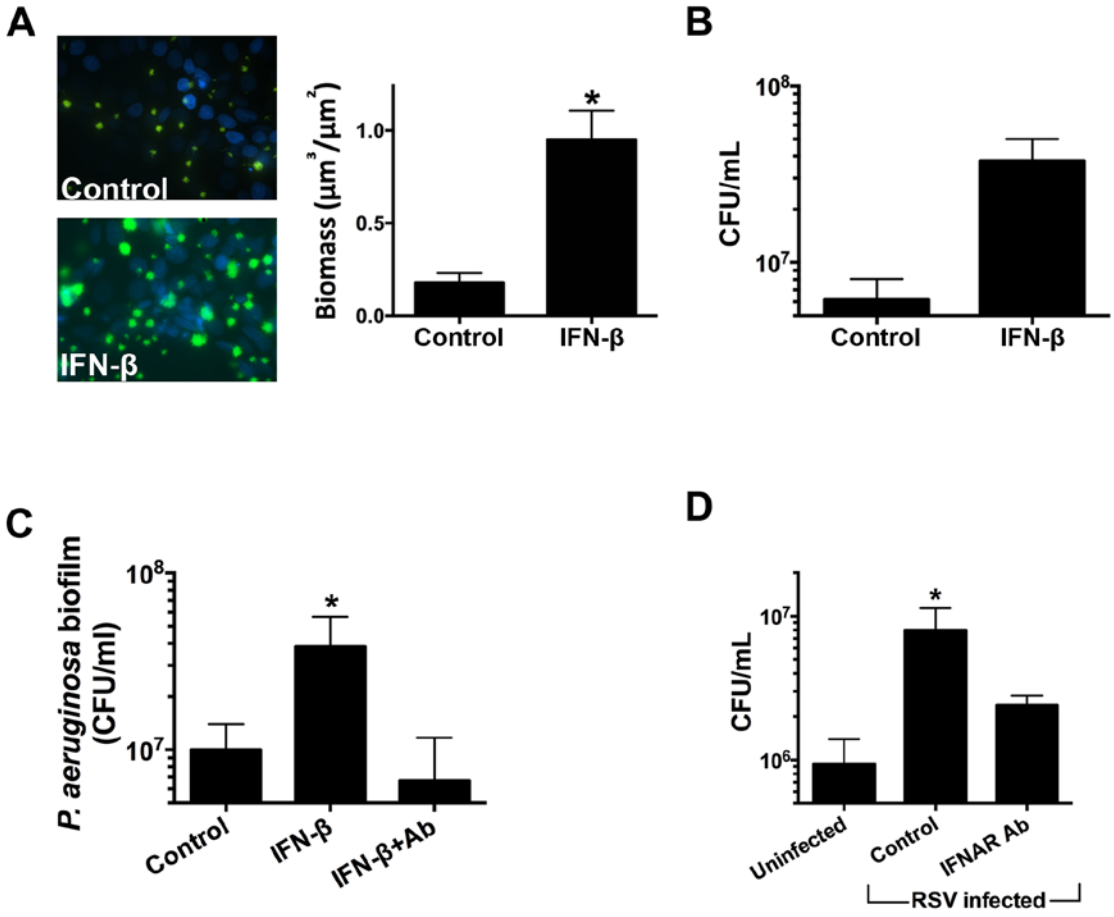

Figure 14: IFN-β treatment enhances the growth of *P. aeruginosa* biofilm.

(A-B) The growth of *P. aeruginosa* biofilm increased on AECs treated with IFN-β (1000 U/mL) for 18 hr, as measured by live-cell microscopy (A) or in static coculture biofilm assays (B). (A) Epithelial cell nuclei are shown with Hoechst (blue) staining and *P. aeruginosa* biofilm (GFP, green) biomass was calculated using COMSTAT. (B) *P. aeruginosa* biofilm was assessed by CFU enumeration. (C) Signaling through IFNAR is required for biofilm growth induced by IFN-β treatment. AECs were treated with IFNAR-neutralizing antibody (5 μg/mL) during 18-hr treatment with IFN-β (1000 U/mL), and *P. aeruginosa* biofilms were grown in a static coculture biofilm assay. Control corresponds to mock IFN-β treatment in the absence of IFNAR-neutralizing antibody. The growth of *P. aeruginosa* biofilm was quantified by CFU enumeration. (D) Neutralizing IFNAR prevents the RSV-stimulated growth of *P. aeruginosa* biofilm. AECs were infected with RSV ("RSV infected") and were treated with neutralizing IFNAR-antibody (5 μg/mL). *P. aeruginosa* biofilms were grown in a static coculture biofilm assay. The

growth of *P. aeruginosa* biofilm was quantified by CFU enumeration. Uninfected, mock infection (MEM control). For all experiments n ≥ 3. Data are presented as mean ± SD; **P* < 0.05 versus control. Data provided by L.P.L., D.K.F, and J.M.B.

Furthermore, these results imply that IFN-β and IFN-λ proteins do not interact directly with *P. aeruginosa* to stimulate biofilm formation and *P. aeruginosa* cannot utilize IFNs as a nutrient source to support biofilm growth. In support of this conclusion, when either IFN-β and IFN-λ was added directly to *P. aeruginosa* in a 96-well microtiter biofilm assay (in the absence of AECs), no biofilm growth was observed (**Figure 15**).

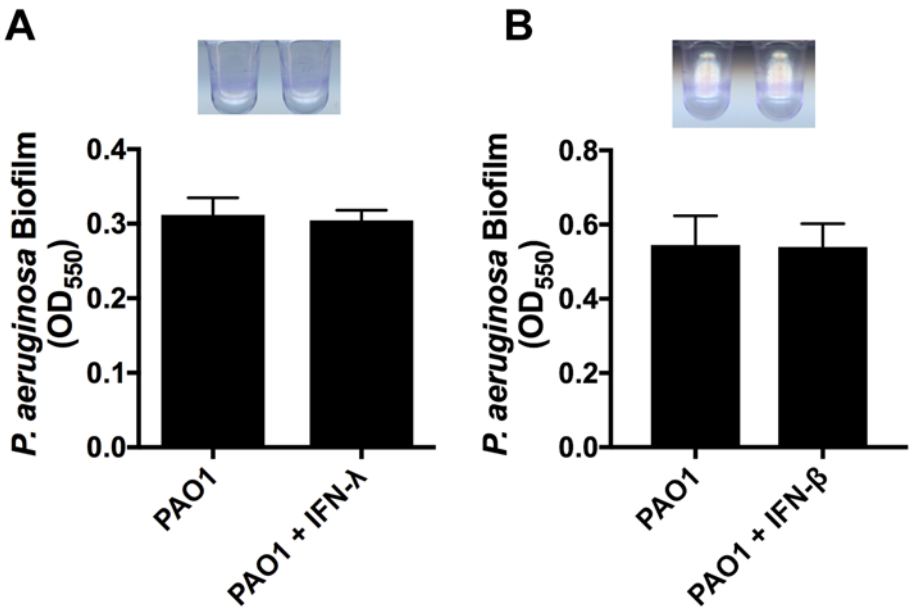

Figure 15: IFN-λ and IFN-β do not interact directly with *P. aeruginosa* and stimulate biofilm growth.

P. aeruginosa was grown in the presence or absence of (A) IFN-λ (200 ng/mL) or (B) IFN-β (1000 U/mL) diluted in MEM for 24 hr in the 96-well microtiter biofilm assay. Biofilm growth was measured as absorbance at 550 nm following crystal violet staining and is presented as OD_{550}. n = 3; data are presented as mean ± SD.

3.2.5 Iron released from RSV-infected AECs stimulates *P. aeruginosa* biofilm growth

Because we did not observe that RSV infection enhanced *P. aeruginosa* adherence to AECs, we next determined whether the apical airway surface liquid [hereafter termed "conditioned medium" (CM)] from RSV-infected cells was capable of enhancing biofilm growth in the absence of AECs. We found that CM from RSV-infected cells increased biofilm growth on abiotic surfaces, as assessed by static abiotic biofilm assay (**Figure 16A**) and a 96-well microtiter biofilm assay (**Figure 16B**). Because we observed that CM from RSV-infected cells stimulated biofilm growth, we hypothesized that RSV infection and induced the release of biofilm stimulatory factor(s). Iron is an essential nutrient for many bacteria and is required for the formation of *P. aeruginosa* biofilm on both abiotic and biotic surfaces [27, 37, 204]. To determine if iron homeostasis is altered during RSV infection, we measured total iron levels in CM from mock- or RSV-infected cells. RSV infection resulted in a time-dependent (**Figure 17A**) and dose-dependent (**Figure 17B**) increase in extracellular iron in the CM collected from AECs. In addition, RSV infection resulted in an increased in extracellular iron in CM collected from primary CF HBEs (**Figure 17C**) and primary non-CF HBEs (**Figure 17D**). Importantly, the presence of iron in CM was required for the enhancement of biofilm growth in response to RSV infection because an iron-chelating agent (Chelex-100) dramatically decreased CM-induced biofilm growth (**Figure 18**). When exogenous iron ($FeCl_3$) was added to CM from RSV-infected cells after treatment with Chelex-100, biofilm growth was restored (**Figure 18**). Collectively, these results indicate that RSV infection enhances iron release by AECs, thus increasing iron availability and biofilm formation by *P. aeruginosa***.**

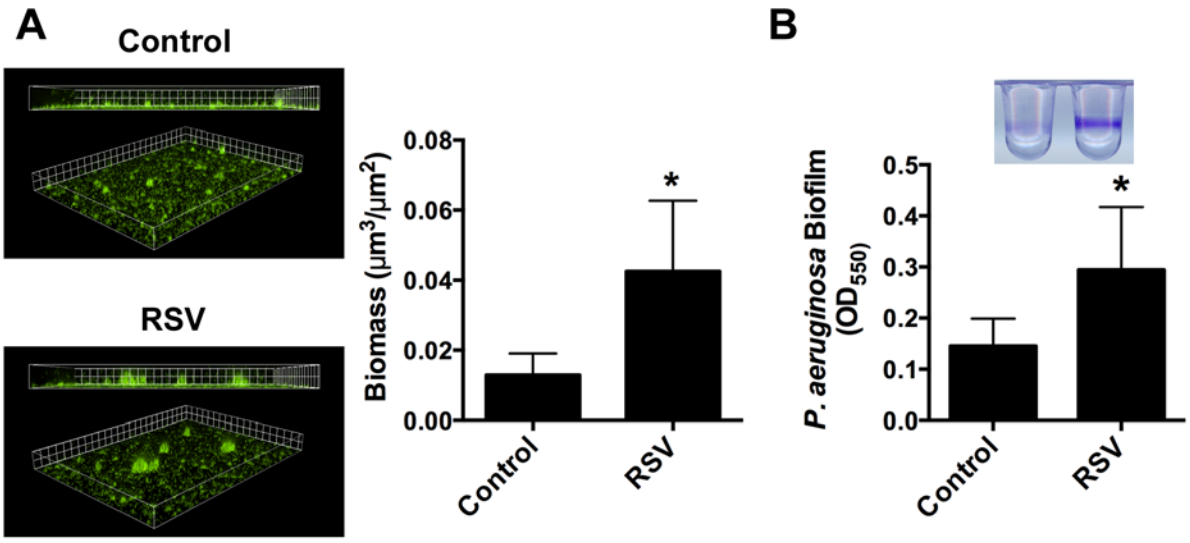

Figure 16: Apical secretions from RSV-infected AECs stimulate *P. aeruginosa* biofilm formation.

RSV infection stimulates the release of a biofilm-stimulatory factor that promotes *P. aeruginosa* formation. AECs were infected with RSV or were mock-infected (MEM control) for 72 hr, and the apical CM was collected. (A) *P. aeruginosa* (GFP) was grown in the presence of CM in static abiotic biofilm assays. Fluorescent microscopy was used to measure the growth of *P. aeruginosa* (GFP, green), and biomass was quantified using Nikon Elements (grid unit = 9 μm). (B) *P. aeruginosa* biofilms were grown in CM for 24 hr in 96-well microtiter biofilm assays. Biomass was quantified by crystal violet staining and absorbance was measured at 550 nm. For all experiments $n \geq 3$. Data are presented as mean ± SD; *$P < 0.05$ versus control.

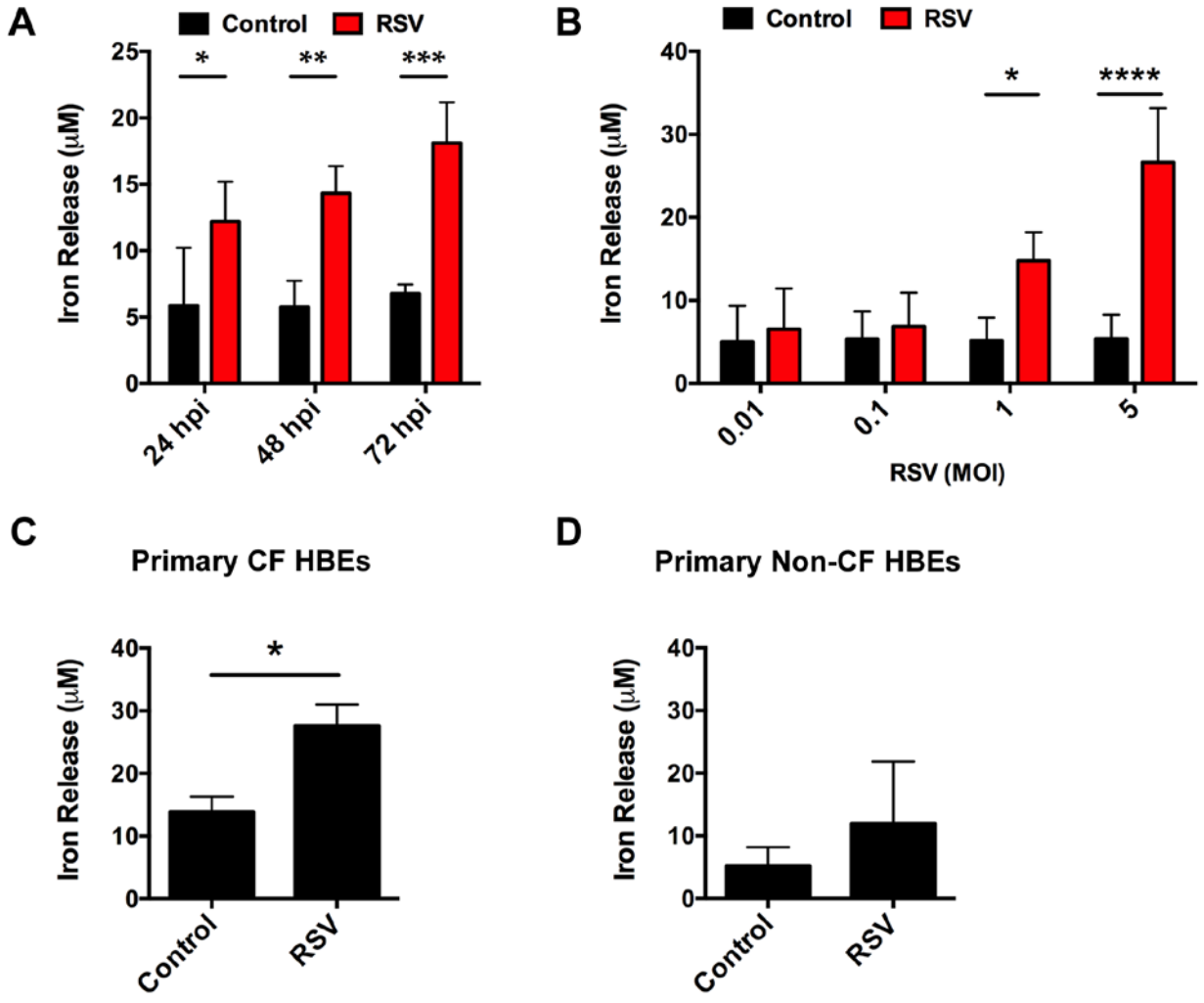

Figure 17: RSV infection enhances iron release from AECs.

(A) Total iron was increased in apical CM collected from AECs infected with RSV or mock-infected (MEM control) for the indicated number of hours post infection (hpi). (B) Total iron in the apical CM collected from AECs infected with RSV at the indicated MOI or mock-infected (MEM control) for 72 hours. (C and D) Total iron in the apical CM collected from primary CF (C) and non-CF (D) HBEs infected with RSV or mock-infected (MEM control). RSV, RSV-infected AECs. For all experiments n ≥ 3. Data are presented as mean ± SD; **P* < 0.05 versus control.

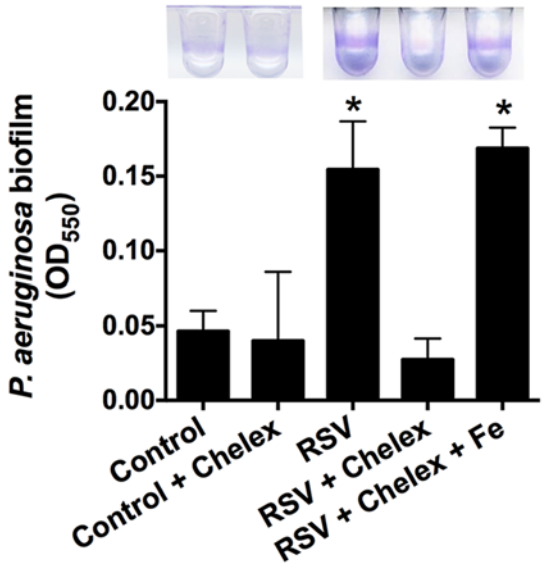

Figure 18: Iron in RSV CM is required for the growth of *P. aeruginosa* biofilm growth.

96-well microtiter biofilm assays were performed to measure the growth of *P. aeruginosa* in CM. Divalent metal cations were chelated with Chelex-100 (labeled "Chelex" in the figure), and iron was added back with $FeCl_3$ (8 μM) after Chelex-100 treatment. RSV, RSV-infected AECs. RSV, RSV-infected AECs. For all experiments $n \geq 3$. Data are presented as mean ± SD; $^*P < 0.05$ versus control.

3.2.6 Transferrin is apically released by AECs in response to RSV infection

Nutritional immunity is a process by which host cells restrict access to free iron and other trace metals by sequestering them inside cells, across anatomical barriers and bound to molecules that have a high affinity for metals ions. Because increased iron abundance in CM contradicts these principles, we sought to identify the mechanism by which RSV infection increases luminal iron release. To begin to examine the mechanism by which RSV infection promotes apical iron release, we investigated whether the abundance of iron transporters and iron-binding proteins in AECs was altered by virus infection. We did not observe a significant difference in the

abundance of the iron exporter, ferroportin, or the iron importer, divalent metal-ion transporter 1 (DMT1), during RSV infection (**Figure 19A**). Similarly, the abundance of iron-biding proteins, including transferrin, ferritin and lactoferrin, was not changed by RSV infection (**Figure 19A**). Although this suggests AECs are not actively changing free iron transport during RSV infection by changing proteins levels of iron transporters, it does not exclude the possibility of either the membrane abundance or the activity of these transporters being altered by RSV infection. To address both of possibilities and test whether free iron was being released by AECs during RSV infection, we measured iron concentrations of CM filtered through 3 kDa filters, which would retain protein bound iron. We found that when CM was filtered through 3 kDa filters, all of the iron was retained by the filter in the concentrate (**Figure 19B**), implying that iron present in CM is protein-bound. Because we observed that iron was required for *P. aeruginosa* biofilm formation in CM from RSV-infected cells (**Figure 18**), we also probed whether CM filtered through 3 kDa filters was capable of stimulating biofilms. Using a 96-well microtiter biofilm assay, we found that *P. aeruginosa* biofilm growth was not increased in the presence of CM from RSV-infected cells that had been filtered through 3 kDa filters and the biofilm stimulatory activity was retained in the concentrate from these filtrations (**Figure 19C**). Taken together, these results support the conclusion that *P. aeruginosa* is utilizing protein-bound iron, and not free ionic iron, in CM to form biofilms in the presence of RSV coinfection.

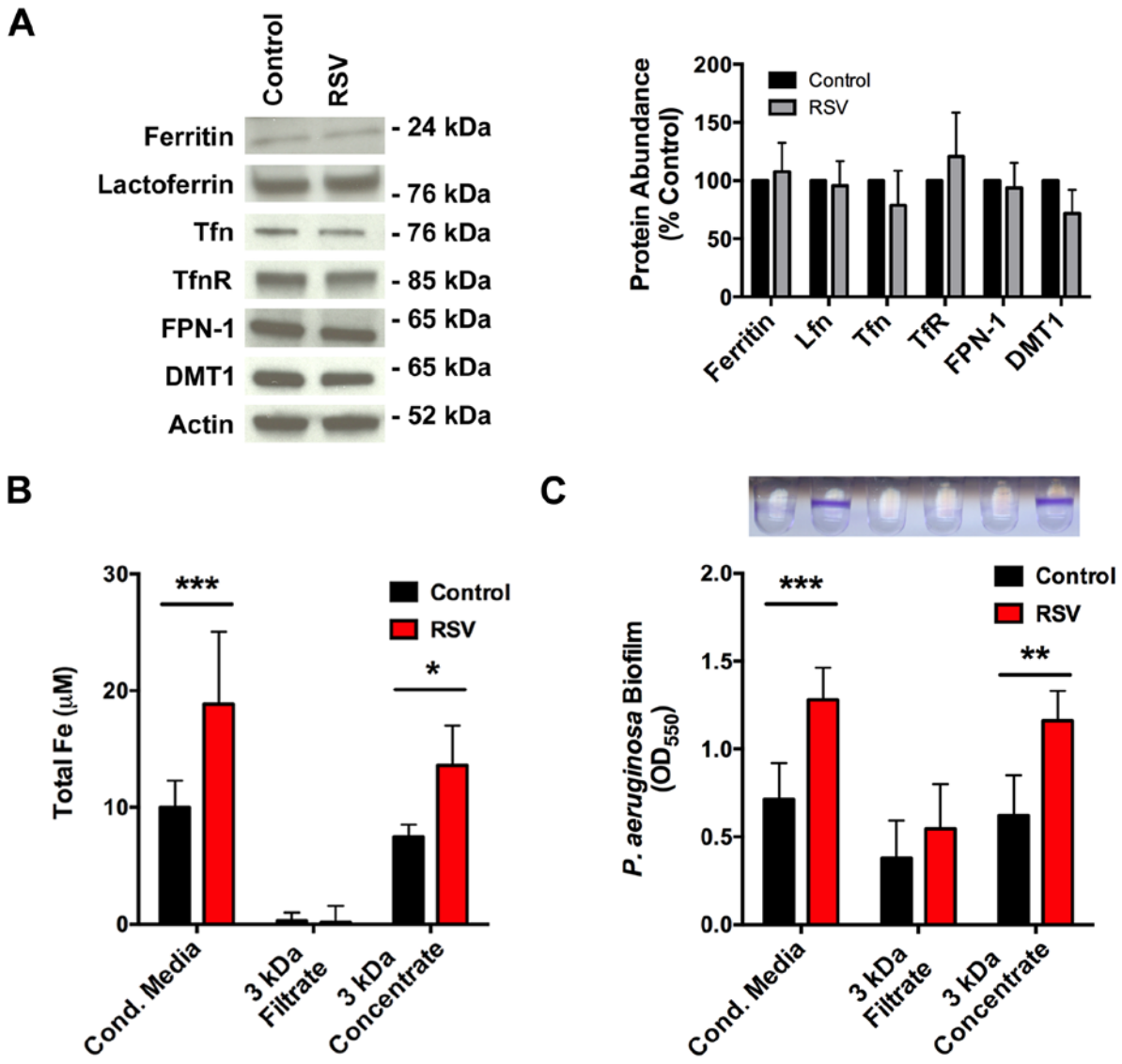

Figure 19: RSV infection does not increase free-iron release from AECs.

(A) RSV infection does not affect the abundance of iron transporter proteins in AECs infected with RSV or mock-infected (MEM control) for 72 hr, as measured by Western blot analysis. (B-C) Apical CM was collected from AECs infected with RSV or mock-infected (MEM control) for 72 hr and subjected to 3 kDa filtration. Cond. Media, CM not filtered; 3 kDa Filtrate, flow-through from 3 kDa filtration; 3 kDa Concentrate, media that did not flow through 3 kDa filter. (B) Total iron levels in apical CM following 3 kDa filtration. (C) *P. aeruginosa* biofilms were grown in apical CM following 3 kDa filtration for 24 hr in 96-well microtiter biofilm assay. Biofilm growth was measured as absorbance at 550 nm following crystal violet staining. For all experiments $n \geq 3$. Data are presented as mean ± SD; *$P < 0.05$ versus control. J.A.M. provided data for panels C and D.

Since we observed increased iron levels in CM from RSV-infected cells (**Figure 17**), with no corresponding changes in the expression of iron transporters or free iron in CM, we next examined whether RSV infection alters the release of iron-binding proteins into CM. Indeed, we found increased abundance of transferrin in the CM from RSV-infected AECs (**Figure 20A**). Transferrin is a host iron-binding protein that can be used as a source of iron and can support the growth of multiple bacterial species, including *P aeruginosa* [197-199, 211]. Notably, transferrin promotes biofilm growth by *P. aeruginosa* in a dose-dependent manner [27]. To determine whether transferrin is necessary for the stimulation of biofilm growth by CM from RSV-infected cells, we grew *P. aeruginosa* in transferrin-depleted CM and found that a significant reduction in biofilm growth when CM from RSV-infected cells was depleted of transferrin (**Figure 20B**). We confirmed that our immunoprecipitation reactions completely removed transferrin from CM by western blot analysis (**Figure 20C**). Collectively, these data suggest that RSV infection stimulates the apical release of transferrin from AECs to promote the formation of *P. aeruginosa* biofilms.

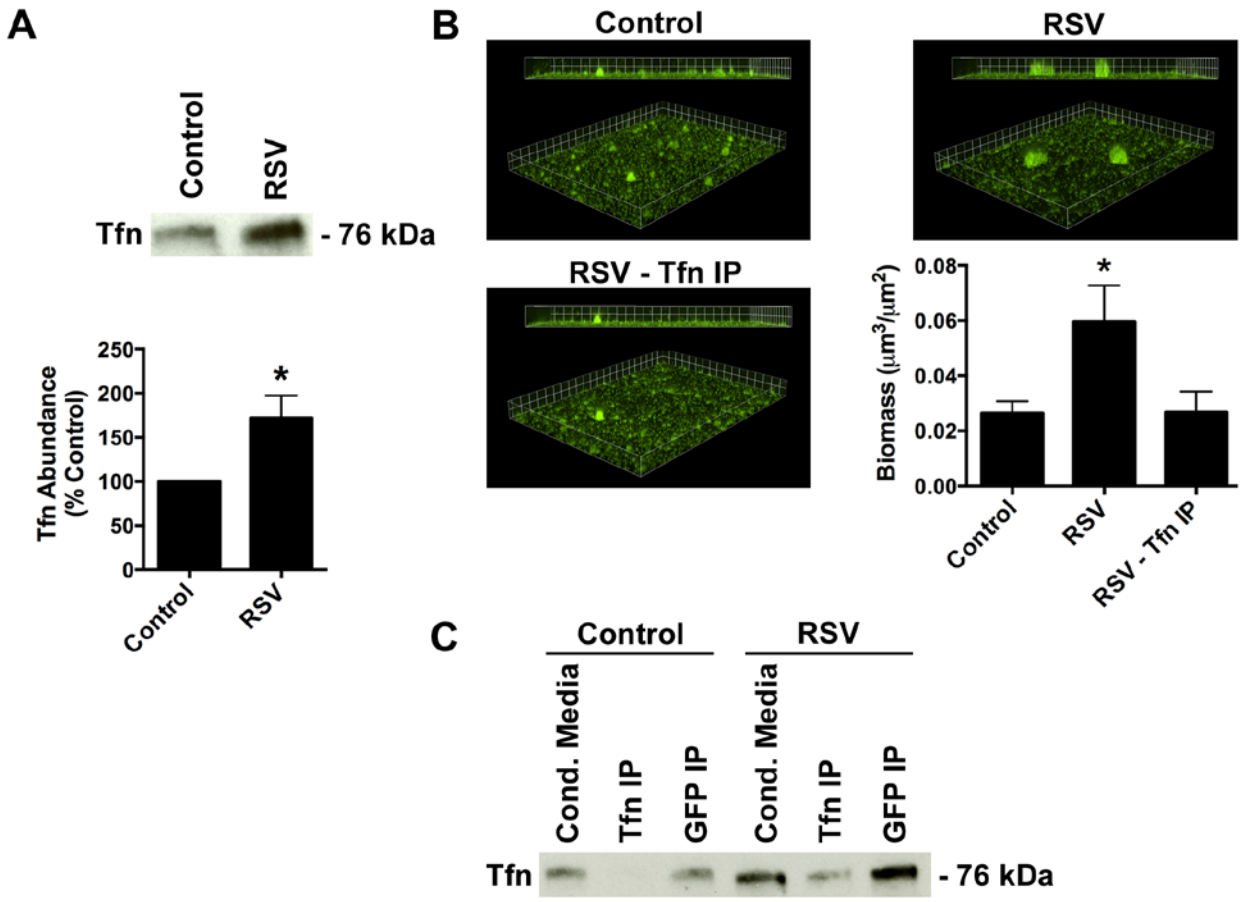

Figure 20: Transferrin release increases in response to virus infection *in vitro.*

AECs were infected with RSV or were mock-infected (MEM control) for 72 hr and then apical CM was collected. (A) RSV infection increases transferrin abundance in apical CM, as measured by Western blot analysis. (B) Transferrin depletion reduces the growth of *P. aeruginosa* biofilm in RSV CM. Apical CM was collected from RSV-infected AECs depleted of transferrin by immunoprecipitation (RSV-Tfn IP). *P. aeruginosa* (GFP) biofilms were grown in transferrin-replete and –depleted RSV CM in static abiotic biofilm assays. Biofilm biomass was quantified using Nikon Elements (grid unit = 8.5 μm). (C) Transferrin depletion was achieved by immunoprecipitation of transferrin from CM using an anti-transferrin polyclonal antibody. Western blot analysis was used to verify transferrin depletion from CM. For all experiments n ≥ 3. Data are presented as mean ± SD; *$P <$ 0.05 versus control.

3.2.7 RSV infection increases the availability of airway iron *in vivo*

To extend our *in vitro* findings to what might occur *in vivo*, we used a neonatal mouse model of RSV infection [315] and measured iron levels in the bronchoalveolar lavage fluid (BALF) up to 1 week post infection. RSV infection increase iron concentrations in the airways significantly, compared with mock-infected controls (**Figure 21A**). In agreement with the increased abundance of iron, BALF from RSV-infected mice was able to support *in vitro P. aeruginosa* biofilm growth (**Figure 21C**). Although RSV infection resulted in increased inflammation, there was no evidence of server bronchiolar epithelial damage or of sloughing or rupture of the epithelial barrier, which could account for the increase of iron in the airways (**Figure 21D-E**). In addition, consistent with our finding in polarized human AECs, transferrin abundance was increased in the BALF of RSV-infected mice (**Figure 21B**), further supporting a role for iron release as a key mediator of biofilm formation in response to RSV infection of AECs.

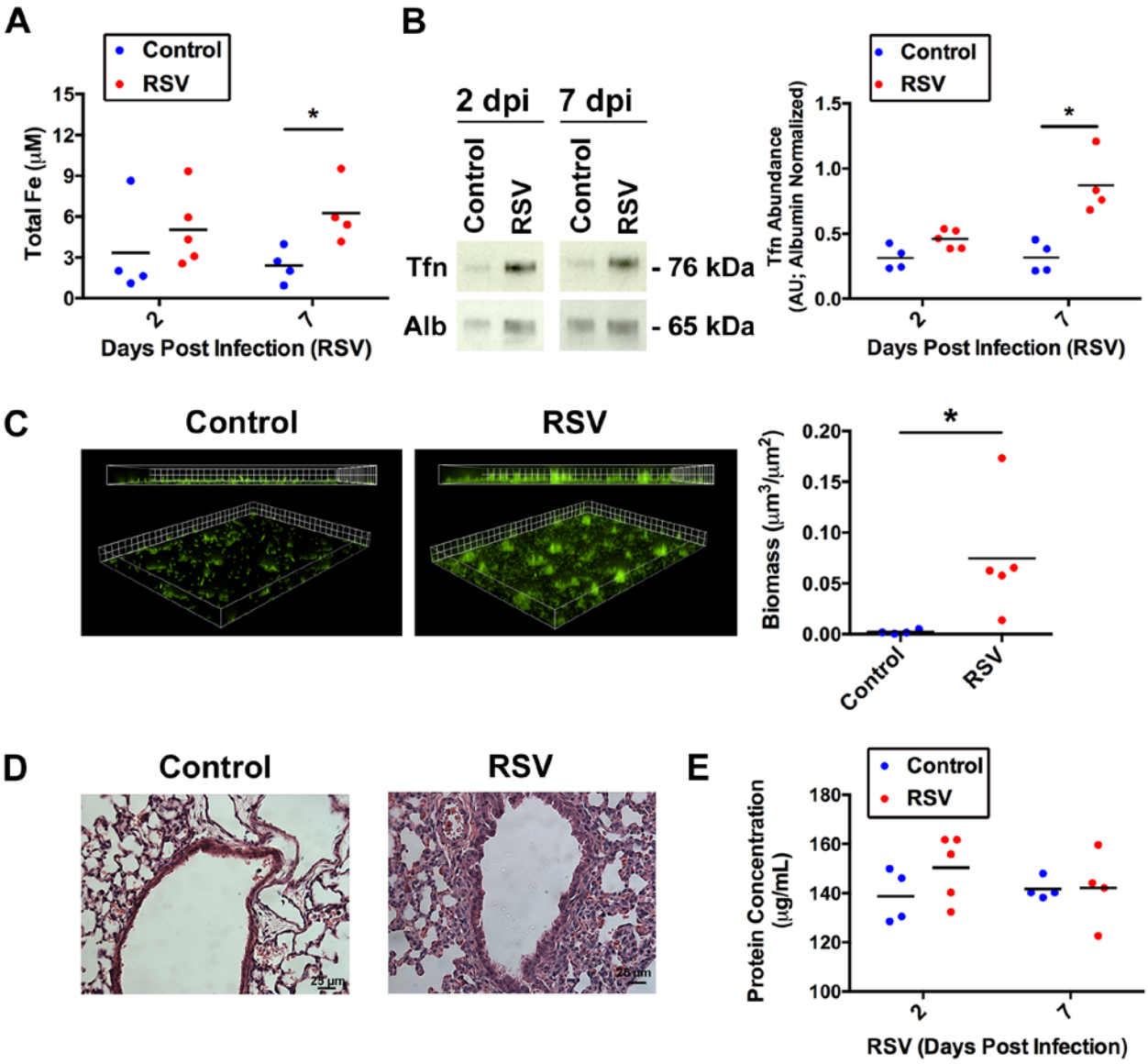

Figure 21: Transferrin release increases in response to RSV infection *in vivo*.

(A and B) Total iron (A) and transferrin abundance (B) were increased in BALF recovered from neonatal mice infected with RSV or mock-infected (PBS control) for the indicated number of days post infection (dpi), as measured by iron assay or Western blot analysis, respectively. (C) BALF recovered from neonatal mice infected with RSV stimulates the growth of *P. aeruginosa* biofilm growth *in vitro*. *P. aeruginosa* (GFP) biofilms grown in BALF recovered from neonatal mice infected with RSV 5 dpi in static abiotic biofilm assays. Biofilm biomass was quantified using Nikon Elements (grid unit = 7.5 μm). (D) Lung pathology in mice following infection. Mice were infected with RSV for 7 days; then lungs were harvested, sliced, and stained with H&E. Each panel represents an

individual mouse from the indicated group. (Scale bar, 25 μm). (D) At 2 and 7 dpi, BALF was collected and assayed for protein content by Bradford assay. N=4 or 5 mice per treatment group. Means are not significantly different from PBS controls. Horizontal lines indicate mean values. Alb, albumin; RSV, RSV infection; Tfn, transferrin. All experiments were repeated, with at least four mice per group. * $P < 0.05$. Katherine Eichinger and Kerry Empey performed mouse infections, H&E staining, and collected BALF. All assays with BALF performed in Bomberger Lab by myself.

3.3 DISCUSSION

Respiratory viral infections trigger exacerbations in chronic lung disease such as CF and predispose patients to bacterial colonization, but identifying the molecular mechanism(s) underlying viral-bacterial interactions has been elusive [53, 54, 56, 71, 72, 79]. Because of the paucity of animal models to study the development of chronic bacterial infections, we used a unique coculture model in which the early stages of *P. aeruginosa* biofilm development in association with polarized human AECs can be observed by high-resolution, live-cell imaging. We demonstrate that respiratory virus infection of CF and non-CF AECs results in the increased formation of bacterial biofilm. Moreover, in this study we show that biofilm growth is increased through a dysregulation of host nutritional immunity mechanisms, resulting in the increased release of iron-bound transferrin during virus infection, which originates in at the basolateral membrane of AECs and is transcytosed to the apical compartment of cells. This release of iron-bound transferrin promotes the transition of *P. aeruginosa* to a biofilm mode of growth. Importantly, our findings propose a molecular mechanism underlying the common clinical observation that respiratory virus infection in patients with chronic lung disease promotes

chronic bacterial colonization and disease progression [51, 53, 56, 71, 72, 79, 330]. Our study has important implications, beyond CF pathogenesis, for understanding how complex microbial communities interact during disease in the lung.

Few studies have investigated the interaction between viruses and *P. aeruginosa* in the airways. It has been shown that *P. aeruginosa* may modulate the antiviral response, although the consequences of these interactions on the progression of *P. aeruginosa* infection and virus infection remain unclear [121, 173]. Previous studies have shown that RSV coinfection promotes bacterial adherence to nonpolarized and ciliated AECs [152, 154, 331]. In our model using well-differentiated AECs, we show that preceding RSV infection decreased *P. aeruginosa* adherence to AECs while greatly enhancing the development of bacterial biofilm. We interpret these results, coupled with abiotic biofilm assays that are not altered with virus exposure, as indicating that a direct interaction between virus and bacteria is not responsible for enhancement of *P. aeruginosa* biofilm growth during respiratory viral infection. Instead, using a coculture model of biofilm development in association with the respiratory epithelium, our data suggest a mechanism by which the host innate immune response to the viral pathogen creates a local environment at the mucosal surface that promotes chronic bacterial infection. The molecular details of this mechanism are explored further in this dissertation.

Although the antiviral effects of IFNs are well recognized [332], studies now suggest that an appropriate antiviral IFN response to respiratory viral infection has unfavorable effects on secondary bacterial infections. For example, in acute models of influenza-bacterial coinfections, the increased bacterial load in the airways of mice after influenza challenge has been attributed to the antiviral IFN response to the virus [156-158]. Little is known about how IFN induction or signaling pathways influence chronic bacterial infection. In acute models of *P. aeruginosa*

infection, the ability to clear *P. aeruginosa* infection is improved significantly in mice lacking IL-28Rα, indicating that IFN-λ signaling may contribute adversely to pulmonary *P. aeruginosa* infection *in vivo* [127]. Our data extend previous findings to suggest that IFN signaling also promotes the growth of *P. aeruginosa* biofilms.

Our study suggests the dysregulation of nutritional immunity, specifically iron homeostasis, as a primary mechanism by which RSV promotes the transition of *P. aeruginosa* to a biofilm mode of growth. Iron plays an essential role in the development of biofilms on abiotic surfaces and in association with AECs for *P. aeruginosa* and other bacterial species [27, 37, 43, 204]. A strong positive correlation has been reported among increased iron levels, *P. aeruginosa* burden and disease severity in the CF lung, but the effect of respiratory viral infection on iron levels has not been investigated [24, 25, 28]. In our studies we found that, during the corse of infection, RSV increased apical iron release from the airway epithelium and that iron chelation dramatically reduced biofilm growth, implying that iron chelation is effective in counteracting virus-mediated iron release and biofilm growth. Although *P. aeruginosa* biofilms grown on AECs display significantly high antibiotic resistance than biofilms formed on abiotic surfaces, the use of iron chelation compounds significantly increases antibiotic-mediated disruption of biofilms on cells [49]. Moreover, it has been demonstrated recently that *P. aeruginosa* dispersed from biofilms by chemical induction is highly sensitive to iron stress [333]. This high sensitivity to iron limitation suggests that iron chelation compounds may play a role in preventing the spread of bacteria to new infection sites. A novel approach to inhibiting *P. aeruginosa* growth and biofilm formation uses the transition metal gallium (Ga^{3+}) to disrupt *P. aeruginosa* iron metabolism [334, 335]. Therefore, the co-administration of iron chelators that can prevent bacterial iron acquisition and compounds that disrupt bacterial iron metabolism may be an

important therapeutic strategy during respiratory virus seasons to prevent the development and spread of chronic bacterial infections in CF patients.

Iron is a critical nutrient for many cellular processes in humans, but the quantity and location of iron must be regulated tightly to prevent infection [182]. Even in the absence of infection, extracellular iron is bound to high-affinity iron-binding proteins, such as transferrin, to maintain extremely low levels of free iron. We found that RSV infection promoted the apical release of transferrin from AECs and that transferrin contributed significantly to the formation of *P. aeruginosa* biofilms. Moreover, our data suggest that RSV infection does not promote the release of free iron and therefore, that the iron released during viral infection is protein-bound. Our data suggest that the iron is bound to transferrin. The mechanism(s) by which *P. aeruginosa* responds to the environmental conditions imposed by RSV infection, including the presence of transferrin, are important to consider. One mechanism by which *P. aeruginosa* overcomes iron sequestration is through the siderophore pyoverdine, which facilitates iron acquisition from transferrin and is important for bacterial growth and biofilm formation [204, 206]. The presence of pyoverdine in CF sputum suggests the importance of pyoverdine-mediated iron uptake by *P. aeruginosa* in the CF lung [336]. Taken together, these studies suggest that pyoverdine-mediates acquisition of iron from transferrin may be an important mechanism by which chronic *P. aeruginosa* infections initially develop in the CF lung and that respiratory viral infection may instigate such a microenvironment. In support of this hypothesis, longitudinal analyses of CF clinical isolates suggest that *P. aeruginosa* pyoverdine production is high early in infection and then production decreases as chronic infections continue to progress over the life time of patients [212, 213].

In summary, many clinical studies in patients with chronic lung disease report viral-bacterial interactions that result in poor bacterial clearance and disease progression. In the current study, we demonstrate that respiratory viral infections dysregulate host iron homeostasis mechanisms, promoting harmful secondary bacterial infections. By improving our mechanistic understanding of viral-bacterial coinfections, these studies aid in the development of new treatments to target complex infectious diseases. Moreover, because mounting clinical evidence suggest that many infectious diseases are polymicrobial in nature, our studies likely have implications for studying complex microbial communities during other disease processes.

4.0 EXTRACELLULAR VESICLES RELEASED BY AIRWAY EPITHELIAL CELLS DURING RESPIRATORY VIRUS INFECTION PROMOTE *PSEUDOMONAS AERUGINOSA* BIOFILM GROWTH

This chapter is adapted from the manuscript in preparation:

Matthew R. Hendricks[a], Jeffrey A. Melvin[a], Yingshi Ouyang[b], Donna B. Stolz[c], Yoel Sadovsky[b], John V. Williams[d] and Jennifer M. Bomberger[a]

Extracellular vesicles released by airway epithelial cells during respiratory virus infection enhance *Pseudomonas aeruginosa* biofilm growth.

[a]Department of Microbiology and Molecular Genetics, University of Pittsburgh School of Medicine, Pittsburgh, PA 15219

[b]Magee-Womens Research Institute, Department of OBGYN and Reproductive Sciences, University of Pittsburgh, Pittsburgh, PA 15213

[c]Department of Cell Biology, University of Pittsburgh School of Medicine, Pittsburgh, PA 15213

[d]Department of Pediatrics, University of Pittsburgh School of Medicine, Children's Hospital of the University of Pittsburgh Medical Center, Pittsburgh, PA 15224

Unless otherwise specified, all data presented in this chapter will be included in the manuscript outlined above. Contributions of authors to individual figures are indicated in the figure legends.

4.1 INTRODUCTION

Extracellular communication is a critical component of many host processes. Extracellular vesicles (EVs) are small membrane-enclosed vesicles that are produced by most cell types, and secreted into the extracellular environment. Biologically active proteins, RNAs and lipids can be packaged into EVs and delivered to target cells, where they impact many biological processes [216, 218, 221, 337]. EVs have been isolated from lung epithelial cells, as well as from the bronchoalveolar lavage fluid (BALF) and sputum collected from patients with chronic lung diseases, such as asthma and cystic fibrosis (CF) [338-342]. Although EVs seem to play roles in both normal tissue homeostasis and in the progression of inflammation in the airways, little is known about what function EVs have in the airways during an infection [343].

During viral infection, EVs mediate intercellular communication that is beneficial to the viral life cycle by delivering viral particles and genetic elements between neighboring cells that help establish productive infections [217]. For example, EVs released from hepatitis C virus (HCV) infected cells contained replication competent viral RNA that successfully establish infection in naïve cells [251, 252]. In addition, EVs transport molecules that promote viral replication by suppressing host immune responses, such as the antiviral interferon (IFN) response, as has been demonstrated during enterovirus 71 (EV71) infection [250]. However, viral infections do not often occur in isolation and there is an increasing appreciation for the prevalence and severity of polymicrobial infections involving viruses. Viral-bacterial interactions in the respiratory tract have received notable attention due to the severity of secondary bacterial infection following viral infection in both acute infections, such as pneumonias, and chronic diseases, such as CF lung disease. Although synergistic virulence is commonly observed in these

infections, it remains poorly understood how EVs impact viral-bacterial polymicrobial infections in the airways.

CF is a genetic disease caused by mutations within the cystic fibrosis transmembrane conductance regulator (CFTR) ion channel. Reduced CFTR function in the airways results in thick mucus secretions that are difficult to clear due to decreased innate defenses, such as mucociliary clearance [325, 344]. This creates a favorable environment for microbial colonization and persistence. *Pseudomonas aeruginosa* is a commonly isolated bacterial pathogen in the CF lung that forms chronic infections in the airways of most adult CF patients, and causes much of morbidity and mortality in patients. The development of chronic *P. aeruginosa* infections in the CF lung often involves the transition to a biofilm-associated lifestyle, which can protect the bacteria from the host immune response and antibiotics [44, 46]. *P. aeruginosa* is rarely the only microbe that is present in the CF lung [6]. Extensive amount of research has focused on bacterial communities and bacterial-bacterial interactions in the CF lung. However, much less is known about the mechanisms underlying viral-bacterial interactions in the CF lung, despite clinical studies strongly linking respiratory viral infection with *P. aeruginosa* coinfection and the development of chronic *P. aeruginosa* infection in patients [53, 55, 71, 72, 79, 330]. Because antimicrobials are ineffective at treating chronic infections in the CF lung, a better understanding of the factors that drive biofilm development in the airways may help identify alternative therapeutic strategies to either prevent chronic bacterial infections or treat already established biofilms.

Many environmental factors contribute to *P. aeruginosa* biofilm growth, including the nutrient iron. Although iron is essential for microbial growth and the host tightly regulates iron accessibility to prevent infection, iron levels in the CF lung are significantly increased compared

to non-CF airways [23, 24, 26, 29]. Increased iron levels are correlated with increased bacterial burden and decreased pulmonary function in the CF lung, but the mechanisms that contribute to increased iron levels in the CF airways are unknown [25, 28]. We have shown the respiratory viral infection produces an environment that promotes *P. aeruginosa* biofilm growth through the increased release of iron into the airways (**Chapter 3**), suggesting virus infection alters iron homeostasis in the lung. Many proteins involved in metal homeostasis have been identified on EVs [345], but it is not known what function EVs have in metal homeostasis, and which metal and metal-binding proteins are loaded onto EVs in the lung and how airway infection alters metal abundance in EV populations in the airways.

To gain a better understanding of how EVs impact viral-bacterial interactions at a mucosal surface, we determined whether EVs isolated from AECs influence *P. aeruginosa* biofilm development during respiratory viral coinfection in a model of CF lung disease. In this study, we show that EVs isolated from AECs during respiratory viral infections enhance *P. aeruginosa* biofilm growth. In addition, we show that virus infection increases iron accessibility to promote *P. aeruginosa* biofilm growth. Our results demonstrate that the release of EVs in the respiratory tract is an important factor in the interactions that occur during polymicrobial infections. Additionally, our study offers new insight into our understanding of nutritional immunity in the lung and how the host contributes to the development of bacterial biofilm-associated infections during respiratory viral infection.

4.2 RESULTS

4.2.1 Extracellular vesicles isolated from AECs stimulate *P. aeruginosa* biofilm growth during respiratory viral infection

Previously, we have observed that in the apical secretions collected from RSV-infected AECs [termed "conditioned media" (CM)], was capable of enhancing *P. aeruginosa* biofilm growth (**Figure 22A**). To determine if EVs were required for CM-mediated bacterial biofilm formation, we depleted apical secretions from RSV-infected cells of EVs and measured biofilm formation in the presence of vesicle-depleted CM. We found that CM from RSV-infected cells that had been depleted of EVs by ultracentrifugation was unable to stimulate *P. aeruginosa* biofilm growth (**Figure 22A**), implying that EVs are required for virally-induced *P. aeruginosa* growth in CM. In addition, we filtered CM through 100 kDa filters, which would trap any large protein complexes or vesicles but allow smaller, soluble proteins to flow-through. Filtrate from RSV-infected AECs was unable to stimulate *P. aeruginosa* biofilm formation compared to CM (**Figure 22B**). However, we observed that concentrate from RSV-infected cells maintained the ability to greatly increase biofilm growth, similar to CM that had not been filtered (**Figure 22B**). Taken together, these results suggest that respiratory viral infection increases EV release from AECs, which can be utilized by *P. aeruginosa* to form biofilms.

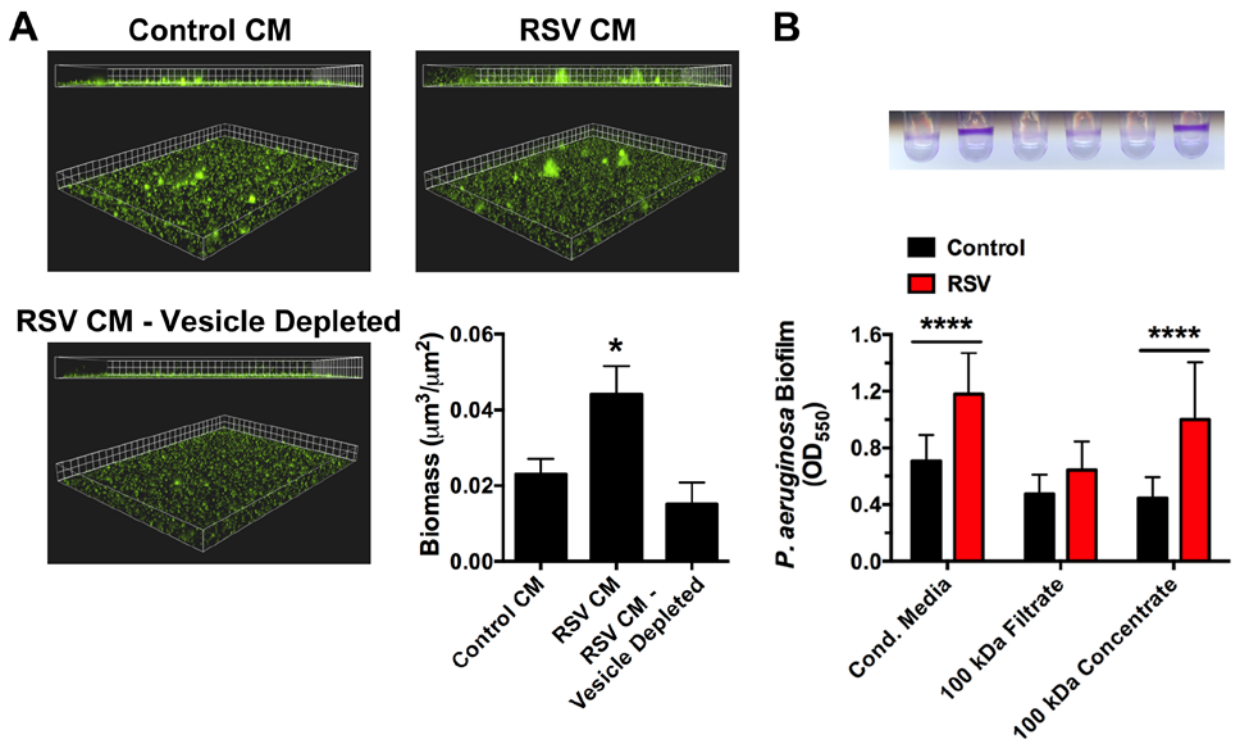

Figure 22: EVs are required for *P. aeruginosa* biofilm growth in apical secretions from RSV-infected AECs. AECs were infected with RSV or mock-infected (MEM control) for 72 hr and the apical CM was collected. CM was depleted of EVs by (A) ultracentrifugation or (B) 100 kDa filtration. (A) *P. aeruginosa* (GFP) biofilms were grown in the presence of CM in static abiotic biofilm assays. Fluorescent microscopy was used to measure biofilm growth. Biomass was quantified using Nikon Elements (unit grid = 7.5 μm). (B) *P. aeruginosa* were grown in CM for 24 hr in a 96-well microtiter biofilm assay following 100 kDa filtration. Biofilm growth was measured as absorbance at 550 nm following crystal violet staining. Cond. Media, CM not filtered; 100 kDa Filtrate, flow-through from 100 kDa filtration; 100 kDa Concentrate, media that did not flow through 100 kDa filter. For all experiments $n \geq 3$. Data are presented as mean ± SD; $^*P < 0.05$ versus control.

To determine if EVs released from airway epithelial cells, ΔF508/ΔF508 cystic fibrosis bronchial epithelial cells (CFBE41o-, referred to as "AECs" hereafter), during respiratory viral infection were capable of enhancing *P. aeruginosa* biofilm growth, we isolated EVs from AECs infected with RSV using ultracentrifugation. We measured biofilm growth in the presence of EVs but in the absence of AECs, as described previously [346]. Interestingly, we found that EVs from RSV-infected cells significantly increases biofilm growth in the absence of AECs on abiotic surfaces, as measured by fluorescent microscopy and 96-well microtiter biofilm assays (**Figure 23A-B**). Further experiments are planned to determine whether EVs isolated from RSV-infected, non-CF AECs also stimulate *P. aeruginosa* biofilm growth. Based on our observations that RSV co-infection increases biotic biofilm growth of *P. aeruginosa* on non-CF HBEs (**Figure 7A**), we hypothesize that EVs isolated from non-CF cells infected with RSV will also stimulate *P. aeruginosa* biofilm growth. We observed that many of the proteins commonly used as protein markers for EVs were also present in the EVs we isolated from AECs, while the absence of GM130 (a Golgi marker) and calnexin (an endoplasmic reticulum marker) confirmed no cell debris in our EV preparations (**Figure 24A**). Furthermore, the size and morphology of the isolates EVs were confirmed by electron microscopy and Nanoparticle Tracking Analysis (NTA) (**Figure 24B-C**). RSV infection increased the release of EVs from AECs, as assessed by both western blot and NTA. We observed that although EVs contained RSV proteins and RNA (**Figure 24D-E**), the EVs population we isolated did not contain infectious viral particles, as measured by plaque assay (**Figure 24F**). These data suggest that infectious RSV particles are not responsible for the biofilm stimulatory activity of EVs isolated from RSV-infected AECs. These results are consistent with previous observations that purified RSV does not stimulate *P. aeruginosa* biofilm formation (**Figure 9A**), further suggesting that infectious RSV particles are

not responsible for virus-mediated biofilm growth. To examine whether EV-mediated *P. aeruginosa* biofilm growth was specific to RSV infection, we isolated EVs from AECs infected with another respiratory virus commonly found in CF patients, human rhinovirus (hRV). Interestingly, we observed that EVs from hRV-infected cells also increased *P. aeruginosa* biofilm growth in the absence of AECs, as measured by fluorescent microscopy (**Figure 23C**).

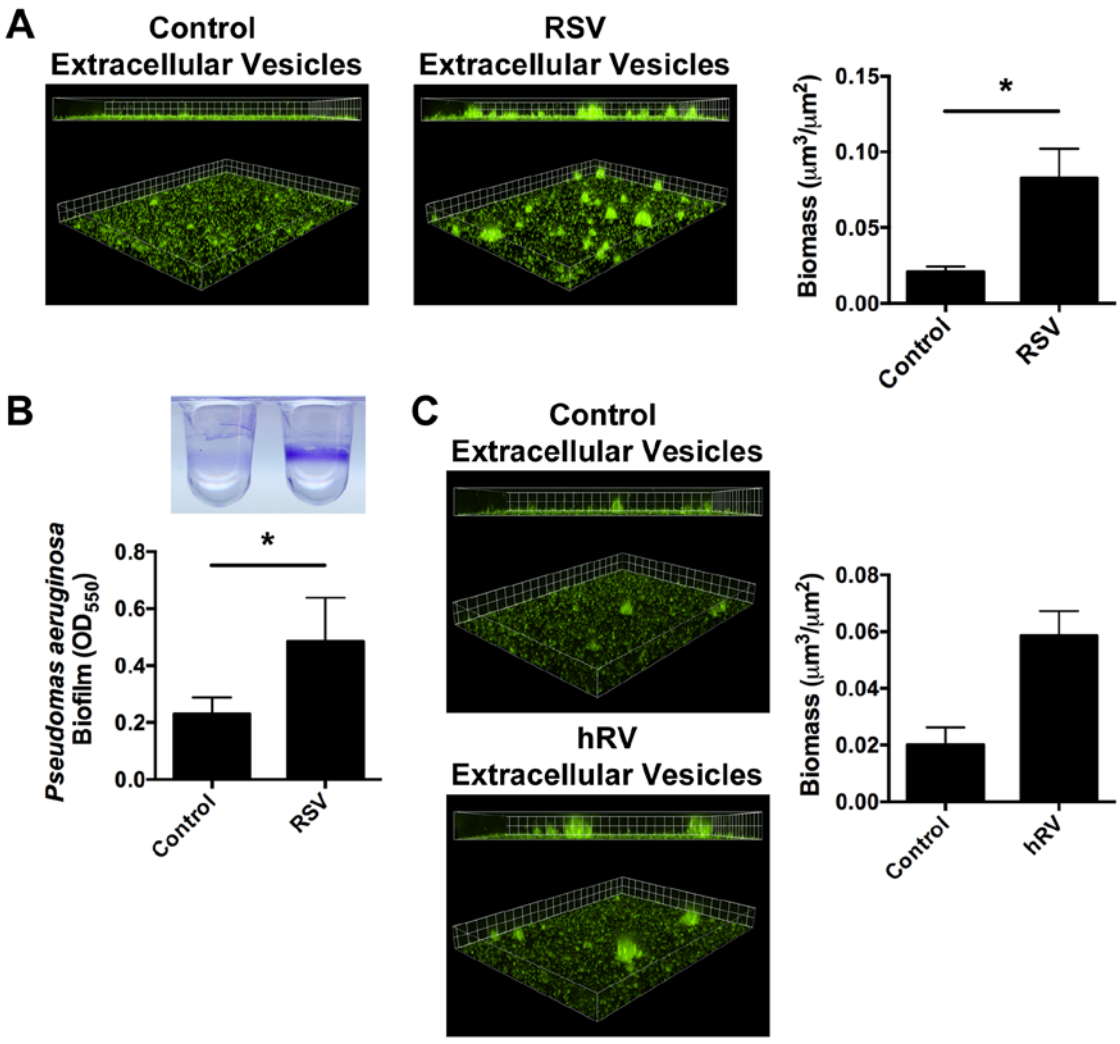

Figure 23: Respiratory viral-infected AECs release EVs that stimulate *P. aeruginosa* biofilm growth.

(A and B) AECs were infected with RSV or mock infected (MEM control) for 72 hr and then EVs were isolated from apical CM. (A) *P. aeruginosa* (GFP) was grown in the presence of isolated EVs in static abiotic biofilm assays. Fluorescent microscopy was used to measure the growth of *P. aeruginosa*, and biomass was quantified by Nikon Elements (grid unit = 8 μm) (B) *P. aeruginosa* biofilms were grown for 24 hr in 96-well microtiter biofilm assay. Biomass was quantified by crystal violet staining and absorbance was measured at 550 nm. (C) AECs were infected with hRV (MOI = 0.1) or mock infected (MEM control) for 72 hr and then EVs were isolated from apical CM. *P. aeruginosa* (GFP) biofilms were grown in the presence of EVs in static abiotic biofilm assays. Biofilm biomass was quantified using Nikon Elements (grid unit = 10 μm). Control, EVs from mock-infected AECs; RSV, EVs from RSV-infected AECs. For all experiments n ≥ 3. Data are presented as mean ± SD; *$P < 0.05$ versus control.

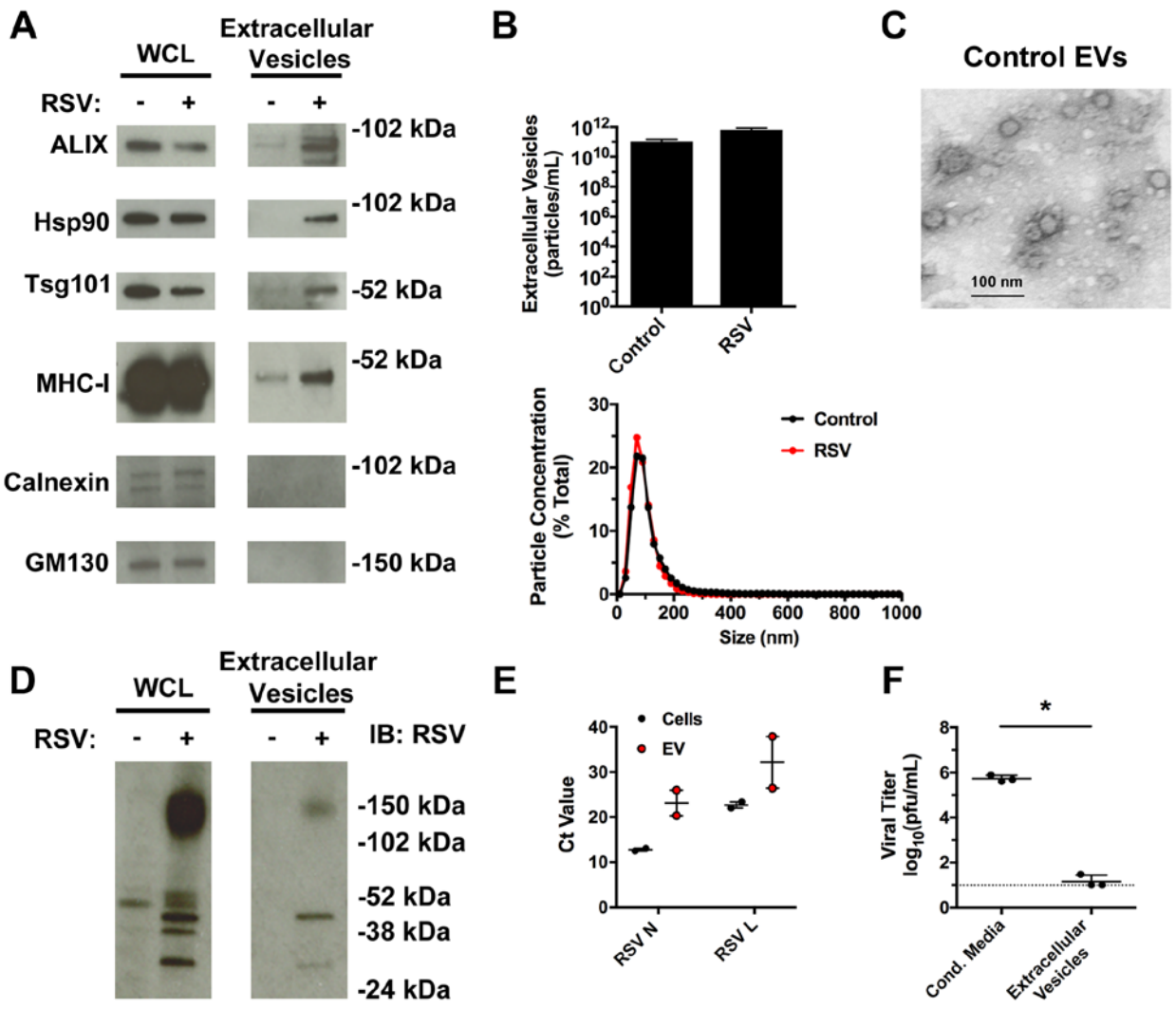

Figure 24: Characterization of EVs released by AECs.

EVs were prepared from AECs following 72 hr infection with RSV or mock infected (MEM control). (A) Western blot analysis of EV and non-EV marker proteins in whole cell lysates (WCL) and EVs. n=3. (B) Nanoparticle Tracking Analysis (NTA) of EVs released by AECs. n=2. (C) Electron microscopy of EVs prepared from mock-infected AECs was performed to verify the size and morphology of AEC-released vesicles. (D) Western blot analysis of RSV proteins in WCL and EV preparations. IB = immunoblot. n=3. (E-F) EVs were prepared from AECs following 72 hr RSV infection. qRT-PCR analysis was performed for the RSV N and L genes in cells and in EVs prepared from those cells. n=2. (F) Plaque assay of conditioned media (Cond. Media) and EVs collected from AECs infected with RSV for 72 hr. n= 3. Data are presented as mean ± SD; *P < 0.05 versus control.

To further examine the mechanism by RSV EVs stimulate *P. aeruginosa* biofilm growth, we next investigated whether EVs from RSV-infected AECs increase bacterial attachment to an abiotic surface. We found that there was no difference in the number of bacteria that attached in the presence of EVs from uninfected and RSV-infected cells (**Figure 25A**). Moreover, there was no difference in *P. aeruginosa* attachment between EVs or in minimal media (MEM) (**Figure 25A**). Because EVs from RSV-infected cells stimulated biofilm growth but did not increase bacterial attachment, we hypothesized that EVs from RSV-infected AECs increase bacterial growth. To test this hypothesis, we compared the growth of *P. aeruginosa* in EVs isolated from uninfected and RSV-infected AECs, and we found that RSV EVs significantly enhanced *P. aeruginosa* growth compared to EVs from uninfected cells (**Figure 25B**). Taken together, these results indicate that EVs isolated from RSV-infected cells contain biofilm stimulatory molecules, which are either absent or present in significantly reduced levels on EVs from uninfected AECs, to promote *P. aeruginosa* bacterial growth and biofilm formation.

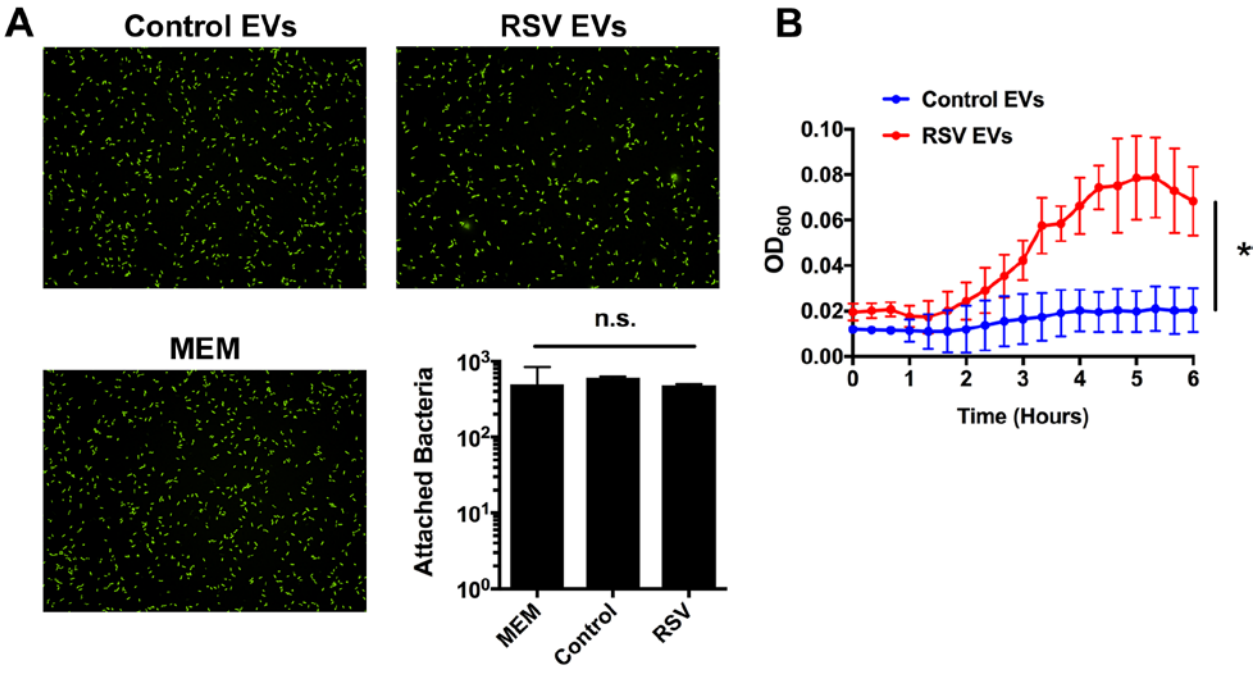

Figure 25: RSV EVs increase *P. aeruginosa* growth but not adherence to abiotic surfaces.

(A) *P. aeruginosa* (GFP) was grown in the presence of EVs isolated from AECs in static abiotic biofilm assays. After 1 hr, any unattached bacteria were washed away and attached bacteria were measured using fluorescent microscopy. Nikon Elements was used to count bacteria. (B) Growth kinetics in EVs isolated from AECs infected with RSV or mock-infected (MEM control) for 72 hr. For all experiments n ≥ 3. Data are presented as mean ± SD; *$P < 0.05$ versus control.

4.2.2 RSV infection increases iron bioavailability on extracellular vesicles to promote biofilm growth

Iron is required for many biological processes, including *P. aeruginosa* biofilm growth on both abiotic and biotic surfaces [27, 37, 43, 204]. We have previously observed that RSV infection increases extracellular iron in CM collected from AECs (**Figure 17**). However, it is not known if iron and other metals are loaded into EVs released by the respiratory epithelium. To examine if

EV contain iron and RSV infection altered iron abundance in EVs, we measured total iron in EVs collected from uninfected and RSV-infected AECs and observed that RSV infection increased total iron in EVs isolated from AECs (**Figure 26A**). Although iron is necessary for *P. aeruginosa* biofilm formation, other transition metals are abundant in biological systems and are involved in important physiological processes. For example, zinc supplementation has recently been shown to increase *P. aeruginosa* biofilm growth [347]. In addition, copper is a redox-active metal that participates in many redox reactions in bacteria and has been shown to be increased in the sputum of CF patients, along with zinc and iron [30, 348]. Therefore, we also measured the abundance of other transition metals in extracellular vesicles to determine if virus infection was increasing the abundance of other metals in EVs. We found that virus infection caused a slight increase in zinc concentrations in EVs, but that copper concentrations were unchanged by RSV infection (**Figure 26B-C**).

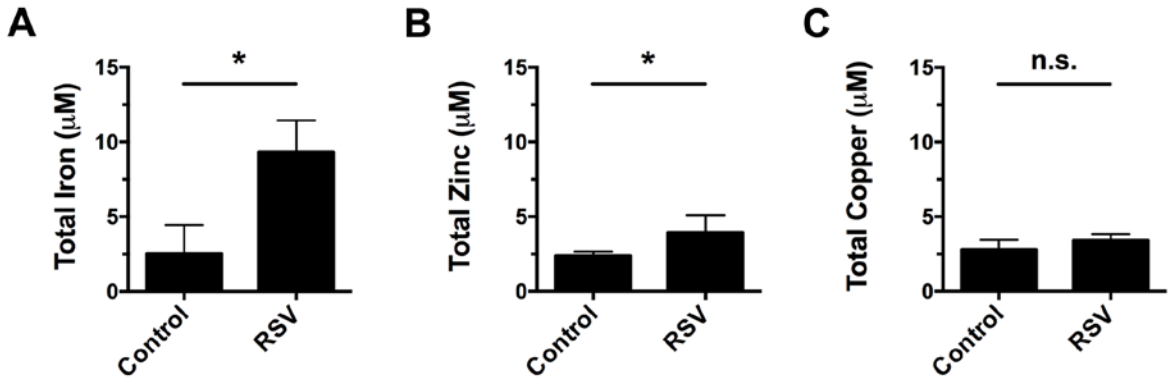

Figure 26: RSV infection increases iron release on EVs.

AECs were infected with RSV or mock-infected (MEM control) for 72 hr and EVs were isolated from apical CM. (A) Total iron, (B) zinc, and (C) copper in the EVs from AECs. RSV, RSV-infected AECs. For all experiments n ≥ 3. Data are presented as mean ± SD; **P* < 0.05 versus control.

Importantly, the presence of iron was necessary for *P. aeruginosa* biofilm growth in the presence of EVs isolated from RSV-infected cells because chelation of iron, using the iron-chelating agent Chelex-100, significantly decreased biofilm formation in the presence of EVs (**Figure 27A**). NTA was performed after Chelex-100 treatment to verify that EV abundance or morphology was not changed by iron chelation (**Figure 27B**). Future experiments will test the hypothesis that adding back exogenous iron sources to chelated EVs will restore biofilm growth. Taken together, these results suggest that *P. aeruginosa* utilizes iron localized on EVs to form biofilms during RSV coinfection. Moreover, RSV infection increases total iron abundance in EVs released by AECs, thereby increasing iron bioavailability for *P. aeruginosa* biofilm growth.

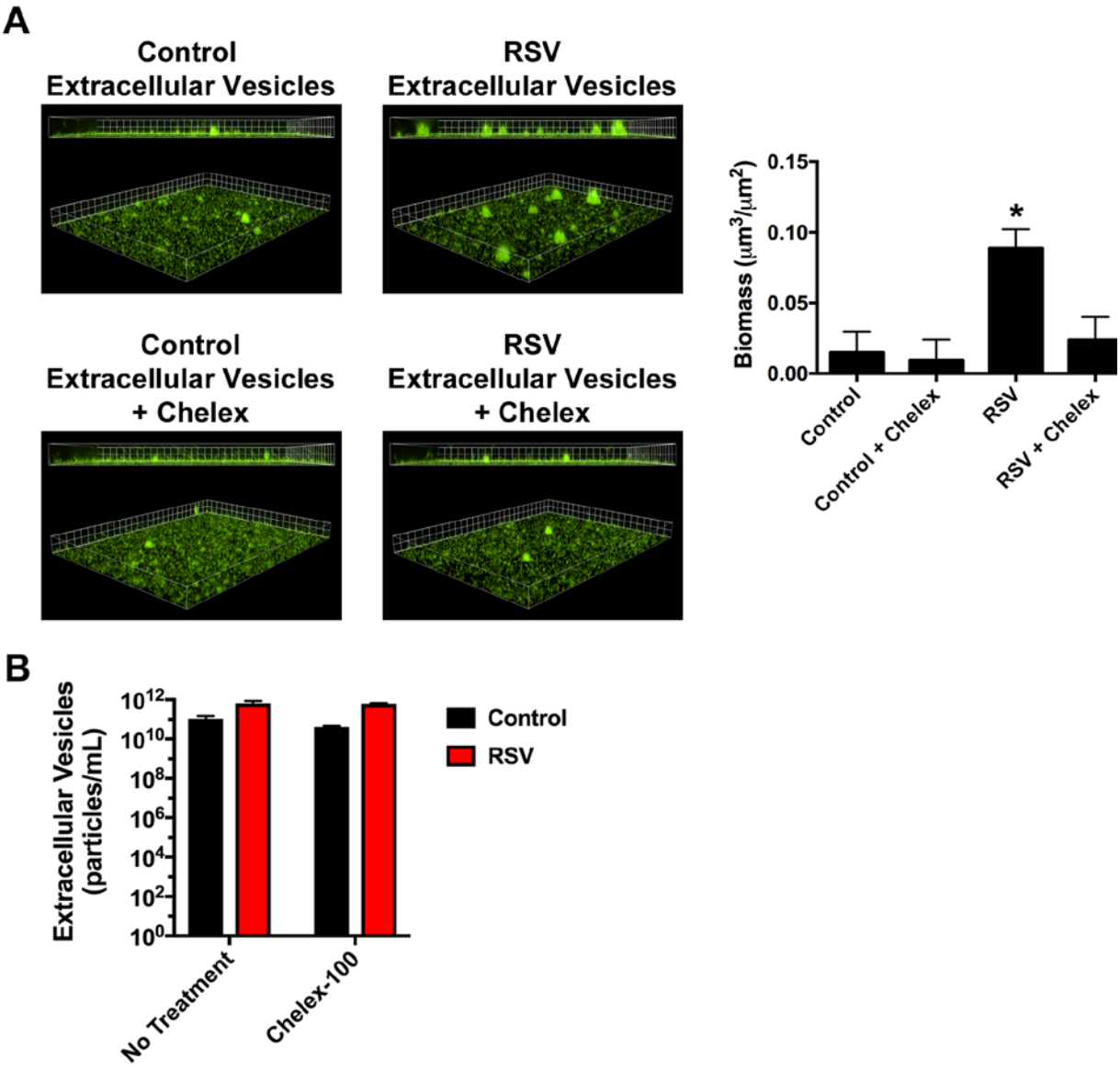

Figure 27: Iron is required for *P. aeruginosa* biofilm growth.

EVs were isolated from AECs infected with RSV or mock-infected (MEM control) for 72 hr. Divalent metal cations were chelated with Chelex-100 (labeled "+ Chelex"). (A) *P. aeruginosa* (GFP) was grown in the presence of EVs in static abiotic biofilm assays and fluorescent microscopy was used to measure biofilm growth. Nikon Elements was used to quantify biofilm growth (grid unit = 8.0 μm). RSV, RSV-infected AECs. For all experiments $n \geq 3$. Data are presented as mean ± SD; *$P < 0.05$ versus control. (B) NTA analysis of EVs before and after Chelex-100 treatment. n=2.

4.2.3 RSV infection increases transferrin abundance on extracellular vesicles

Nutritional immunity postulates that the host restrict the availability of nutrients from bacteria and other pathogenic microorganisms. In regard to metal restriction, one the strategies utilized by the host is the chelation of metals with high-affinity proteins that sequester metals from pathogens, such as lactoferrin and transferrin. In response to iron limitation *P. aeruginosa* increases the production of the siderophores pyochelin and pyoverdine [205]. Thus, we measured pyoverdine production during *P. aeruginosa* biofilm growth in the presence of EVs to determine whether EVs provide an iron-restricted or iron-replete environment for biofilm formation. We observed that pyoverdine production in the presence of EVs is not changed by RSV infection (**Figure 28A**). Moreover, the levels of pyoverdine produced by *P. aeruginosa* grown in the presence of EVs mirrored pyoverdine production in iron-restricted environments (i.e. MEM or iron-bound transferrin) (**Figure 28A**). Conversely, pyoverdine production was significantly higher when *P. aeruginosa* biofilms were grown in the presence of EVs compared to an iron-replete environment (i.e. $FeCl_3$) (**Figure 28A**). In these experiments, we grew *P. aeruginosa* in the same levels of iron as measured in our EV preparations (i.e. 10 μM $FeCl_3$ and 5 μM holo-transferrin). Taken together, these data suggest that iron associated with EVs is sequestered from *P. aeruginosa* and is likely bound to host-iron binding proteins loaded into the vesicles.

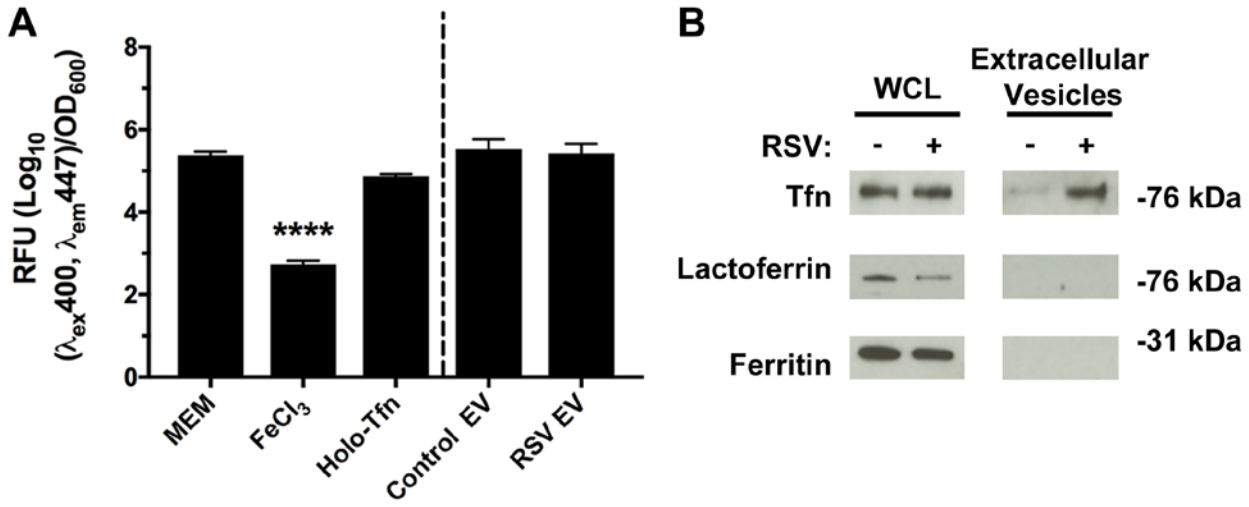

Figure 28: RSV infection increases transferrin abundance in EVs.

EVs were isolated from AECs infected with RSV or mock-infected (MEM control). (A) *P. aeruginosa* was grown in the presence of EVs, $FeCl_3$ (10 μM) or holo-transferrin (5 μM) in static abiotic biofilm assays. At the end of assays, supernatants were removed and analyzed for pyoverdine (excitation: 400 nm, emission: 447 nm) and normalized to the density of bacteria (OD_{600}). (B) RSV infection increases transferrin abundance in EVs, as measured by Western blot analysis. RSV, RSV-infected AECs. For all experiments $n \geq 3$. Data are presented as mean ± SD; $^*P < 0.05$ versus control.

Because RSV infection increases iron abundance in our EV preparations and *P. aeruginosa* responds to EVs with increased pyoverdine production, we next examined whether RSV infection alters the release of iron-binding proteins on EVs that may sequester iron. Interestingly, we found that RSV infection increased the abundance of only transferrin within our preparations of EVs (**Figure 28B**). Transferrin supports the growth of many bacterial species, including *P. aeruginosa*, and is a component of airway secretions that can promote *P. aeruginosa* biofilm growth [27]. Importantly, we have previously shown RSV infection increases the apical release of transferrin, and that biofilm growth in the presence of RSV coinfection

requires transferrin secretion from AECs (**Figure 20B**). Collectively, these results demonstrate that RSV infection of AECs increases apical transferrin release on EVs.

4.2.4 RSV infection increases transcytosed transferrin release on EVs in the apical compartment

Because transferrin is primarily a serum glycoprotein that is taken up and recycled at the basolateral membrane of cells, we next determined whether transferrin in the basolateral compartment of cells is transcytosed and released apically on EVs. We have previously determined that RSV infection promotes the transcytosis of transferrin from the basolateral to apical compartment of cells (**Appendix A**), but it is unknown if the transcytosed transferrin is released on EVs. We determined whether transferrin is transcytosed apically and loaded on EVs during RSV infection by adding biotinylated transferrin to the basolateral media and then assayed for biotinylated transferrin on EVs 24 hours later (**Figure 29A**). We found that biotinylated transferrin was associated with EVs released apically by AECs, and that significantly more biotinylated transferrin was released in association with EVs during RSV infection (**Figure 29B**). Interestingly, we observed that all the transferrin that was associated with apically released EVs was affinity purified due to the absence of transferrin in the supernatant we collected from the streptavidin resin (**Figure 29B**), indicating that the transferrin loaded onto EVs originated in the basolateral compartment. Additionally, we conclude that the transcytosed transferrin was localized to the outside of EVs because streptavidin resin would not have been able to access proteins on the inside of vesicles. This suggests that we would have affinity purified EVs loaded with transferrin in our experiments. To test this hypothesis, probed for marker proteins of EVs and found that ALIX, Tsg101, Hsp90, and MHC-I were affinity

purified with biotinylated transferrin (**Figure 29B**). Interestingly, we observed that CD81 and Flotillin-1, as well as small amounts of ALIX, Tsg101, Hsp90 and MHC-I, were present in the supernatant we collected from the streptavidin resin (**Figure 29B**), indicating these proteins were not affinity purified with biotinylated transferrin. Thus, our data suggest at least two EV populations exist, one of which is transferrin-positive. In addition, we observed that RSV proteins were present in the EV population that was affinity purified with biotinylated transferrin, as well as the vesicle population that was negative for biotinylated transferrin (**Figure 29C**), indicating RSV proteins are present in two EV populations we purified. To determine whether transferrin-positive EVs were necessary for biofilm growth in the presence of EVs from RSV-infected AECs, we grew *P. aeruginosa* in EVs that had been depleted of transferrin-positive vesicles. We found a significant decrease in *P. aeruginosa* biofilm growth in the presence of EVs when transferrin-positive vesicles were removed from our EV preparations (**Figure 29D**). Taken together, these data support that conclusion that at least two EV populations are released by AECs. One of these vesicles populations contains transcytosed transferrin loaded on the outside of vesicles, and are necessary for *P. aeruginosa* biofilm growth in the presence of EVs isolated from RSV-infected AECs.

P. aeruginosa utilizes two siderophores, pyochelin and pyoverdine, to acquire iron. Pyoverdine has a higher affinity for iron and is capable of acquiring iron directly from transferrin [206]. Because we have previously observed that *P. aeruginosa* produces pyoverdine in the presence of EVs and that transferrin is on the outside of EVs, we hypothesized that *P. aeruginosa* acquires iron from EVs using its siderophores during biofilm growth. Our lab has previously demonstrated that a *P. aeruginosa* mutant (Δ*pvdA*Δ*pchE*) unable to produce either of its siderophores (pyoverdine or pyochelin) has a decreased ability to form biofilms during RSV

co-infection where iron-loaded transferrin abundance is increased. We found that *P. aeruginosa* biofilm growth in the presence of EVs from RSV-infected cells was reduced with a Δ*pvdA*Δ*pchE* mutant compared to wild type *P. aeruginosa* (**Figure 30**). Collectively, these results suggest that *P. aeruginosa* siderophores are required for the full biofilm induction observed in the presence of EVs isolated from RSV-infected AECs. EVs are a likely source of multiple nutrients besides iron-loaded transferrin, and our data indicate that the nutrient-rich environment potentially provided by EVs is not able to overcome the absence of this iron acquisition mechanism in *P. aeruginosa*.

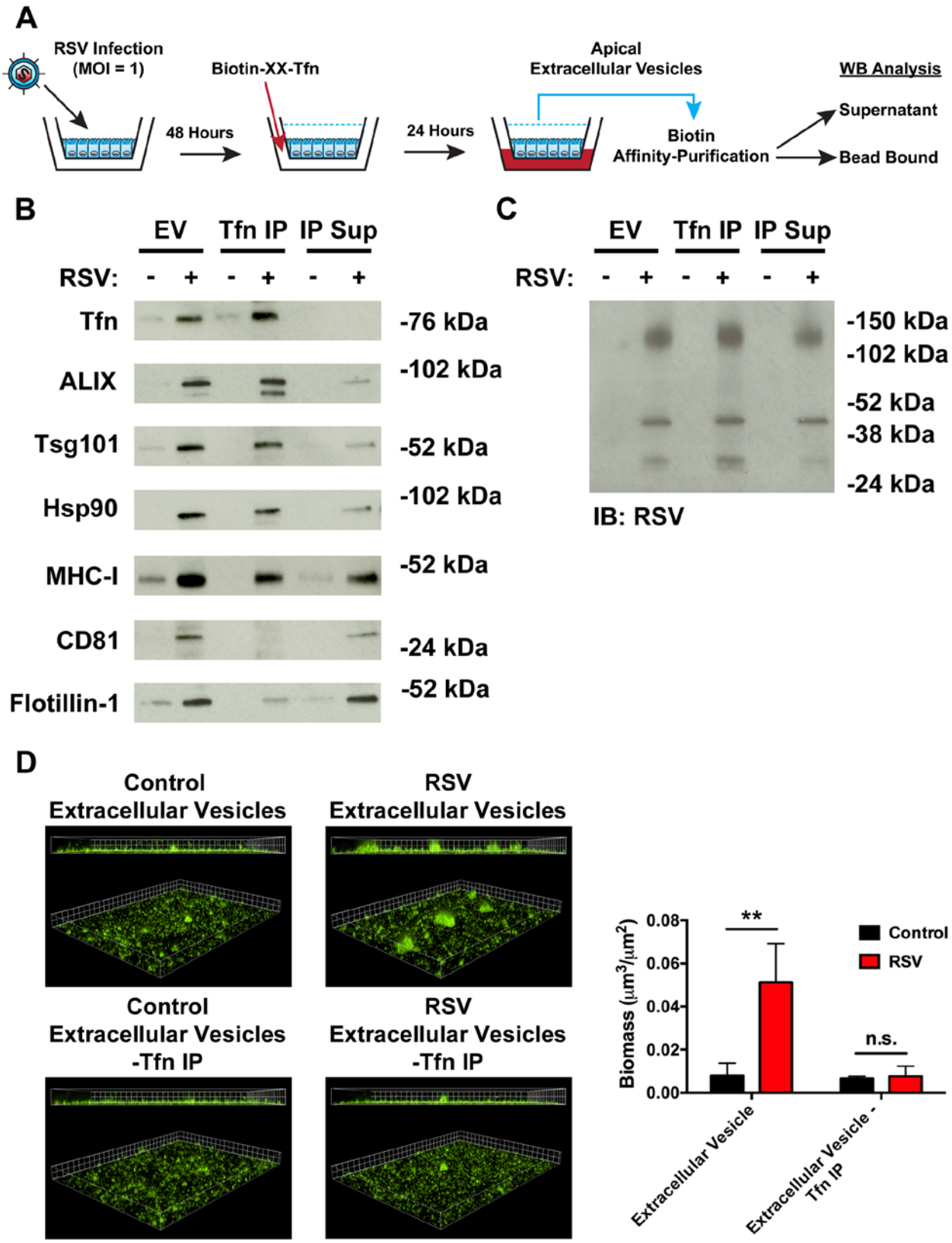
A
RSV Infection
(MOI = 1)
48 Hours
Biotin-XX-Tfn
24 Hours
Apical
Extracellular Vesicles
Biotin
Affinity-Purification
WB Analysis
Supernatant
Bead Bound
B
EV
Tfn IP
IP Sup
RSV: - + - + - +
Tfn
ALIX
Tsg101
Hsp90
MHC-I
CD81
Flotillin-1
-76 kDa
-102 kDa
-52 kDa
-102 kDa
-52 kDa
-24 kDa
-52 kDa
C
EV
Tfn IP
IP Sup
RSV: - + - + - +
-150 kDa
-102 kDa
-52 kDa
-38 kDa
-24 kDa
IB: RSV
D
Control
Extracellular Vesicles
RSV
Extracellular Vesicles
Control
Extracellular Vesicles
-Tfn IP
RSV
Extracellular Vesicles
-Tfn IP
Biomass (μm³/μm²)
0.08
0.06
0.04
0.02
0.00
**
n.s.
Control
RSV
Extracellular Vesicle
Extracellular Vesicle -
Tfn IP

Figure 29: Transferrin released on EVs in the apical compartment of AECs is transcytosed.

(A) AECs were infected with RSV or mock-infected (MEM control) for 48 hr. Biotin-transferrin was added to the basal chamber of RSV or mock-infected AECs at a final concentration of 25 μg/mL. EVs were collected from the apical CM of AECs 24 hours later and biotinylated-transferrin was affinity-purified from EV preparations with streptavidin-coated beads. Bead-bound proteins, which are positive for biotin, were eluted from the resin with Laemmli Sample Buffer supplemented with dithiothreitol (DTT) (Tfn IP) and separated by SDS-PAGE. Supernatant from the streptavidin resin (IP Sup), which are negative for biotin, was also separated by SDS-PAGE. (B) Transcytosed transferrin and protein markers of EVs proteins were measured by Western blot analysis in Tfn IP (biotin-positive) and IP Sup (biotin-negative) fractions. (C) Tfn IP (biotin-positive) and IP Sup (biotin-negative) fractions were analyzed by western blot analysis for RSV proteins. IB = immunoblot. (D) *P. aeruginosa* (GFP) was grown in the presence of EVs in static abiotic biofilm assays following biotin affinity purification to remove transferrin-positive vesicles. Biofilm growth was measured by fluorescent microscopy, and biomass quantified by Nikon Elements (grid unit = 7.5 μm). For all experiments $n \geq 3$. Data are presented as mean ± SD; $*P < 0.05$ versus control.

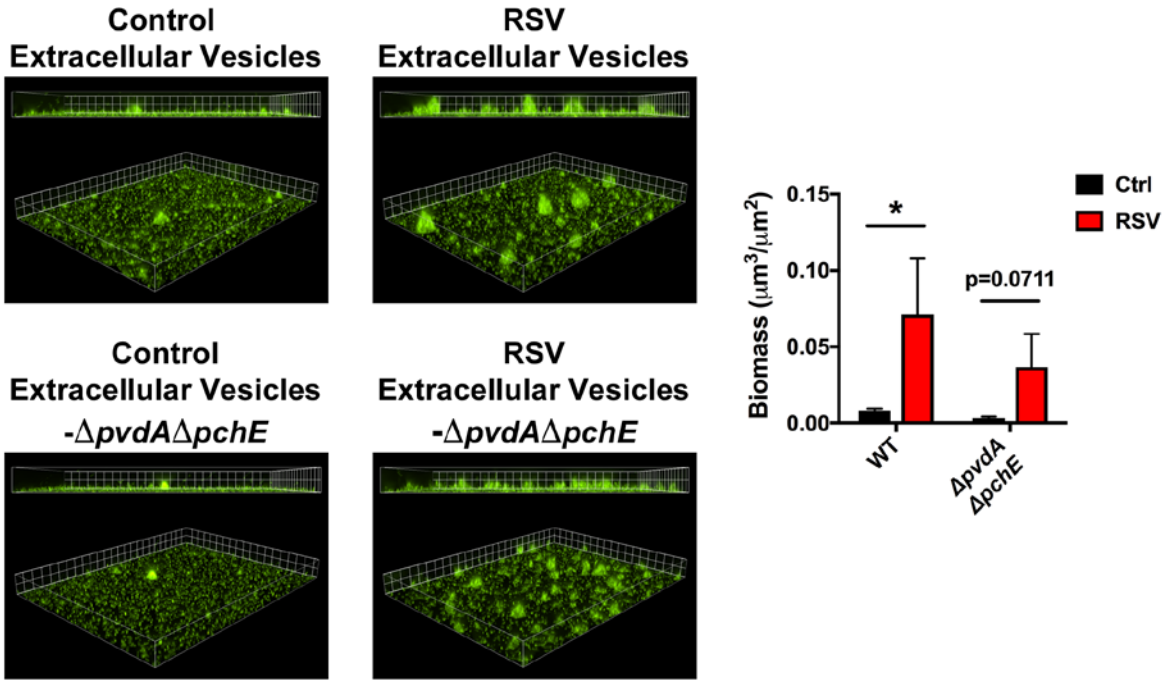

Figure 30: Biofilm formation of *P. aeruginosa* Δ*pvdA*Δ*pchE* mutant in presence of EVs.

(A and B) AECs were infected with RSV or mock infected (MEM control) for 72 hr and then EVs were isolated from apical CM. (A) *P. aeruginosa* WT or Δ*pvdA*Δ*pchE* mutant (GFP) was grown in the presence of isolated EVs in static abiotic biofilm assays. Fluorescent microscopy was used to measure the growth of *P. aeruginosa*, and biomass was quantified by Nikon Elements (grid unit = 9 μm)**.** For all experiments n ≥ 3. Data are presented as mean ± SD; **P* < 0.05 versus control.

4.2.5 Extracellular vesicles interact with *P. aeruginosa*

EVs commonly deliver biologically molecules (i.e. proteins, RNAs and/or lipids) to modify the function of recipient cells. Because we observed that EVs isolated from RSV-infected AECs stimulated *P. aeruginosa* biofilm growth, we focused on determining whether EVs deliver biofilm stimulatory molecules to bacteria during RSV infection. To begin testing this hypothesis,

we first examined whether *P. aeruginosa* can interact with fluorescently labeled EVs from uninfected and RSV-infected AECs. We used the CellTracker Deep Red, a fluorescent dye that labels the cytoplasm of cells, and thus, the inside of EVs released by AECs (**Figure 31A**). We then isolated EVs from uninfected and RSV-infected cells and measured the ability of *P. aeruginosa* to bind fluorescently labeled EVs when grown in the presence of these vesicles. We observed that EV association with *P. aeruginosa* increases over time, and interestingly, that *P. aeruginosa* associated with a greater amount of EVs isolated from RSV-infected than uninfected cells (**Figure 31B**). This is likely a consequence of RSV infection promoting increased EV release from AECs (**Figure 23**). However, these experiments were carried out over short intervals with planktonic bacteria and did not examine whether EVs associated with *P. aeruginosa* during biofilm development. Therefore, to further test whether EVs associate with *P. aeruginosa*, we performed static abiotic biofilm assays with EVs and measured EV association with *P. aeruginosa* biofilms by Western blot analysis. We observed the presence of host EV marker proteins (MHC-I and TfnR) in bacterial biofilms (**Figure 31C**), confirming an increased association of EVs from RSV-infected cells with *P. aeruginosa* biofilms. Further experiments will need to be performed to validate the interaction of EVs with *P. aeruginosa*, and we have plans to perform flow cytometry and fluorescent microscopy to confirm the interaction between *P. aeruginosa* and fluorescent EVs. Collectively, these results demonstrate that AEC-derived EVs interact with *P. aeruginosa*.

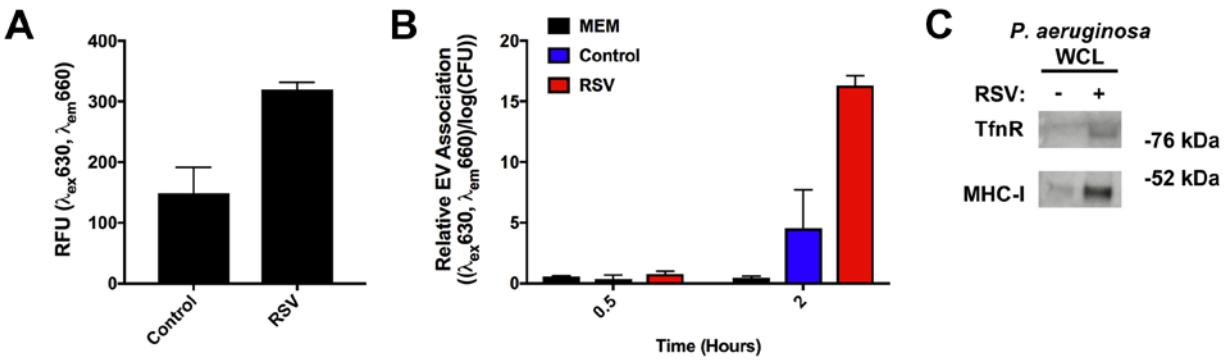

Figure 31: EVs associate with *P. aeruginosa*.

AECs were infected with RSV or mock-infected (MEM control). 48 hpi AECs were stained with CellTracker Deep Red and EVs were isolated from cells 24 hours later. (A) Fluorescence of EV preparations was measured with fluorescent plate reader (excitation: 630 nm, emission: 660 nm). (B) *P. aeruginosa* was grown in the presence of fluorescent EVs for the indicated number of hours and then washed with MEM two times. *P. aeruginosa* fluorescence was measured with plate reader (excitation: 630 nm, emission: 650 nm). (C) *P aeruginosa* biofilms were grown in the presence of EVs in static abiotic biofilm assays, and Western blot analysis of *P. aeruginosa* biofilm whole cell lysate (WCL) was used to measure the association of EVs with *P. aeruginosa* biofilms. RSV, RSV-infected AECs. n=2. Data are presented as mean ± SD.

To validate the importance of transferrin loading onto EVs for *P. aeruginosa* biofilm induction by EVs isolated from RSV-infected AECs, we grew *P. aeruginosa* in the presence of either free iron or free iron-bound transferrin (**Figure 32**) we observed that biofilm formation was significantly less than in the presence of EVs from RSV-infected cells. Because the iron amounts we used were equivalent to what was measured on EVs isolated from RSV-infected cells, these data imply that the delivery of iron on EVs is important for promoting *P. aeruginosa* biofilm growth during RSV coinfection. Taken together, these results are consistent with the conclusion that RSV infection increases transcytosed transferrin on EVs, thereby providing an accessible iron source for *P. aeruginosa* during biofilm growth. Additionally, these results

suggest that EVs released by AECs during RSV infection interact with *P. aeruginosa* and this may be a mechanism by which nutrient-rich microenvironments are created near the bacteria to promote biofilm growth.

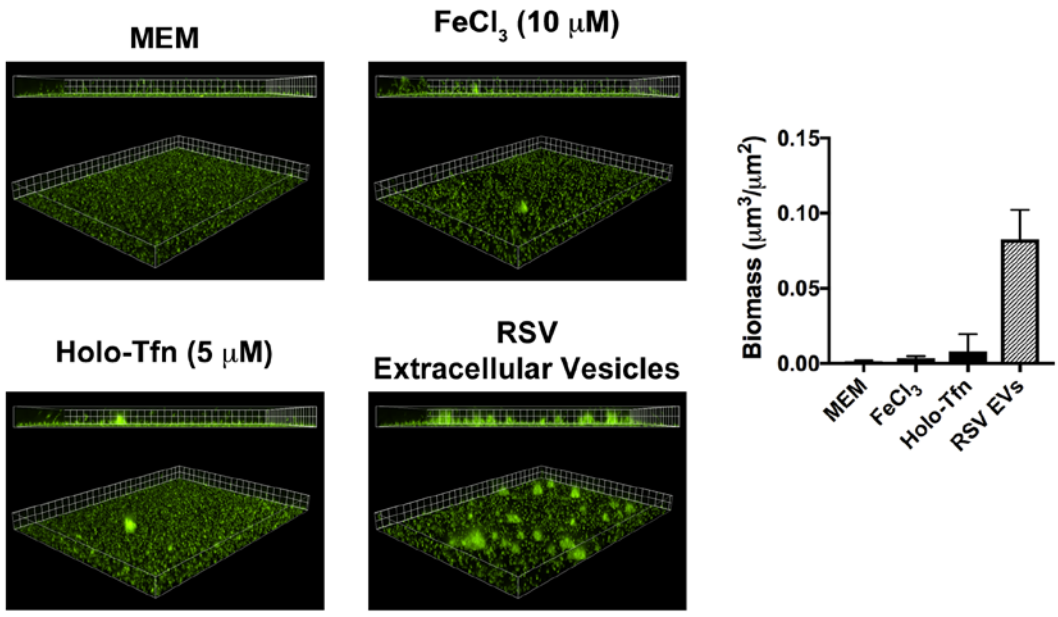

Figure 32: Free iron sources do not stimulate *P. aeruginosa* biofilm growth.

P. aeruginosa was grown in the presence of $FeCl_3$ or holo-transferrin in static abiotic biofilm assays. Biofilm growth was measured by fluorescent microscopy and Nikon Elements was used to quantify biomass (grid unit = 7.5 μm). Representative static abiotic biofilm assay in the presence of EVs isolated from AECs infected with RSV (72 hr infection) is shown for comparison. Biomass of *P. aeruginosa* biofilm growth in the presence of EVs isolated from RSV-infected cells is shown with hatched bar (data obtained from **Figure 23A** for comparison). No significant difference in *P. aeruginosa* biofilm growth was observed between different iron sources and MEM. RSV, RSV-infected AECs. EVs, Extracellular Vesicles. For all experiments n = 3. Data are presented as mean ± SD.

4.3 DISCUSSION

EVs are membrane-encapsulated vesicles released by most cell types, including in the airways, into the extracellular environment that facilitate physiological changes in neighboring cells. Although EVs have been studied in the context of viral pathogenesis to modify the local environment to the benefit of the host or the virus [217], very little is understood about the role of EVs in polymicrobial infections in the respiratory tract. Here, we demonstrated that EVs released from the respiratory epithelium during RSV infection stimulates *P. aeruginosa* biofilm growth through a mechanism dependent upon increased iron-loaded transferrin release on EVs. The transferrin is oriented on the outside of vesicles, which makes it an accessible iron source for *P. aeruginosa* biofilm formation. Moreover, we show the EVs associate with *P. aeruginosa* and that EVs loaded with iron-bound transferrin are much more efficient at stimulating *P. aeruginosa* biofilm growth than free iron or iron-bound transferrin of equal concentrations. Importantly, our findings propose a novel role for EVs during viral-bacterial co-infections as a virally-induced nutrient source for bacteria. Our studies provide further understanding for the clinical observation that respiratory viral infection promotes chronic bacterial infections in patients with chronic lung disease [53, 71, 72, 79]. Importantly, the findings presented here further demonstrate that respiratory viral infection alters the lung environment to make it more susceptible to secondary bacterial infection, and increases our understanding how viruses and bacteria interact in the lung.

Although EVs are known to be secreted into the airways [338, 343], very little is known about the biological function of EVs during respiratory infections. During virus infection in other organs, EVs are known to facilitate viral spread by protecting the genomes from antibody-mediated neutralization or transferring pro-viral molecules between cells [250-252].

Alternatively, it is also known that EVs can transfer antiviral molecules between cells that inhibit virus infection [216, 266], or may contain molecules with neutralizing activity against viruses, as has been shown with respiratory epithelial-derived EVs that contain sialic acid [339]. How EVs impact the outcome of viral-bacterial infections or how host-derived EVs influence bacterial behavior in the airways remain unanswered questions. In our study, RSV infection increases the apical release of EVs from AECs to promote *P. aeruginosa* growth and biofilm development. We interpret these findings to suggest that during respiratory viral infection the airway epithelium releases EVs that interact with bacterial pathogens to create a local nutrient-rich environment at the mucosal surface that promotes bacterial biofilm growth, which are associated with chronic infections. The increased release of EVs from the respiratory epithelium is consistent with other studies that have observed epithelial cells increase EV release in response to stress (i.e. infection.) [250, 349-351]. Interestingly, our study demonstrates that increased EV release in response to one infection promotes a secondary infection.

Previous studies of viral-bacterial interactions in the respiratory tract have mainly identified two mechanisms by which virus infection promotes secondary bacterial infections and decreases bacterial clearance: (i) increased bacterial adherence to virally infected cells, and (ii) alterations in the antibacterial immune response induced by viral infection [352]. Recently, studies have begun investigating how the nutritional environment in the airways is altered by respiratory viral infections to the benefit of bacteria. For example, it has been shown that influenza A infection increases the abundance of sialylated mucins in the airways, which is used as a nutrient source that promotes *S. pneumoniae* growth [353]. In the work presented in this dissertation, we have shown the RSV infection increases iron levels in the airway surface liquid to promote *P. aeruginosa* biofilm growth (**Chapter 3**). Here, we have extended these studies to

show that the release of iron on EVs released by AECs is one mechanism by which RSV infection promotes *P. aeruginosa* biofilm growth. EVs contain biologically active proteins, lipids and RNAs, and our study demonstrates that iron, and potentially other nutrients, are also present on host-derived EVs and contribute to host-pathogen interactions in the airways.

Iron is required for many biological processes in humans, but it is tightly regulated to limit the levels of accessible iron during an infection and to prevent iron intoxication by a process that is termed nutritional immunity [182, 187]. Previous studies have demonstrated the requirement of iron for *P. aeruginosa* biofilm formation [27, 37, 43, 204]. Moreover, bacterial burden and decreased pulmonary function are correlated with increased iron levels in the CF lung [25, 28], but the impact of respiratory viral infections on the nutritional environment in the airways is not well understood. We have previously shown that RSV infection dysregulates this process to promote the apical release of iron-loaded transferrin to stimulate *P. aeruginosa* biofilm growth (**Chapter 3**), but the mechanism by which iron-loaded transferrin was released by AECs was unidentified. Our current study suggests that one mechanism by which RSV infection increases the release of iron-loaded transferrin is on EVs from the respiratory epithelium. Importantly, the transferrin is localized on the outside of EVs, making it accessible to bacterial pathogens, and iron chelation significantly reduced biofilm growth in the presence of EVs released by RSV infected cells, suggesting that iron chelation is a potential therapeutic strategy to disrupt EV-mediated biofilm growth during virus infection. Previous results have demonstrated that iron chelation inhibits *P. aeruginosa* biofilm growth on AECs and that iron chelators augment antibiotic-mediated disruption of biofilms on cells [27, 49, 354]. Due to our incomplete knowledge on the biological importance of EVs to airway physiology, iron chelators may be an important and most effective therapeutic strategy that effectively counteracts EV-

mediated bacterial infections in the airways of CF patients during respiratory viral seasons. Furthermore, it will be imperative in future studies to determine if other nutrients besides iron are loaded onto EVs and can be utilized as a nutrient source by *P. aeruginosa*.

Our study demonstrates that iron-loaded transferrin is localized to the outside of EVs, thereby making the iron accessible to bacterial pathogens that are able to circumvent transferrin-mediated iron sequestration. *P. aeruginosa* is particularly proficient at acquiring iron from the environment, and has been shown to overcome transferrin-mediated iron sequestration through the production of siderophores [206]. Our data demonstrate that a Δ*pvdA*Δ*pchE* mutant unable to produce siderophores has a reduced ability to form biofilms in the presence of EVs from RSV-infected cells. Whether *P. aeruginosa* uses other mechanisms to overcome transferrin-mediated iron sequestration and acquire iron from EVs is an area of future investigation. Previously, we have demonstrated *P. aeruginosa* produces proteases capable of degrading transferrin (**Appendix A**), but determining whether transferrin and other surface proteins loaded onto EVs are degraded by *P. aeruginosa* is unknown but could help define the interaction that exists between *P. aeruginosa* and EVs. Moreover, longitudinal analysis of *P. aeruginosa* clinical isolates from CF patients suggest that pyoverdine production is higher in early isolates and that later isolates have increased expression of other iron-acquisition systems (i.e. heme-acquisition systems) [212, 213]. It will be of interest to see if EVs from RSV-infected cells stimulate *P. aeruginosa* biofilm growth with early and late clinical isolates, or if the interaction between EVs and *P. aeruginosa* changes over time.

EVs commonly exert their biological effects on the local environment by delivering biologically molecules (i.e. proteins, RNAs and/or lipids) to recipient cells. Although the interaction between host-derived EVs and bacteria has not been investigated before, our data

suggest that EVs derived from the airway epithelium associate with *P. aeruginosa*, regardless of RSV infection. We interpret these results, coupled with increased iron-bound transferrin bound to EVs-derived from RSV infected cells, to indicate that EV association with *P. aeruginosa* during RSV coinfection creates a microenvironment that is rich in nutrients and promotes bacterial biofilm formation. Previous reports have demonstrated that host-derived EVs bind to the surface of parasites, which either protects parasites from immune-mediated lysis or promotes parasite killing depending upon the type of infection and cell type that produces the EVs [351, 355]. It is not clear what mechanism is responsible for EV association with *P. aeruginosa*, but interesting areas of future investigation will be aimed at understanding if the association of EVs with bacteria is specific to *P. aeruginosa*, how EVs associate with bacteria, and what bacterial and host factors are required for the interaction between *P. aeruginosa* and EVs. Moreover, it will be interesting to see if host molecules are delivered directly into the periplasm of *P. aeruginosa* and thereby, bypassing its outer membrane. Also, it is not known if EVs derived from other cell types also interact with bacteria. Although these questions were beyond the scope of this study, they are interesting areas of future investigation that could potentially have implications for drug delivery.

Due to the structural similarity between RNA virus particles and EVs, which may contain viral components, it is extremely difficult to specifically separate virions and EVs, and it has been suggested that during virus infection a diverse population of vesicles are released from cells [217, 226]. We observed that at least two distinct subpopulations of EVs were released from AECs during RSV infection, one of which were transferrin-positive EVs. Because depletion of transferrin-positive EVs significantly reduced *P. aeruginosa* biofilm growth in the presence of EVs from RSV-infected cells, we conclude that this subpopulation of EVs was responsible for

the biofilm stimulatory effect of EVs released during RSV infection. Thus, we interpret our findings to suggest that during RSV infection a diverse population of EVs are released by AECs, and that it is specifically the increase in the subpopulation of transferrin-positive EVs that is responsible for increased *P. aeruginosa* biofilm growth.

Clinical studies strongly correlate respiratory viral infection with the acquisition of chronic *P. aeruginosa* infection in CF patients, as well as poor bacterial clearance in other lung diseases as a result of viral-bacterial coinfections, but the mechanisms underlying these interactions remain poorly understood. In this report, we demonstrate that respiratory viral infection increases the release of EVs from epithelial cells in the airways and are utilized as a nutrient source for secondary bacterial infection. Our data suggest a novel nutrient acquisition pathway for bacteria and provide mechanistic insight into nutritional immunity in the lung. Because it is appreciated that many infectious diseases are polymicrobial and EVs are released by most cell types throughout the body, our studies likely have implications for host-pathogen and pathogen-pathogen interactions in other diseases.

5.0 IMPLICATIONS OF DISSERTATION: CONCLUSIONS AND FUTURES DIRECTIONS

In this dissertation, we have provided mechanistic understanding for the clinical observation that respiratory viral infection is well correlated with *P. aeruginosa* colonization and infection in CF patients by coupling biochemical, cell biological and novel live-cell imaging approaches. Whereas the majority of studies on viral-bacterial interactions in the respiratory tract have focused on alterations in bacterial attachment or host immunity, our studies provide evidence that respiratory viral infections also alter nutrient levels in the airways. Complex and incompletely understood interactions between the host, virus and bacteria determine disease outcomes in these infections. In this body of work, we have specifically addressed questions involving *P. aeruginosa* biofilm growth during viral-bacterial coinfections in the lung, and outlined one mechanism by which respiratory viruses interact with *P. aeruginosa* to promote biofilm formation. Because synergy is often reported between viral and bacterial pathogens and there is a growing appreciation for the prevalence of polymicrobial infections, identifying functional relationships between viruses and bacteria likely has implications for other disease settings besides the CF lung and will provide new insight into important biology at mucosal surfaces.

Our studies demonstrate that respiratory viral infection stimulates the formation of *P. aeruginosa* biofilms on the airway epithelium. We further showed that RSV infection increases the apical release of iron and the host-iron binding protein transferrin from AECs, which were

required for the *P. aeruginosa* biofilm growth during RSV coinfection. We extended these studies to a mouse model of RSV infection and showed that the virus infection increased both iron and transferrin in the airways of mice. Interestingly, BALF from RSV-infected mice was sufficient to stimulate *P. aeruginosa* biofilm growth *in vitro*. Together, these data demonstrated that respiratory viral infection alters iron homeostasis in the lung to increase bioavailable iron to promote secondary bacterial infection. Interestingly, we have also demonstrated that EVs isolated from RSV-infected cells stimulate *P. aeruginosa* biofilm growth. During RSV infection, EV secretion from AECs was significantly enhanced, which led to an increase in iron and transcytosed transferrin associated with EVs. Importantly, we observed that free iron or iron-bound transferrin, added at the same concentration as found in EVs released by RSV-infected cells, did not stimulate *P. aeruginosa* biofilm growth, suggesting that (i) EVs interact with *P. aeruginosa* to bring nutrients into proximity with the bacteria or (ii) EVs contain other molecules that work in tandem with iron to promote the development of biofilms. These are not mutually exclusive hypotheses. We show preliminary data that suggests EVs associate with *P. aeruginosa*, but more experiments are required to validate this observation. Collectively, the two studies presented in this dissertation demonstrate that RSV infection alters the nutritional environment in the airways by promoting the release of iron-bound transferrin. Finally, the innate immune response to virus infection, measured by type I and III interferon (IFN–β and –λ, respectively) production, peaks at the same time as virus-induced biofilm growth, and interestingly, treatment of AECs with IFN–β or –λ replicates the enhanced biofilm formation observed during virus co-infection. However, we did not observe that IFN treatment alone was sufficient to increase iron and transferrin release from AECs (**Appendix B**), suggesting that IFN treatment activates a parallel pathway that stimulates *P. aeruginosa* biofilm growth in the absence of virus infection.

Follow-up studies are now underway to address how IFN treatment enhances *P. aeruginosa* biofilm growth (**Appendix B**). The observations presented here provide the foundation for answering important questions about the early acquisition of bacterial infections in the airways and provide novel insight into nutritional immunity in the lung.

5.1 THERAPEUTIC IMPLICATIONS

By understanding the mechanisms that contribute to the development of chronic bacterial infections, we have an opportunity to identify new therapeutic targets that limit the development of these infections. The studies presented in this dissertation suggest that respiratory viral infection alters the nutritional environment, in the airways, making it more hospitable for *P. aeruginosa* colonization. We specifically focused on the nutrient iron in this dissertation, but as we have shown, EVs play a role in the ability of respiratory viral infection to promote *P. aeruginosa* biofilm growth. Because EVs contain proteins, lipids and RNAs that can exert biological effects on recipient cells, it is also conceivable that EVs may also be a source of additional nutrients that promote secondary bacterial infection. Therefore, based on our results, we hypothesize that EVs are a source of metals, such as iron and other nutrients, that are utilized by bacteria to colonize and survive in the host. Because iron is critical for *P. aeruginosa* growth and biofilm development, targeting bacterial iron uptake may represent a novel therapeutic strategy to prevent and/or treat chronic *P. aeruginosa* infections in the CF lung. Currently, a number of approaches are being pursued in the CF field to develop such therapeutics that disrupt bacterial iron homeostasis, and we propose that these therapeutic strategies will be useful

prophylactics during respiratory viral seasons to limit iron availability and prevent the acquisition of bacterial infections in the CF lung.

5.1.1 Iron Chelators

In the CF lung, a strong correlation has been reported between bacterial load, disease severity, and increased iron levels [28]. Iron is required for *P. aeruginosa* growth and biofilm development [27, 37, 43, 204], which has led to many investigations of iron chelation as a therapeutic strategy to limit iron availability in the airways of CF patients and limit bacterial colonization. Although the effect of respiratory viral infection on iron levels has not been previously examined, the studies presented in this dissertation have found that RSV infection increases the apical iron release on EVs from the respiratory epithelium. Importantly, we demonstrate that iron chelation reduces virus-mediated *P. aeruginosa* biofilm growth, suggesting exogenous iron chelators may be an effective therapeutic strategy to counteract virus-mediated iron release and biofilm growth.

Lactoferrin is a multifunctional glycoprotein of the transferrin-family of host iron-binding proteins that sequesters iron from bacteria and has been shown to inhibit *P. aeruginosa* biofilm growth *in vitro* [37]. In these studies, the antibiofilm activity of lactoferrin is attributed to its ability to sequester iron based on the observation that iron-loaded lactoferrin was unable to inhibit *P. aeruginosa* biofilm growth, suggesting that iron saturation neutralized the antibiofilm activity of lactoferrin [37]. Further studies have also demonstrated that iron chelation reduces *P. aeruginosa* biofilm growth on respiratory epithelial cells [27]. In addition to its iron sequestration abilities, lactoferrin possesses antimicrobial activity due to the cationic domains found in the N lobe of the protein that facilitate interaction with microbial membranes. The dual

functionality of lactoferrin could make it a particularly effective therapeutic supplement that chelates iron and thus, neutralizes virus-mediated iron release and *P. aeruginosa* biofilm growth in the CF lung. However, lactoferrin undergoes proteolytic degradation in the airways of CF patients due to the presence of host and bacterial proteases; not surprisingly, *P. aeruginosa* infection was associated with greater lactoferrin cleavage [210, 356]. This may limit of the efficacy lactoferrin supplementation *in vivo*, but further studies will be required to determine the impact of exogenous lactoferrin on *P. aeruginosa* burden in the airways of CF patients.

The effect of the FDA-approved iron chelators deferasirox (DSX) and deferoxamine (DFO), used for the treatment of conditions associated with iron overload (i.e. thalassemia and hemochromatosis), have also been investigated for their ability to inhibit *P. aeruginosa* biofilm growth on respiratory epithelial cells. These studies found that DSX is much more effective at chelating iron and inhibiting *P. aeruginosa* biofilm formation on AECs [49], which is likely due to the fact that *P. aeruginosa* can use DFO as an iron source [204]. Although *P. aeruginosa* biofilms grown on AECs have significantly higher antibiotic resistance than biofilms formed on abiotic surfaces, these studies demonstrated that in combination with tobramycin, both DSX and DFO can significantly disrupt and reduce established *P. aeruginosa* biofilms [49]. A combination of lactoferrin and hypothiocyanite have also been shown to increase the ability of antibiotics to disrupt established *P. aeruginosa* biofilms [354]. Taken together, these studies strongly suggest that iron chelation used in combination with other therapies may be an effective therapeutic strategy for preventing and treating *P. aeruginosa* infections in the CF lung. The significance of this observation is important to consider in the context of the data presented in this dissertation. We have shown that respiratory viral infection enhances apical iron release from AECs, implying that prophylactic iron chelation or co-administration of antibiotics with

iron chelators may be effective strategy to limit *P. aeruginosa* infections in the CF lung during respiratory viral seasons. However, it is not known if prophylactic iron chelation therapy can be used in CF patients or if this may exacerbate lung disease, and it is not known if these compounds would be stable in the CF lung.

5.1.2 Gallium: Disruption of bacterial iron metabolism with an iron mimetic

The transition metal gallium (Ga^{3+}) shares many chemical properties with iron and can bind to iron-binding proteins, including transferrin [357]. Because of its ability to disrupt iron homeostasis in bacteria and *P. aeruginosa* biofilm growth, $Ga(NO_3)_3$ has been proposed as a potential therapeutic to inhibit *P. aeruginosa* chronic colonization in CF patients [334, 335]. Whereas iron has the potential to redox cycle between Fe^{2+} and Fe^{3+} oxidation states, which is important for many of its biological functions, Ga^{3+} lacks this ability. Thus, Ga^{3+} competitively inhibits iron-dependent processes by disrupting proteins that function by utilizing iron as a cofactor. Currently, Ga^{3+} is FDA-approved to treat hypercalcemia and is administered intravenously as gallium nitrate ($Ga(NO_3)_3$; Ganite®) and its use as an antimicrobial therapeutic is currently being investigated. Because of the ability to interfere with iron-dependent processes, a potential approach to inhibiting and treating *P. aeruginosa* growth and biofilm formation in the CF lung is the use of Ga^{3+} to disrupt bacterial iron metabolism. *In vitro* studies have shown that $Ga(NO_3)_3$ both inhibited *P. aeruginosa* biofilm growth and disrupted established *P. aeruginosa* biofilms [334]. This observation is notable since current antibiotic treatment strategies do not prevent the establishment of chronic *P. aeruginosa* infections and are not effective in clearing chronic infections. Clinical studies are now underway to determine the efficacy $Ga(NO_3)_3$ in improving pulmonary function and for the treatment of *P. aeruginosa* infections in CF patients

[clinicaltrials.gov/ct2 (Identification Numbers: NCT01093521 and NCT02354859)]. Moreover, Ga^{3+} conjugated to DFO (Ga-DFO) has also been investigated, and shown to also inhibit *P. aeruginosa* biofilm growth and disrupt established biofilms [335]. Whether DFO-Ga is more effective than $Ga(NO_3)_3$ in the CF lung is not known. Moreover, Ga^{3+} compounds are also effective against other bacterial pathogens, suggesting the Ga^{3+}-based therapeutics may be useful for the treatment of other bacterial infections in the CF lung, as well at other sites [357].

In regards to the data presented in this dissertation and the potential use of $Ga(NO_3)_3$ as a therapeutic strategy to limit virus-mediated *P. aeruginosa* biofilm growth, two important points need to be considered. First, what is the bioavailability of Ga^{3+} in the respiratory tract after $Ga(NO_3)_3$ has been administered to patients? In previous studies where the *in vitro* antibiofilm activity of $Ga(NO_3)_3$ was shown, $Ga(NO_3)_3$ was added directly to bacteria [334]. However, $Ga(NO_3)_3$ is currently administered intravenously, and it is currently not known how much Ga^{3+} is found in the lungs during treatment. Second, is Ga^{3+} able to competitively inhibit microbial iron homeostasis in the high iron environment of the CF lung? It has been shown that iron levels in the CF airway are significantly elevated [23-26, 29, 30]. Our results show that RSV infection further increases iron levels, respiratory viral infection may further exacerbate potential competition between iron and Ga^{3+} and reduce the effectiveness of $Ga(NO_3)_3$ as a therapeutic for *P. aeruginosa* infection in the CF lung. We have also demonstrated in this dissertation that RSV infection enhances the transcytosis of transferrin from the basolateral to apical compartment of the respiratory epithelium (**Chapter 4 and Appendix A**). Because Ga^{3+} binds transferrin and undergoes TfnR-dependent uptake into cells, our work also has implications for the delivery of Ga^{3+} into the airways. One hypothesis, based on our results, is that respiratory viral infection enhances Ga^{3+}-loaded transferrin transcytosis from the basolateral to apical compartment of

AECs. This directional transport of Ga^{3+} corresponds to the movement of Ga^{3+} into the lumen of the respiratory tract during $Ga(NO_3)_3$ treatment. Whether respiratory viral infection facilitates such a process is an area of interesting investigation and should be included in future research that focuses on understanding Ga^{3+} trafficking in patients.

5.1.3 Other treatment strategies

It has been previously shown that respiratory viral infection predisposes the airways to secondary bacterial pneumonias by modifying the immune response in the lung [156-158, 160]. The connection between respiratory viral infection and the increased release of nutrients (i.e. iron and EVs) provides another mechanism by which respiratory viral infection reshapes the environment in the respiratory tract to promote secondary bacterial infection. Taken together, the data in the respiratory viral-bacterial coinfection field combined with our data emphasize that preventing respiratory viral infection through the use of vaccines or prophylaxis may be a strategy that limits the acquisition of severe secondary bacterial infections in the airways, such as the chronic bacterial infections that are associated with respiratory virus infection in CF patients [53, 55, 71, 72, 79, 330].

Influenza virus, hRV and RSV are the three most common viruses detected in CF patients. RSV is the most common cause of early respiratory tract morbidity, and palivizumab (a monoclonal antibody targeting RSV) prophylaxis has been investigated in CF patients to determine its effectiveness on RSV-related infections. These studies have indicated that CF patients that received palivizumab prophylaxis had slightly, but not significantly, decreased hospitalization rates compared to patients that did not receive prophylaxis [358, 359]. Conflicting results have been reported for the effect of palivizumab on first *P. aeruginosa* acquisition [359,

360]. Several factors could contribute to these results, but most importantly to our studies, multiple respiratory viruses trigger *P. aeruginosa* biofilm growth. Thus, targeting a single virus may not be efficacious in preventing virally–mediated exacerbations and bacterial infections in CF patients. Broader approaches will likely be required to successfully treat viral-bacterial coinfections. As an example, it was recently demonstrated by our lab that an engineered antimicrobial peptide, WLBU2, was effective at reducing both biomass and viability of *P. aeruginosa* biofilms as well RSV infectivity [361].

5.2 OUTSTANDING QUESTIONS AND FUTURE DIRECTIONS

The studies in this dissertation demonstrate that respiratory viral infections promote the formation of *P. aeruginosa* biofilms through a mechanism dependent upon the release of iron-bound transferrin. Iron is required for *P. aeruginosa* biofilm growth, and our studies now extend the role of iron to viral-bacterial interactions in the airway. Although our research demonstrates that RSV increases iron-loaded transferrin in the airway, further research is required to fully determine the mechanism by which RSV promotes the release of iron into the airways. As a follow-up to the studies presented in this dissertation, we have preliminary results showing that iron and transferrin levels in paranasal sinus washes of CF patients are elevated during respiratory viral infection. These preliminary studies were conducted in collaboration with Dr. Stella Lee in the Department of Otolaryngology at the University of Pittsburgh, who collected the sinonasal washes. The therapeutic implications for this work focuses mainly on ways to limit iron abundance in the CF respiratory tract during respiratory viral seasons. However, this body of work has other important implications that will be discussed below.

5.2.1 Viral-bacterial interactions

An interesting observation from this dissertation is that respiratory viral infection stimulates *P. aeruginosa* biofilm growth through the release of iron-bound transferrin. Viral-bacterial interactions are mostly studied in the context of a preceding or concurrent virus infection predisposing to secondary bacterial infection. Multiple mechanisms have been described by which respiratory viral infections promote secondary bacterial infection, but in general, the net result is a failure to clear bacterial infections due to increased bacterial adherence to cells or augmented mucosal immunity during a respiratory viral infection [352, 362]. Our study is one of the first to demonstrate that a preceding viral infection alters the nutritional landscape in the airways to promote secondary bacterial infection. Previously, it has been demonstrated that influenza infection increases the abundance of sialylated mucins in the respiratory tract, promoting *S. pneumoniae* growth [353]. Additionally, our studies demonstrate virus infection increases iron abundance in the airways to promote bacterial infection. This is consistent with previous reports that lipocalin-2 levels are decreased in the airways during influenza A virus infection, and exogenous lipocalin-2 decreases *S. aureus* growth during influenza A co-infection by reducing levels of iron in the airway [160]. Lipocalin-2 is a host-derived protein that sequesters siderophores, and thus, inhibits bacterial growth by sequestering iron from bacteria [363]. Collectively, these studies provide novel insight into viral-bacterial interactions in the lung, suggesting that viral dysregulation of nutritional immunity is another important aspect of viral-bacterial coinfections in the airway. Further investigation will be required to determine if other nutrients or host molecules are released by the airway epithelium during respiratory viral infection to increase bacterial colonization of the respiratory tract.

In this dissertation, we focused on the interaction between a preceding RSV infection and *P. aeruginosa*. However, it is important to note that bacteria influence virus infectivity as well. For example, in the gastrointestinal tract, the microbiome directly interacts with enteric viruses to promote enteric virus infection [364]. Whether such interactions occur in the respiratory tract is unknown, but it would be intriguing to test if bacteria in the respiratory tract interact with respiratory viruses to promote infection.

5.2.2 Extracellular vesicles in respiratory viral infections

EVs are membrane-enclosed vesicles secreted by most cell types and transfer biologically active molecules between cells, and were one mechanism by which we observed iron-loaded transferrin was present in apical secretions from RSV-infected AECs. Interestingly, EVs released by RSV-infected cells robustly stimulate *P. aeruginosa* biofilm growth, indicating a unique interaction between host cells, viruses and bacteria in the airways that involves iron. However, whether other nutrients besides iron are present on EVs released by AECs during RSV infection still needs to be elucidated. Moreover, whether viral infections of other mucosal sites produce EVs that have increased amounts of iron and other nutrients will be of interest to viral-bacterial interactions at other sites in the host. During viral infection, EVs have been shown to have both pro-viral and antiviral effects on uninfected neighboring cells [217, 226]. However, no function has yet been described for EVs during viral infection in the airways. In this regard, several interesting areas of investigation remain: What are the mechanisms by which EVs affect respiratory viral infections? Are EVs pro-viral or antiviral in the respiratory tract? Previous studies have suggested that EVs transfer antiviral molecules to uninfected cells as a mechanism to prevent viral infection [216, 266]. Whether this also occurs in the airways still requires

investigation. And more generally, will new technologies be developed that allow for purification of functional EVs from viruses and virus-like particles during a virus infection? This will be key to addressing whether the net biological effect of EV production during viral infection is due to the entire mixed populations of EVs, or whether certain EV subpopulations drive biological outcomes to disease. In this regard, a two-step purification process has been described that utilizes CD63 (a common protein found on exosomes) immunoprecipitation to separate EVs from virions [250]. The limitation of this approach is that EVs are eluted from $CD63^+$ beads with low pH wash. In our own studies, we have demonstrated that the biological activity of our EVs is sensitive to low pH wash (**Figure 33**). This likely occurs because low pH disrupts the interaction between iron and transferrin, and therefore, a low pH wash would potentially release iron and transferrin from EVs in our studies. This suggests that two-step purification approach may have limitations for studying biologically active molecules loaded on the outside of EVs. In addition, this selects only for $CD63^+$ EVs, which may mask important biology that occurs with $CD63^-$ EVs. In our own studies, we could also use RSV antibodies to separate EVs from RSV virions by immunoprecipitation, but this approach has its own limitations. Namely, we observed that the EV population that contained transferrin and was responsible for the biofilm stimulatory activity of EVs isolated from RSV-infected cells also contained RSV antigens (**Figure 29**). Thus, important considerations must be made in future studies in the field to determine the proper method for the purification of functional EVs from viruses to address whether certain EV subpopulations drive biological phenotypes.

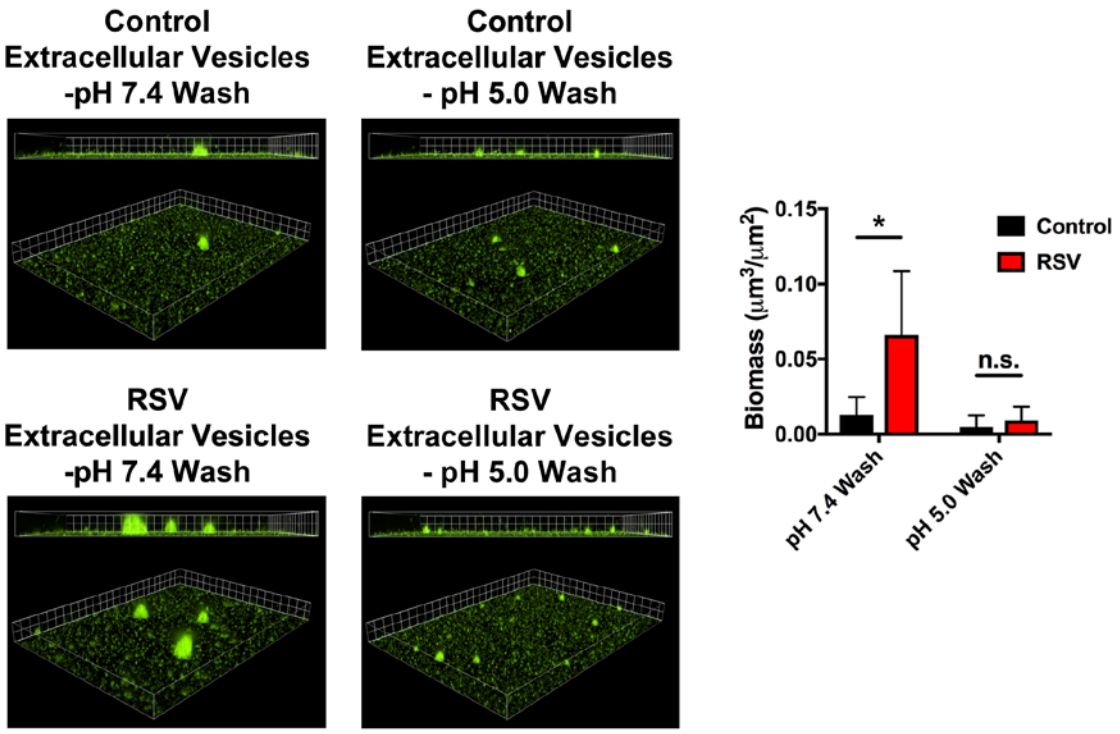

Figure 33: Low pH wash disrupts the biofilm stimulatory activity of EVs isolated from RSV-infected AECs. AECs were infected with RSV or mock-infected (MEM control). EVs were isolated from apical CM as outlined in section 2.2.6 after 72 hr but were resuspended in minimal essential media (MEM) supplemented with 2 mM L-glutamine pH 7.4 or pH 5.0. EV pellets resuspended in pH 7.4 MEM are referred to as "Extracellular Vesicles – pH 7.4 Wash" and EV pellets resuspended in pH 5.0 MEM are referred to as "Extracellular Vesicles – pH 5.0 Wash." All EVs were pelleted again using ultracentrifuge and all pellets were resuspended in MEM supplemented with 2 mM L-glutamine pH 7.4 before biofilm assays. *P. aeruginosa* (GFP) biofilms were grown in the presence of EVs in static abiotic biofilm assays. Fluorescent microscopy was used to measure the growth of *P. aeruginosa*. Nikon Elements (grid unit = 9.0 μm) was used to quantify *P. aeruginosa* biomass. $n \geq 3$. Data are presented as mean ± SD; *$P < 0.05$ versus control.

Our preliminary data suggest that *P. aeruginosa* associates with EVs released from AECs, which raises several questions: Do bacteria interfere with EV functions in the airways and thus, affect respiratory viral infection? Do EVs interact with other bacteria besides *P. aeruginosa*? Is this interaction limited to Gram-negative pathogens or does it extend to Gram-positive pathogens? How do EVs associate with *P. aeruginosa*? Understanding the interaction between host-derived EVs and bacteria in the respiratory tract is very exciting as it hypothesizes an additional component that likely influences the outcome of viral-bacterial infections in the CF lung and at other mucosal sites. If precise host-pathogen relationships are identified at the molecular level, it presents an entirely novel direction for therapeutic intervention in which specific processes could be targeted to minimize nutritional abundance and/or microbial utilization of nutrients in the airways to limit infections.

5.2.3 Transferrin transcytosis at mucosal surfaces

An interesting observation in this study was that respiratory viral infection increased transferrin transcytosis across the airway epithelium to the apical compartment of cells (**Appendix A**). It is known that cells, notably neutrophils, increases lactoferrin and calprotectin (a zinc and manganese-binding protein) concentration in infectious sites as part of the immune response, but less is known about transferrin. The ability of transferrin inhibit bacterial growth increases as transferrin saturation decreases due to its ability to sequester iron. Therefore, it is plausible that apo-transferrin would inhibit microbial growth at the site of infection. Regarding this hypothesis and the evolutionary arms race between iron sequestration and acquisition between host and microbes, an interesting question remains. That is, do pathogens actively increase the abundance of iron-loaded transferrin at the site of infection to promote their own growth? Recently, it was

shown that *Helicobacter pylori*, which colonizes the apical membrane of gastrointestinal epithelial cells, alters iron trafficking of host epithelial cells by promoting transferrin receptor mislocalization from the basolateral to apical membrane of cells [203]. This perturbation in transferrin trafficking results in the apical release of transferrin to promote *H. pylori* growth on cells [203], suggesting that pathogens have evolved mechanisms that increase the amounts of iron-loaded transferrin at the site of infection. More interestingly, this study demonstrated that microbes alter transferrin trafficking within epithelial cells, but the mechanism by which this trafficking pathway is altered remains undefined. It has previously been reported that transferrin transcytosis is increased in polarized epithelial cells due to loss of function of the epithelial basolateral sorting adaptor AP-1B, and that this mechanism is dependent upon Rab11a, Rab11a-FIP2 and galectin-4 [365, 366]. The data from these studies support a model whereby transferrin and other basolateral proteins are trafficked to apical recycling endosomes and delivered via Rab11a-positive endosomes to the apical plasma membrane. Whether microbes target AP-1B or any of these other proteins to promote transferrin trafficking is unknown and an intriguing area of future investigation.

Although our work has demonstrated that respiratory viral infection promotes transferrin transcytosis in AECs, a few stimulating questions remain: Why is iron-loaded transferrin transcytosed (i.e. why is the iron not delivered to cells)? What role do STEAP proteins play in transcytosis? In regards to our own work, why does RSV infection promote transferrin transcytosis, and are specific RSV proteins required for stimulating transcytosis? It is known that RSV utilizes proteins involved in the apical recycling pathway in cells to bud [97, 98]. Thus, one hypothesis that explains the increased transcytosis of transferrin during RSV infection is that while the virus hijacks apical recycling proteins it also downregulates or represses basolateral

recycling, which consequently would direct basolateral proteins to the apical membrane. Whether RSV stimulates the transcytosis of other basolateral proteins besides transferrin and if RSV degrades basolateral recycling proteins are interesting questions that would start testing this hypothesis.

5.3 FINAL THOUGHTS

Although clinical observations have noted for the last twenty years that respiratory viral infections trigger exacerbations and are associated with chronic *P. aeruginosa* infections in CF patients, the mechanisms underlying these interactions have remained poorly understood. This dissertation has contributed to our mechanistic understanding to fill this knowledge gap and demonstrated that respiratory viral infection of the airway epithelium alters nutritional abundance in the airways, creating an environment permissive to the growth of bacterial biofilms by increasing the release of iron-bound transferrin. We also observed that activation of the antiviral IFN response [via treatment of AECs with type I and type III IFNs (IFN-β and IFN-λ, respectively)] in the absence of viral infection was sufficient to stimulate *P. aeruginosa* biofilm growth. Although apical secretions from AECs infected with a respiratory virus or treated with IFN were sufficient to stimulate *P. aeruginosa* biofilms in the absence of cells, our data suggest the biofilm-stimulatory activity is driven by different factors in these two conditions. Whereas respiratory viral infection enhanced *P. aeruginosa* biofilm growth by increasing the abundance of iron and the host iron-binding protein transferrin in the airways, IFN treatment did not alter iron or transferrin release by AECs but still stimulated *P. aeruginosa* biofilm growth. Together, we interpret these observations to suggest that at least two parallel pathways contribute to

increased *P. aeruginosa* biofilm growth during respiratory viral infection. These two pathways are likely key components of the interactions that exist between respiratory viruses and secondary bacterial infection that determine host outcome. Although this dissertation has focused on *P. aeruginosa* biofilm formation in the airways during respiratory viral infection, the observations made here offer new insight into the complex interactions that occur between the host and pathogens at mucosal surfaces during polymicrobial infections. In addition, it is important to consider that while this dissertation has focused on how viral infection benefits secondary bacterial infection, the relationship between these two microbes is not a one-way road and there is a growing body of literature demonstrating the impact bacteria have on viral infection. For example, work in the gastrointestinal tract has shown that the intestinal microbiome promotes enteric viral infection through modulation of the immune system and by directly interacting with virions [367]. Confirming the precise interactions that exist between viruses and bacteria will be critical as this would be among the first steps needed for designing therapeutics that disrupt these relationships to limit the severity of secondary infections.

The final portion of this thesis has demonstrated that RSV infection increases the release of EVs from the airway epithelium and importantly that these EVs stimulate *P. aeruginosa* biofilm growth through a mechanism dependent upon the release of iron-loaded transferrin on EVs. Although our studies expand our understanding of how a respiratory virus alters the nutritional landscape of the airways through EV release, these results set the stage for an interesting set of new studies that investigates the biological function of EVs in the airways during an infection. In particular, it will be of great interest to see what role EVs may play in transferring antiviral molecules between cells, and what other consequences EV association with *P. aeruginosa* has on bacterial infection besides promoting biofilm growth. In conclusion, the

work presented in this dissertation suggests that during viral infection, the nutritional landscape of the airways is altered, promoting secondary bacterial infections. Microbes do not exist in a vacuum and understanding the complex interplay between viruses, bacteria and the host environment is a very active area of research that may uncover novel therapeutic strategies for treating complex microbial infections, including the chronic bacterial infections found in CF patients.

APPENDIX A

RESPIRATORY SYNCYTIAL VIRUS INFECTION DISRUPTS TRANSFERRIN TRAFFICKING IN THE RESPIRATORY EPITHELIUM

The data included in this appendix is data I generated for a manuscript being prepared by Dr. Jeffrey Melvin, a postdoctoral associate in the Bomberger Lab, to understand how *P. aeruginosa* responds to the environment created by respiratory viral infection to form biofilms.

A.1 RESULTS

Our data suggest a model in which RSV infection increases apical release of transferrin to promote *P. aeruginosa* biofilm growth. To understand why increased levels of transferrin are released into CM during RSV infection, we looked at the transcription of transferrin in AECs, and found that the expression of transferrin is reduced in AECs in response to RSV infection (**Figure 34A**), implying that apically released transferrin originates outside the cell. Transferrin is responsible for shuttling iron throughout the body in the circulatory system. In our model, the only extracellular location that transferrin can originate from is the basolateral compartment of cells. Thus, we examined whether transferrin is transcytosed from the basolateral to apical

compartment of polarized AECs during RSV infection by adding biotinylated transferrin to the media in the basolateral compartment of cells 48 hours post-RSV infection. After 24 hours, we then measured the abundance of biotinylated transferrin in CM. We found that biotinylated transferrin was transcytosed across the epithelial layer to the apical compartment by both control and RSV-infected AECs, but during RSV infection there was approximately a three-fold increase in the amount of biotinylated transferrin in CM collected from RSV-infected cells as compared to uninfected monolayers after a total of 72-hour virus infection (**Figure 34B**). Additionally, the increase in transferrin transcytosis during RSV infection was time-dependent, since we observed no difference in the amount of biotinylated transferrin in CM collected from RSV-infected cells after only 24-hour virus infection (**Figure 34B**). We also measured the transcytosis of fluorescently-labeled, 70 kDa dextran from the basolateral to apical compartment of AECs during RSV infection to determine if the increase in transferrin transcytosis was due to paracellular leakage. Because paracellular leakage would rapidly increase transferrin transcytosis to the apical compartment, we added FITC-dextran to cells infected with RSV for 72 hours and measured FITC dextran transcytosis over time compared to either uninfected cells or filters alone (no cells; positive control for paracellular leakage). We found that the amount of dextran that was transported into the apical compartment of cells was unchanged after 72-hour RSV infection, and the overall amount of dextran transcytosed into the apical compartment by infected and uninfected cells was very low (**Figure 34C**). Because we did not observe an increase in dextran in the apical compartment of AECs, we concluded that RSV infection was not damaging the epithelial monolayers and causing non-specific leakage of basolateral proteins into the apical compartment of cells. This supports out earlier findings that RSV infection did not significantly damage the epithelial monolayer, as measured by lactate dehydrogenase (LDH) release and

transepithelial electrical resistance (TEER) (**Figure 10**). In addition, we found very little transcytosis from the apical to the basolateral compartment of cells, and RSV infection had no impact on this process (**Figure 34D**). This suggests that the transcytosis from the basolateral to apical compartment is a directionally specific process. Consistent with the transcytosis from the basolateral to apical compartment, we observed a slight, although not statistically significant, reduction in transferrin receptor (TfnR) abundance on the basolateral membrane (**Figure 34E**). Interestingly, we observed that RSV infection increased the apical release of TfnR that originated in the basolateral plasma membrane, suggesting that virus infection promoted the trafficking of TfnR from the basolateral membrane to the apical compartment of AECs. In light of our observations in **Chapter 4** of this dissertation, we suspect this increase in basolateral TfnR that is secreted during RSV infection is due to the release of EVs. We hypothesize that basolateral TfnR is loaded onto EVs and is bound to transferrin. Whether this EV population is due to trafficking of the basolateral TfnR-transferrin complex to multivesicular bodies (MVBs) and released on exosomes, or the complex is trafficked the apical membrane of AECs and released on EVs that bleb from the apical plasma membrane is still to be determined and is an intriguing question moving forward. Taken together, these results support the conclusion that RSV infection promotes the transcytosis of transferrin into the apical compartment of AECs, increasing the abundance of accessible transferrin for *P. aeruginosa* biofilm growth.

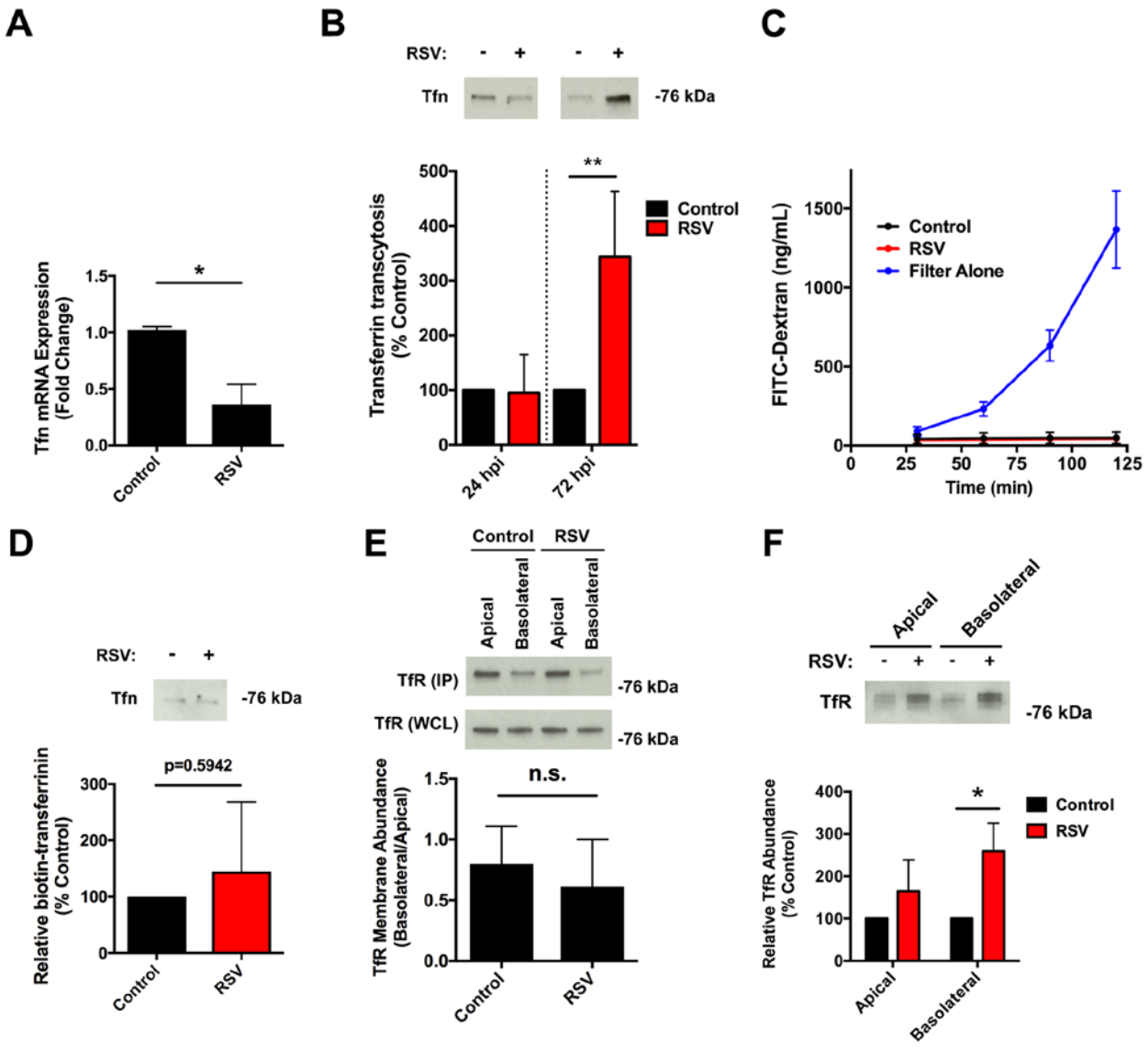

Figure 34: RSV infection increases transferrin transcytosis.

(A) RNA was prepared from AECs infected with RSV or mock-infected (MEM control) for 72 hr and probed by qRT-PCR for transferrin expression. (B) Biotin-transferrin was added to the basal chamber of RSV or mock-infected AECs 48 hpi at a final concentration of 25 μg/mL. The apical supernatants of AECs were collected 24 hours later. Biotinylated-transferrin was affinity-purified from apical secretions with streptavidin beads. Proteins were eluted from beads and separated by SDS-PAGE. Transcytosed transferrin was measured by Western blot analysis. (C) 70 kDa FITC-dextran was added to the basal chamber of RSV or mock-infected AECs 72 hpi at a final concentration of 25 μg/mL. The apical secretions were collected from cells were analyzed for FITC fluorescence by plate reader at the indicated time points after addition of FITC-dextran. RSV, RSV-infected AECs. (D) Biotin-transferrin was

added to the apical chamber of RSV or mock-infected (control MEM) AECs 48 hpi at a final concentration of 25 μg/mL. The basolateral media was collected from AECs 24 hr later and biotinylated-transferrin was affinity-purified from apical secretions with streptavidin beads. Proteins were eluted from beads and separated by SDS-PAGE. Transcytosed transferrin was measured by Western blot analysis. (E) AECs were infected with RSV or mock-infected (MEM control) for 72 hr. The apical and basolateral cell surface was biotinylated and biotinylated proteins were affinity purified from whole cell lysates (WCLs) with streptavidin beads. Proteins were eluted from beads, followed by SDS-PAGE and Western blot analysis to analyze the effect of RSV infection on apical and basolateral membrane TfnR abundance. Quantification of results found below representative blots. All quantifications were normalized to TfnR in whole cell lysate (WCL). (F) AECs were infected with RSV or mock-infected (MEM control) for 48 hr, followed by cell surface biotinylation of the apical or basolateral cell surface. CM was collected from cells 24 hr later and biotinylated proteins from CM were affinity-purified with streptavidin beads followed by SDS-PAGE and Western blot analysis was performed to analyze the effect of RSV infection on the apical release of cell surface proteins from AECs. For all experiments $n \geq 3$. Data are presented as mean ± SD; $*P < 0.05$ versus control.

APPENDIX B

INTERFERON-STIMULATED REGULATORS OF *PSEUDOMONAS AERUGINOSA* BIOFILM GROWTH ON AIRWAY EPITHELIAL CELLS

All data presented here is unpublished and represents a collaborative ongoing study in the Bomberger Lab interested in understanding how the innate antiviral IFN response and more specifically, individual interferon-stimulated genes (ISGs) contribute to *P. aeruginosa* biofilm growth. Dr. Jeffrey Melvin, a post-doc in the Bomberger Lab, and myself performed the ISG screen, and Brian R. Kocak, a laboratory technician in the Bomberger Lab, is now in the process of validating the hits from the ISG screen. Contributions of authors to individual figures are indicated in the figure legends. The cell-based screen used in this study was initially developed by Dr. John Schoggins (Department of Microbiology, University of Texas Southwestern Medical Center, Dallas, TX, United States of America), who we have collaborated with as part of the ISG screen described here.

B.1 RESULTS

B.1.1 Apical secretions from IFN treated AECs promotes the growth of *P. aeruginosa* biofilms independent of transferrin and extracellular vesicles

In the previous chapters, it has been established that AECs increase apical release of the host-iron binding protein transferrin (**Chapter 3**) and extracellular vesicles (**Chapter 4**) during respiratory virus infection and that these factors are important for increased *P. aeruginosa* biofilm growth following viral co-infections. However, it is unknown if IFN signaling influences the release of iron from AECs, or whether extracellular vesicles isolated from cells treated with IFN interact with and stimulate bacterial growth. To begin addressing these questions, we first asked if CM from IFN treated AECs stimulated *P. aeruginosa* biofilm growth to determine if cells treated with IFN release factors that stimulate biofilm growth. We found that CM from IFN-β-treated AECs increased biofilm growth in static abiotic biofilm assays (**Figure 35**), suggesting that IFN treatment increases the release of factors that promote *P. aeruginosa* biofilm growth.

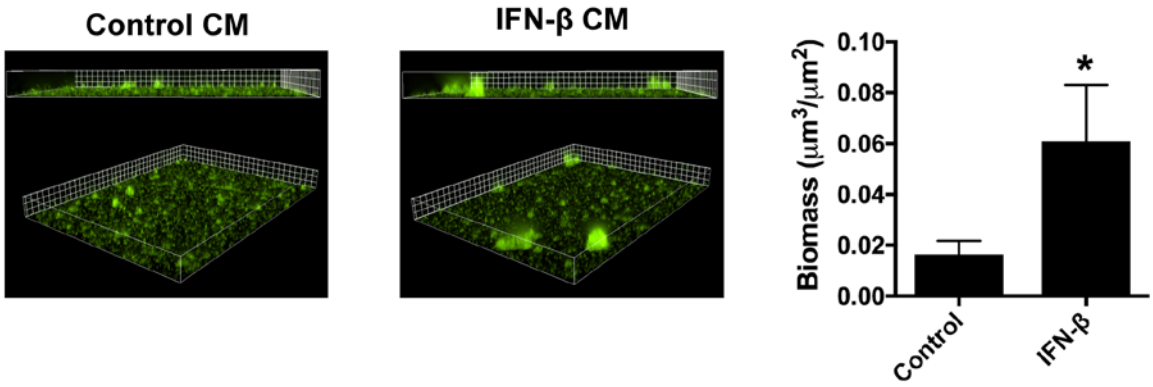

Figure 35: CM from IFN-β treated AECs enhance *P. aeruginosa* biofilm growth.

CM was collected from AECs were treated with IFN-β (1000 U/mL) for 18 hrs, and *P. aeruginosa* (GFP) was grown in the presence of CM in static abiotic biofilm assay and epifluorescence microscopy was used to measured biofilm growth (GFP, green). *P. aeruginosa* biofilm biomass was quantified using Nikon Elements (grid unit = 6 μm). *$P < 0.05$, $n > 3$.

Because we observed that apical secretions from both RSV infected and IFN-β treated AECs enhanced *P. aeruginosa* biofilm growth and we have shown that RSV enhances iron release from AECs to stimulate *P. aeruginosa* biofilm growth, we next examined if IFN-β treatment alters the release of iron from AECs. Interestingly, we found that IFN-β treatment did not change total iron levels in CM collected from IFN-treated cells (**Figure 36A**). This suggests that IFN signaling does not mediate the release of iron from AECs, or at the very least is not sufficient to promote iron release. In addition, this implies that the antiviral IFN response is not responsible for the increased iron release we observed from AECs during respiratory viral infection (**Chapter 3**). However, this does not rule out the possibility that IFN signaling increases the release of non-iron bound transferrin from AECs. Such a phenotype could be considered an appropriate immune response during viral infection as transferrin could sequester any free iron that is released during the course of the infection, specifically for the purpose of

preventing secondary bacterial infections. However, we observed that IFN-β treatment did not alter the transcytosis and apical release of transferrin into CM (**Figure 36B**). Collectively, these results demonstrate that IFN signaling does not disrupt nutritional immunity in AECs and increase the release of iron or the iron-binding protein transferrin. This implies that iron is not the only factor that is altered by respiratory viral infection, and that IFN signaling activates a parallel biofilm stimulatory mechanism. Thus, we hypothesized that IFN treatment activates specific ISGs that stimulate *P. aeruginosa* biofilm growth. To test this hypothesis and begin to understand the mechanism by which IFN treatment stimulates *P. aeruginosa* biofilm growth, we performed an ISG screen that will be described in the next section.

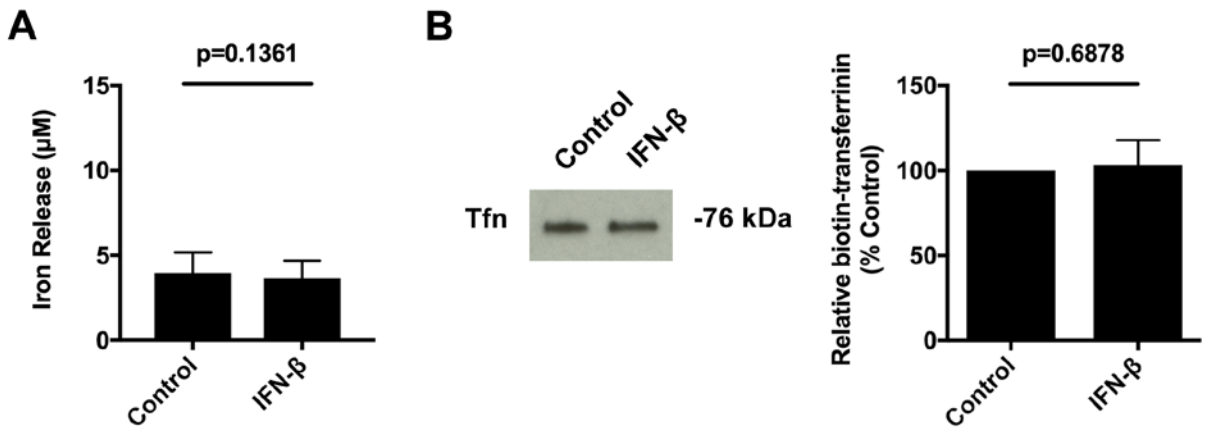

Figure 36: Iron release and transferrin transcytosis from AECs treated with IFN-β.

AECs were treated with IFN-β (1000 U/mL) for 18 hrs. (A) Total iron was measured in apical CM. (B) IFN-β treatment does not increase transferrin transcytosis from the basolateral to apical compartment of AECs. At the time of IFN-β treatment, 25 μg/mL of transferrin biotin-XX-conjugate was added to the basolateral compartment of AECs. Transferrin biotin-XX-conjugate was affinity purified from the apical CM and transferrin was measured by western blot analysis. n = 3.

B.1.2 ISG screen identifies potential regulators of *P. aeruginosa* biofilm growth in response to IFN signaling

Because we observed that IFN treatment did not increase iron release from AECs, we propose that respiratory viruses and the antiviral IFN response to virus infection stimulate *P. aeruginosa* biofilm growth by two distinct but parallel mechanisms. We utilized a gain-of-function screening approach to identify ISGs that increase *P. aeruginosa* biofilm growth in CM, to gain a better understanding of the mechanisms by which IFN signaling enhances the release of biofilm stimulatory factor(s). To screen CM from hundreds of ISGs for biofilm stimulatory activity we utilized our static abiotic biofilm assay. Briefly, AECs were transduced, in a one-gene one well format, with bicistronic lentiviral vectors driving constitutive expression of genes for a single ISG and red fluorescent protein [368]. CM was collected from cells 72 hours post-transduction, and GFP-expressing bacteria were grown in the presence of the CM in static abiotic biofilm assays for 6 hours and biofilm growth was assessed by fluorescent microscopy (**Figure 37A**). Firefly luciferase was used as a negative control to ensure that protein overexpression was not driving the biofilm stimulatory activity of cells. As has been shown throughout this dissertation, this method allows for visualization of biofilm growth in the absence of AECs, which makes it possible to ascertain whether individual ISGs stimulate biofilm growth by promoting the secretion of biofilm stimulatory factor(s). Additionally, by visualizing biofilm growth, biofilm architecture can be analyzed to identify unique structures that may result due to environment changes in the CM induced by individual ISGs. Finally, our Nikon Ti-inverted fluorescent microscope is fitted with an automated stage, which allows for automated, unbiased imaging of biofilm formation in CM.

We expressed a library of approximately 390 ISGs previously described [368], and performed static abiotic biofilm assays as described above. Biofilm growth of *P. aeruginosa* from the average of two screen replicates is shown as a dot plot (**Figure 37B**). Some ISGs very robustly stimulate *P. aeruginosa* biofilm growth, whereas the majority had relatively little effect on biofilm formation. We determined ISGs that enhance *P. aeruginosa* biofilm growth as those ISGs that increased biofilm biomass 1.5 standard deviations above the population mean (Z-score greater than 1.5). Most of the ISGs had little effect on *P. aeruginosa* biofilm growth, as bacterial biomass for the majority of ISGs had a Z-score less than 1.5 (**Figure 37B**). Six ISGs were identified based on this criteria including MYDD88, APOBEC3A, HK2, TNFRSF10A, EHD4 and PML.

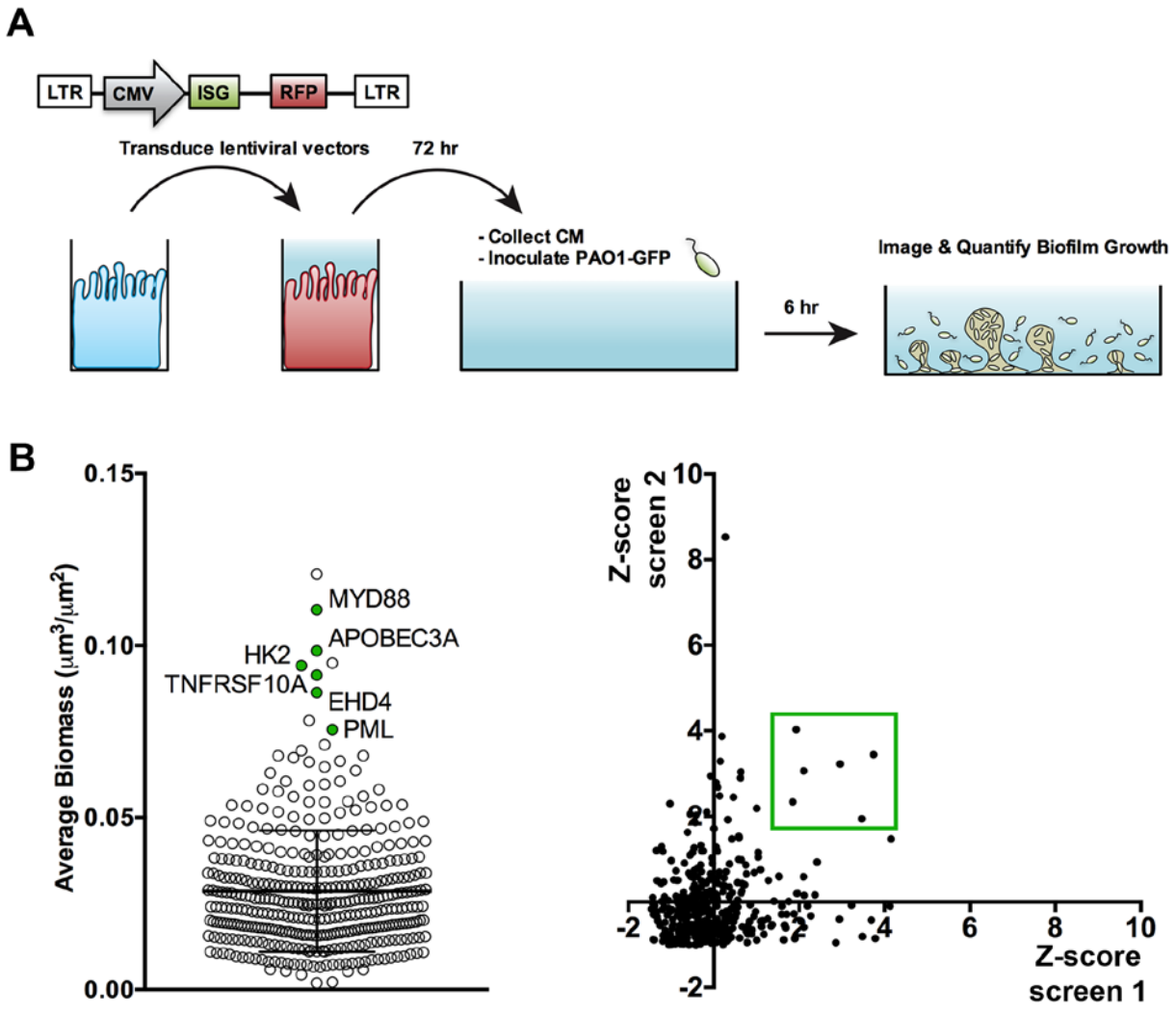

Figure 37: Gain-of-function screen identifies regulators of *P. aeruginosa* biofilm growth.

(A) Schematic of gain-of-function screen for ISGs that enhance abiotic *P. aeruginosa* biofilm growth. Diagram of bicistronic lentiviral vector is shown; CMV, immediate early promoter from human cytomegalovirus; LTR, HIV-1 long terminal repeat; RFP, red fluorescent protein. AECs were transduced with biscistronic lentiviral vector for 72 hours, and CM was collected. *P. aeruginosa* (GFP) was grown in the presence of CM in static abiotic biofilm assays. Epifluorescence microscopy was used to measure biofilm growth. (B) (*Left*) Dot plot of *P. aeruginosa* biofilm growth in the presence of CM in two replicate screens and presented as an averaged (error bars represent s.d.). n=2. (*Right*) Scatter plot of Z-scores of screen replicates 1 and 2. Genes selected as positive hits for further confirmation are boxed in scatter plot (*Right*) and labeled in dot plot (*Left*).

We are currently in the process of performing repeat trials of static abiotic biofilm assays with full-length cDNA clones of all six ISGs to confirm the biofilm stimulatory activity of these ISGs. Preliminary experiments using these cDNA clones have confirmed that overexpression of HK2 and EHD4 increase *P. aeruginosa* biofilm growth (**Figure 38**). As a negative control, we are using GFP, which does not stimulate biofilm growth. In addition, we have also measured the expression of all six ISGs in AECs during RSV infection and found that expression of five of the six ISGs are significantly increased 72 hours post-RSV infection (**Figure 39**).

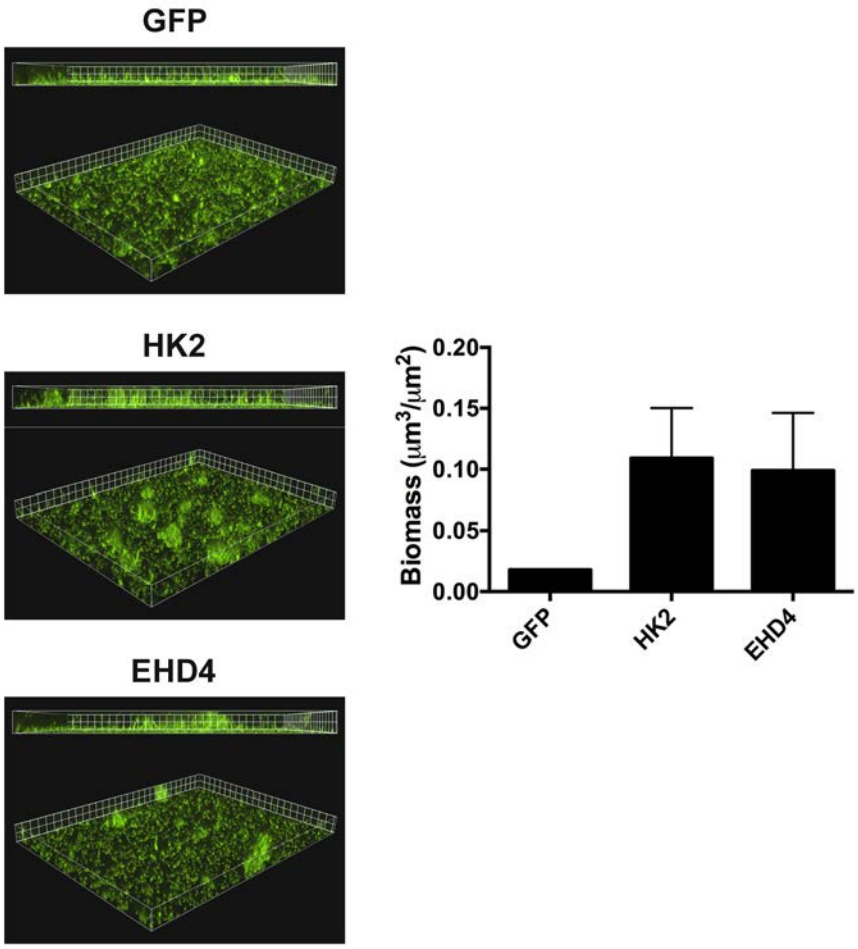

Figure 38: Validation of biofilm stimulatory activity of ISG screen hits.

AECs were transfected with full-length cDNA clones of two genes identified in the gain-of-function ISG screen for 72 hours, and CM was collected. *P. aeruginosa* (GFP) was grown in the presence of CM in static abiotic biofilm assay. Epifluorescence microscopy was used to measured biofilm growth (GFP, green) and biofilm biomass was quantified using Nikon Elements (grid unit = 6 μm). GFP cDNA clone was used as negative control to verify that gene overexpression by cDNA clones did not promote *P. aeruginosa* biofilm growth. Static abiotic biofilm assays performed by Brian R. Kocak. n=2.

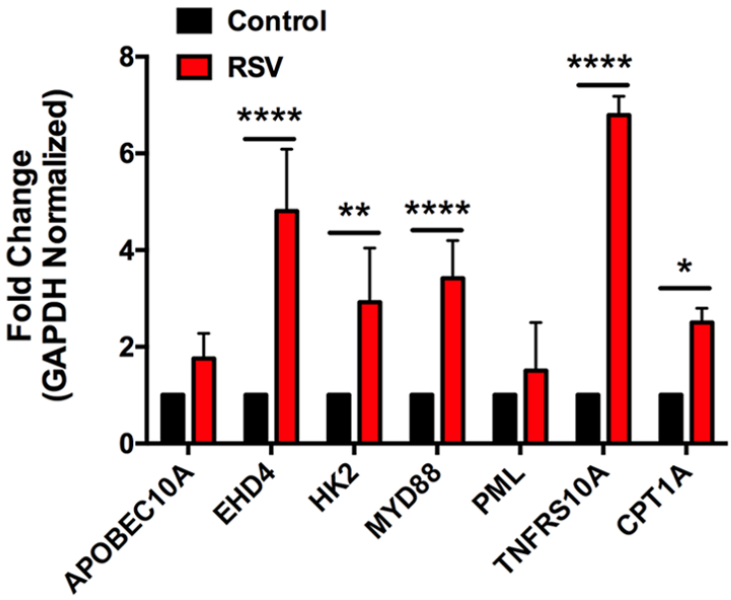

Figure 39: Gene expression of ISG screen hits during RSV infection.

AECs were infected with RSV or were mock-infected (MEM control) for 72 hours and RNA was collected. Gene expression was measured by quantitative RT-PCR (qRT-PCR) to monitor gene expression during RSV infection (red bar) compared to uninfected cells (black bar). *P < 0.05, **P < 0.005, ****P < 0.00005, n=3. Data provided by Brian R. Kocak.

BIBLIOGRAPHY

1. Kato, A. and R.P. Schleimer, *Beyond inflammation: airway epithelial cells are at the interface of innate and adaptive immunity.* Curr Opin Immunol, 2007. **19**(6): p. 711-20.

2. Hammad, H. and B.N. Lambrecht, *Barrier Epithelial Cells and the Control of Type 2 Immunity.* Immunity, 2015. **43**(1): p. 29-40.

3. Hooper, L.V., *Epithelial cell contributions to intestinal immunity.* Adv Immunol, 2015. **126**: p. 129-72.

4. Davis, P.B., *Cystic fibrosis since 1938.* Am J Respir Crit Care Med, 2006. **173**(5): p. 475-82.

5. Sosnay, P.R., et al., *Defining the disease liability of variants in the cystic fibrosis transmembrane conductance regulator gene.* Nat Genet, 2013. **45**(10): p. 1160-7.

6. Lipuma, J.J., *The changing microbial epidemiology in cystic fibrosis.* Clin Microbiol Rev, 2010. **23**(2): p. 299-323.

7. Rosenfeld, M., B.W. Ramsey, and R.L. Gibson, *Pseudomonas acquisition in young patients with cystic fibrosis: pathophysiology, diagnosis, and management.* Curr Opin Pulm Med, 2003. **9**(6): p. 492-7.

8. Stanton, B.A., *Effects of Pseudomonas aeruginosa on CFTR chloride secretion and the host immune response.* Am J Physiol Cell Physiol, 2017. **312**(4): p. C357-C366.

9. Matsui, H., et al., *Evidence for periciliary liquid layer depletion, not abnormal ion composition, in the pathogenesis of cystic fibrosis airways disease.* Cell, 1998. **95**(7): p. 1005-15.

10. Tarran, R., et al., *Normal and cystic fibrosis airway surface liquid homeostasis. The effects of phasic shear stress and viral infections.* J Biol Chem, 2005. **280**(42): p. 35751-9.

11. Bals, R., et al., *The peptide antibiotic LL-37/hCAP-18 is expressed in epithelia of the human lung where it has broad antimicrobial activity at the airway surface.* Proc Natl Acad Sci U S A, 1998. **95**(16): p. 9541-6.

12. Bals, R., et al., *Human beta-defensin 2 is a salt-sensitive peptide antibiotic expressed in human lung.* J Clin Invest, 1998. **102**(5): p. 874-80.

13. Singh, P.K., et al., *Production of beta-defensins by human airway epithelia.* Proc Natl Acad Sci U S A, 1998. **95**(25): p. 14961-6.

14. Singh, P.K., et al., *Synergistic and additive killing by antimicrobial factors found in human airway surface liquid.* Am J Physiol Lung Cell Mol Physiol, 2000. **279**(5): p. L799-805.

15. Travis, S.M., et al., *Activity of abundant antimicrobials of the human airway.* Am J Respir Cell Mol Biol, 1999. **20**(5): p. 872-9.

16. Nakayama, K., et al., *Acid stimulation reduces bactericidal activity of surface liquid in cultured human airway epithelial cells.* Am J Respir Cell Mol Biol, 2002. **26**(1): p. 105-13.

17. Coakley, R.D., et al., *Abnormal surface liquid pH regulation by cultured cystic fibrosis bronchial epithelium.* Proc Natl Acad Sci U S A, 2003. **100**(26): p. 16083-8.

18. Pezzulo, A.A., et al., *Reduced airway surface pH impairs bacterial killing in the porcine cystic fibrosis lung.* Nature, 2012. **487**(7405): p. 109-13.

19. Abou Alaiwa, M.H., et al., *Neonates with cystic fibrosis have a reduced nasal liquid pH; a small pilot study.* J Cyst Fibros, 2014. **13**(4): p. 373-7.

20. Hoegger, M.J., et al., *Impaired mucus detachment disrupts mucociliary transport in a piglet model of cystic fibrosis.* Science, 2014. **345**(6198): p. 818-22.

21. Tang, X.X., et al., *Acidic pH increases airway surface liquid viscosity in cystic fibrosis.* J Clin Invest, 2016. **126**(3): p. 879-91.

22. Abdullah, L.H., et al., *Defective postsecretory maturation of MUC5B mucin in cystic fibrosis airways.* JCI Insight, 2017. **2**(6): p. e89752.

23. Reid, D.W., et al., *Iron deficiency in cystic fibrosis: relationship to lung disease severity and chronic Pseudomonas aeruginosa infection.* Chest, 2002. **121**(1): p. 48-54.

24. Reid, D.W., et al., *Airway iron and iron-regulatory cytokines in cystic fibrosis.* Eur Respir J, 2004. **24**(2): p. 286-91.

25. Reid, D.W., et al., *Increased airway iron as a potential factor in the persistence of Pseudomonas aeruginosa infection in cystic fibrosis.* Eur Respir J, 2007. **30**(2): p. 286-92.

26. Stites, S.W., et al., *Increased concentrations of iron and isoferritins in the lower respiratory tract of patients with stable cystic fibrosis.* Am J Respir Crit Care Med, 1999. **160**(3): p. 796-801.

27. Moreau-Marquis, S., et al., *The DeltaF508-CFTR mutation results in increased biofilm formation by Pseudomonas aeruginosa by increasing iron availability.* Am J Physiol Lung Cell Mol Physiol, 2008. **295**(1): p. L25-37.

28. Hunter, R.C., et al., *Ferrous iron is a significant component of bioavailable iron in cystic fibrosis airways.* MBio, 2013. **4**(4).

29. Stites, S.W., et al., *Increased iron and ferritin content of sputum from patients with cystic fibrosis or chronic bronchitis.* Chest, 1998. **114**(3): p. 814-9.

30. Gray, R.D., et al., *Sputum trace metals are biomarkers of inflammatory and suppurative lung disease.* Chest, 2010. **137**(3): p. 635-41.

31. Folkesson, A., et al., *Adaptation of Pseudomonas aeruginosa to the cystic fibrosis airway: an evolutionary perspective.* Nat Rev Microbiol, 2012. **10**(12): p. 841-51.

32. Costerton, J.W., P.S. Stewart, and E.P. Greenberg, *Bacterial biofilms: a common cause of persistent infections.* Science, 1999. **284**(5418): p. 1318-22.

33. Burmolle, M., et al., *Biofilms in chronic infections - a matter of opportunity - monospecies biofilms in multispecies infections.* FEMS Immunol Med Microbiol, 2010. **59**(3): p. 324-36.

34. Lee, K. and S.S. Yoon, *Pseudomonas aeruginosa Biofilm, a Programmed Bacterial Life for Fitness.* J Microbiol Biotechnol, 2017. **27**(6): p. 1053-1064.

35. Mann, E.E. and D.J. Wozniak, *Pseudomonas biofilm matrix composition and niche biology.* FEMS Microbiol Rev, 2012. **36**(4): p. 893-916.

36. Harmsen, M., et al., *An update on Pseudomonas aeruginosa biofilm formation, tolerance, and dispersal.* FEMS Immunol Med Microbiol, 2010. **59**(3): p. 253-68.

37. Singh, P.K., et al., *A component of innate immunity prevents bacterial biofilm development.* Nature, 2002. **417**(6888): p. 552-5.

38. Winstanley, C. and J.L. Fothergill, *The role of quorum sensing in chronic cystic fibrosis Pseudomonas aeruginosa infections.* FEMS Microbiol Lett, 2009. **290**(1): p. 1-9.

39. Lee, J. and L. Zhang, *The hierarchy quorum sensing network in Pseudomonas aeruginosa.* Protein Cell, 2015. **6**(1): p. 26-41.

40. Parsek, M.R. and E.P. Greenberg, *Sociomicrobiology: the connections between quorum sensing and biofilms.* Trends Microbiol, 2005. **13**(1): p. 27-33.

41. Rutherford, S.T. and B.L. Bassler, *Bacterial quorum sensing: its role in virulence and possibilities for its control.* Cold Spring Harb Perspect Med, 2012. **2**(11).

42. Davies, D.G., et al., *The involvement of cell-to-cell signals in the development of a bacterial biofilm.* Science, 1998. **280**(5361): p. 295-8.

43. Patriquin, G.M., et al., *Influence of quorum sensing and iron on twitching motility and biofilm formation in Pseudomonas aeruginosa.* J Bacteriol, 2008. **190**(2): p. 662-71.

44. Singh, P.K., et al., *Quorum-sensing signals indicate that cystic fibrosis lungs are infected with bacterial biofilms.* Nature, 2000. **407**(6805): p. 762-4.

45. Baltimore, R.S., C.D. Christie, and G.J. Smith, *Immunohistopathologic localization of Pseudomonas aeruginosa in lungs from patients with cystic fibrosis. Implications for the pathogenesis of progressive lung deterioration.* Am Rev Respir Dis, 1989. **140**(6): p. 1650-61.

46. Bjarnsholt, T., et al., *Pseudomonas aeruginosa biofilms in the respiratory tract of cystic fibrosis patients.* Pediatr Pulmonol, 2009. **44**(6): p. 547-58.

47. Whitchurch, C.B., et al., *Extracellular DNA required for bacterial biofilm formation.* Science, 2002. **295**(5559): p. 1487.

48. Frederiksen, B., et al., *Effect of aerosolized rhDNase (Pulmozyme) on pulmonary colonization in patients with cystic fibrosis.* Acta Paediatr, 2006. **95**(9): p. 1070-4.

49. Moreau-Marquis, S., G.A. O'Toole, and B.A. Stanton, *Tobramycin and FDA-approved iron chelators eliminate Pseudomonas aeruginosa biofilms on cystic fibrosis cells.* Am J Respir Cell Mol Biol, 2009. **41**(3): p. 305-13.

50. Wang, E.E., et al., *Association of respiratory viral infections with pulmonary deterioration in patients with cystic fibrosis.* N Engl J Med, 1984. **311**(26): p. 1653-8.

51. Smyth, A.R., et al., *Effect of respiratory virus infections including rhinovirus on clinical status in cystic fibrosis.* Arch Dis Child, 1995. **73**(2): p. 117-20.

52. Pribble, C.G., et al., *Clinical manifestations of exacerbations of cystic fibrosis associated with nonbacterial infections.* J Pediatr, 1990. **117**(2 Pt 1): p. 200-4.

53. Collinson, J., et al., *Effects of upper respiratory tract infections in patients with cystic fibrosis.* Thorax, 1996. **51**(11): p. 1115-22.

54. Hiatt, P.W., et al., *Effects of viral lower respiratory tract infection on lung function in infants with cystic fibrosis.* Pediatrics, 1999. **103**(3): p. 619-26.

55. van Ewijk, B.E., et al., *Prevalence and impact of respiratory viral infections in young children with cystic fibrosis: prospective cohort study.* Pediatrics, 2008. **122**(6): p. 1171-6.

56. Wat, D., et al., *The role of respiratory viruses in cystic fibrosis.* J Cyst Fibros, 2008. **7**(4): p. 320-8.

57. de Almeida, M.B., et al., *Rhinovirus C and respiratory exacerbations in children with cystic fibrosis.* Emerg Infect Dis, 2010. **16**(6): p. 996-9.

58. Asner, S., et al., *Role of respiratory viruses in pulmonary exacerbations in children with cystic fibrosis.* J Cyst Fibros, 2012. **11**(5): p. 433-9.

59. Ortiz, J.R., et al., *Influenza-associated cystic fibrosis pulmonary exacerbations.* Chest, 2010. **137**(4): p. 852-60.

60. Esther, C.R., Jr., et al., *Respiratory viruses are associated with common respiratory pathogens in cystic fibrosis.* Pediatr Pulmonol, 2014. **49**(9): p. 926-31.

61. Flight, W.G., et al., *Incidence and clinical impact of respiratory viruses in adults with cystic fibrosis.* Thorax, 2014. **69**(3): p. 247-53.

62. Seemungal, T., et al., *Respiratory viruses, symptoms, and inflammatory markers in acute exacerbations and stable chronic obstructive pulmonary disease.* Am J Respir Crit Care Med, 2001. **164**(9): p. 1618-23.

63. Rohde, G., et al., *Respiratory viruses in exacerbations of chronic obstructive pulmonary disease requiring hospitalisation: a case-control study.* Thorax, 2003. **58**(1): p. 37-42.

64. Papi, A., et al., *Infections and airway inflammation in chronic obstructive pulmonary disease severe exacerbations.* Am J Respir Crit Care Med, 2006. **173**(10): p. 1114-21.

65. Seemungal, T.A., et al., *Effect of exacerbation on quality of life in patients with chronic obstructive pulmonary disease.* Am J Respir Crit Care Med, 1998. **157**(5 Pt 1): p. 1418-22.

66. Yi, M.S., et al., *The impact of treatment of pulmonary exacerbations on the health-related quality of life of patients with cystic fibrosis: does hospitalization make a difference?* J Pediatr, 2004. **144**(6): p. 711-8.

67. Goldbeck, L., S. Zerrer, and T.G. Schmitz, *Monitoring quality of life in outpatients with cystic fibrosis: feasibility and longitudinal results.* J Cyst Fibros, 2007. **6**(3): p. 171-8.

68. Solem, C.T., et al., *Impact of pulmonary exacerbations and lung function on generic health-related quality of life in patients with cystic fibrosis.* Health Qual Life Outcomes, 2016. **14**: p. 63.

69. Britto, M.T., et al., *Impact of recent pulmonary exacerbations on quality of life in patients with cystic fibrosis.* Chest, 2002. **121**(1): p. 64-72.

70. Abman, S.H., et al., *Role of respiratory syncytial virus in early hospitalizations for respiratory distress of young infants with cystic fibrosis.* J Pediatr, 1988. **113**(5): p. 826-30.

71. Armstrong, D., et al., *Severe viral respiratory infections in infants with cystic fibrosis.* Pediatr Pulmonol, 1998. **26**(6): p. 371-9.

72. Petersen, N.T., et al., *Respiratory infections in cystic fibrosis patients caused by virus, chlamydia and mycoplasma--possible synergism with Pseudomonas aeruginosa.* Acta Paediatr Scand, 1981. **70**(5): p. 623-8.

73. Hewitt, R., et al., *The role of viral infections in exacerbations of chronic obstructive pulmonary disease and asthma.* Ther Adv Respir Dis, 2016. **10**(2): p. 158-74.

74. De Serres, G., et al., *Importance of viral and bacterial infections in chronic obstructive pulmonary disease exacerbations.* J Clin Virol, 2009. **46**(2): p. 129-33.

75. Dimopoulos, G., et al., *Viral epidemiology of acute exacerbations of chronic obstructive pulmonary disease.* Pulm Pharmacol Ther, 2012. **25**(1): p. 12-8.

76. Ramsey, B.W., et al., *The effect of respiratory viral infections on patients with cystic fibrosis.* Am J Dis Child, 1989. **143**(6): p. 662-8.

77. Hordvik, N.L., et al., *Effects of acute viral respiratory tract infections in patients with cystic fibrosis.* Pediatr Pulmonol, 1989. **7**(4): p. 217-22.

78. van Ewijk, B.E., et al., *Viral respiratory infections in cystic fibrosis.* J Cyst Fibros, 2005. **4 Suppl 2**: p. 31-6.

79. Johansen, H.K. and N. Hoiby, *Seasonal onset of initial colonisation and chronic infection with Pseudomonas aeruginosa in patients with cystic fibrosis in Denmark.* Thorax, 1992. **47**(2): p. 109-11.

80. Lay, M.K., et al., *Advances in understanding respiratory syncytial virus infection in airway epithelial cells and consequential effects on the immune response.* Microbes Infect, 2013. **15**(3): p. 230-42.

81. Gould, P.S. and A.J. Easton, *Coupled translation of the respiratory syncytial virus M2 open reading frames requires upstream sequences.* J Biol Chem, 2005. **280**(23): p. 21972-80.

82. Gould, P.S. and A.J. Easton, *Coupled translation of the second open reading frame of M2 mRNA is sequence dependent and differs significantly within the subfamily Pneumovirinae.* J Virol, 2007. **81**(16): p. 8488-96.

83. Fearns, R. and P.L. Collins, *Role of the M2-1 transcription antitermination protein of respiratory syncytial virus in sequential transcription.* J Virol, 1999. **73**(7): p. 5852-64.

84. Bermingham, A. and P.L. Collins, *The M2-2 protein of human respiratory syncytial virus is a regulatory factor involved in the balance between RNA replication and transcription.* Proc Natl Acad Sci U S A, 1999. **96**(20): p. 11259-64.

85. Johansson, C., *Respiratory syncytial virus infection: an innate perspective.* F1000Res, 2016. **5**: p. 2898.

86. Chirkova, T., et al., *CX3CR1 is an important surface molecule for respiratory syncytial virus infection in human airway epithelial cells.* J Gen Virol, 2015. **96**(9): p. 2543-56.

87. Johnson, S.M., et al., *Respiratory Syncytial Virus Uses CX3CR1 as a Receptor on Primary Human Airway Epithelial Cultures.* PLoS Pathog, 2015. **11**(12): p. e1005318.

88. Haynes, L.M., et al., *Involvement of toll-like receptor 4 in innate immunity to respiratory syncytial virus.* J Virol, 2001. **75**(22): p. 10730-7.

89. Tayyari, F., et al., *Identification of nucleolin as a cellular receptor for human respiratory syncytial virus.* Nat Med, 2011. **17**(9): p. 1132-5.

90. Krzyzaniak, M.A., et al., *Host cell entry of respiratory syncytial virus involves macropinocytosis followed by proteolytic activation of the F protein.* PLoS Pathog, 2013. **9**(4): p. e1003309.

91. Garcia, J., et al., *Cytoplasmic inclusions of respiratory syncytial virus-infected cells: formation of inclusion bodies in transfected cells that coexpress the nucleoprotein, the phosphoprotein, and the 22K protein.* Virology, 1993. **195**(1): p. 243-7.

92. Carromeu, C., et al., *Intracellular localization of human respiratory syncytial virus L protein.* Arch Virol, 2007. **152**(12): p. 2259-63.

93. Rincheval, V., et al., *Functional organization of cytoplasmic inclusion bodies in cells infected by respiratory syncytial virus.* Nat Commun, 2017. **8**(1): p. 563.

94. Mitra, R., et al., *The human respiratory syncytial virus matrix protein is required for maturation of viral filaments.* J Virol, 2012. **86**(8): p. 4432-43.

95. Shaikh, F.Y., et al., *A critical phenylalanine residue in the respiratory syncytial virus fusion protein cytoplasmic tail mediates assembly of internal viral proteins into viral filaments and particles.* MBio, 2012. **3**(1).

96. Forster, A., et al., *Dimerization of matrix protein is required for budding of respiratory syncytial virus.* J Virol, 2015. **89**(8): p. 4624-35.

97. Brock, S.C., J.R. Goldenring, and J.E. Crowe, Jr., *Apical recycling systems regulate directional budding of respiratory syncytial virus from polarized epithelial cells.* Proc Natl Acad Sci U S A, 2003. **100**(25): p. 15143-8.

98. Utley, T.J., et al., *Respiratory syncytial virus uses a Vps4-independent budding mechanism controlled by Rab11-FIP2.* Proc Natl Acad Sci U S A, 2008. **105**(29): p. 10209-14.

99. San-Juan-Vergara, H., et al., *Cholesterol-rich microdomains as docking platforms for respiratory syncytial virus in normal human bronchial epithelial cells.* J Virol, 2012. **86**(3): p. 1832-43.

100. Chang, T.H., et al., *Cholesterol-rich lipid rafts are required for release of infectious human respiratory syncytial virus particles.* Virology, 2012. **422**(2): p. 205-13.

101. Greve, J.M., et al., *The major human rhinovirus receptor is ICAM-1.* Cell, 1989. **56**(5): p. 839-47.

102. Hofer, F., et al., *Members of the low density lipoprotein receptor family mediate cell entry of a minor-group common cold virus.* Proc Natl Acad Sci U S A, 1994. **91**(5): p. 1839-42.

103. Bochkov, Y.A., et al., *Cadherin-related family member 3, a childhood asthma susceptibility gene product, mediates rhinovirus C binding and replication.* Proc Natl Acad Sci U S A, 2015. **112**(17): p. 5485-90.

104. Suomalainen, M. and U.F. Greber, *Uncoating of non-enveloped viruses.* Curr Opin Virol, 2013. **3**(1): p. 27-33.

105. van der Linden, L., K.C. Wolthers, and F.J. van Kuppeveld, *Replication and Inhibitors of Enteroviruses and Parechoviruses.* Viruses, 2015. **7**(8): p. 4529-62.

106. Roulin, P.S., et al., *Rhinovirus uses a phosphatidylinositol 4-phosphate/cholesterol counter-current for the formation of replication compartments at the ER-Golgi interface.* Cell Host Microbe, 2014. **16**(5): p. 677-90.

107. Chen, Y.H., et al., *Phosphatidylserine vesicles enable efficient en bloc transmission of enteroviruses.* Cell, 2015. **160**(4): p. 619-30.

108. Feng, Z., et al., *A pathogenic picornavirus acquires an envelope by hijacking cellular membranes.* Nature, 2013. **496**(7445): p. 367-71.

109. Robinson, S.M., et al., *Coxsackievirus B exits the host cell in shed microvesicles displaying autophagosomal markers.* PLoS Pathog, 2014. **10**(4): p. e1004045.

110. Vareille, M., et al., *The airway epithelium: soldier in the fight against respiratory viruses.* Clin Microbiol Rev, 2011. **24**(1): p. 210-29.

111. Zhang, L., et al., *Respiratory syncytial virus infection of human airway epithelial cells is polarized, specific to ciliated cells, and without obvious cytopathology.* J Virol, 2002. **76**(11): p. 5654-66.

112. Villenave, R., et al., *In vitro modeling of respiratory syncytial virus infection of pediatric bronchial epithelium, the primary target of infection in vivo.* Proc Natl Acad Sci U S A, 2012. **109**(13): p. 5040-5.

113. Okabayashi, T., et al., *Type-III interferon, not type-I, is the predominant interferon induced by respiratory viruses in nasal epithelial cells.* Virus Res, 2011. **160**(1-2): p. 360-6.

114. Selvaggi, C., et al., *Interferon lambda 1-3 expression in infants hospitalized for RSV or HRV associated bronchiolitis.* J Infect, 2014. **68**(5): p. 467-77.

115. Villenave, R., et al., *Induction and Antagonism of Antiviral Responses in Respiratory Syncytial Virus-Infected Pediatric Airway Epithelium.* J Virol, 2015. **89**(24): p. 12309-18.

116. Whitcutt, M.J., K.B. Adler, and R. Wu, *A biphasic chamber system for maintaining polarity of differentiation of cultured respiratory tract epithelial cells.* In Vitro Cell Dev Biol, 1988. **24**(5): p. 420-8.

117. Devor, D.C., R.J. Bridges, and J.M. Pilewski, *Pharmacological modulation of ion transport across wild-type and DeltaF508 CFTR-expressing human bronchial epithelia.* Am J Physiol Cell Physiol, 2000. **279**(2): p. C461-79.

118. Gruenert, D.C., et al., *Established cell lines used in cystic fibrosis research.* J Cyst Fibros, 2004. **3 Suppl 2**: p. 191-6.

119. Zheng, S., et al., *Impaired innate host defense causes susceptibility to respiratory virus infections in cystic fibrosis.* Immunity, 2003. **18**(5): p. 619-30.

120. Kieninger, E., et al., *High rhinovirus burden in lower airways of children with cystic fibrosis.* Chest, 2013. **143**(3): p. 782-790.

121. Chattoraj, S.S., et al., *Pseudomonas aeruginosa suppresses interferon response to rhinovirus infection in cystic fibrosis but not in normal bronchial epithelial cells.* Infect Immun, 2011. **79**(10): p. 4131-45.

122. Parker, D., et al., *Induction of type I interferon signaling by Pseudomonas aeruginosa is diminished in cystic fibrosis epithelial cells.* Am J Respir Cell Mol Biol, 2012. **46**(1): p. 6-13.

123. Dauletbaev, N., et al., *Rhinovirus Load Is High despite Preserved Interferon-beta Response in Cystic Fibrosis Bronchial Epithelial Cells.* PLoS One, 2015. **10**(11): p. e0143129.

124. Schogler, A., et al., *Interferon response of the cystic fibrosis bronchial epithelium to major and minor group rhinovirus infection.* J Cyst Fibros, 2016. **15**(3): p. 332-9.

125. Xu, W., et al., *Cystic fibrosis and normal human airway epithelial cell response to influenza a viral infection.* J Interferon Cytokine Res, 2006. **26**(9): p. 609-27.

126. Parker, D. and A. Prince, *Type I interferon response to extracellular bacteria in the airway epithelium.* Trends Immunol, 2011. **32**(12): p. 582-8.

127. Cohen, T.S. and A.S. Prince, *Bacterial pathogens activate a common inflammatory pathway through IFNlambda regulation of PDCD4.* PLoS Pathog, 2013. **9**(10): p. e1003682.

128. John, G., et al., *TLR-4-mediated innate immunity is reduced in cystic fibrosis airway cells.* Am J Respir Cell Mol Biol, 2010. **42**(4): p. 424-31.

129. Kieninger, E., et al., *Lack of an exaggerated inflammatory response on virus infection in cystic fibrosis.* Eur Respir J, 2012. **39**(2): p. 297-304.

130. Sutanto, E.N., et al., *Innate inflammatory responses of pediatric cystic fibrosis airway epithelial cells: effects of nonviral and viral stimulation.* Am J Respir Cell Mol Biol, 2011. **44**(6): p. 761-7.

131. Message, S.D., et al., *Rhinovirus-induced lower respiratory illness is increased in asthma and related to virus load and Th1/2 cytokine and IL-10 production.* Proc Natl Acad Sci U S A, 2008. **105**(36): p. 13562-7.

132. Mallia, P., et al., *Experimental rhinovirus infection as a human model of chronic obstructive pulmonary disease exacerbation.* Am J Respir Crit Care Med, 2011. **183**(6): p. 734-42.

133. Wark, P.A., et al., *Asthmatic bronchial epithelial cells have a deficient innate immune response to infection with rhinovirus.* J Exp Med, 2005. **201**(6): p. 937-47.

134. Contoli, M., et al., *Role of deficient type III interferon-lambda production in asthma exacerbations.* Nat Med, 2006. **12**(9): p. 1023-6.

135. Sykes, A., et al., *Rhinovirus-induced interferon production is not deficient in well controlled asthma.* Thorax, 2014. **69**(3): p. 240-6.

136. Gielen, V., et al., *Increased nuclear suppressor of cytokine signaling 1 in asthmatic bronchial epithelium suppresses rhinovirus induction of innate interferons.* J Allergy Clin Immunol, 2015. **136**(1): p. 177-188 e11.

137. Kloepfer, K.M., et al., *Detection of pathogenic bacteria during rhinovirus infection is associated with increased respiratory symptoms and asthma exacerbations.* J Allergy Clin Immunol, 2014. **133**(5): p. 1301-7, 1307 e1-3.

138. Wilkinson, T.M., et al., *Effect of interactions between lower airway bacterial and rhinoviral infection in exacerbations of COPD.* Chest, 2006. **129**(2): p. 317-24.

139. George, S.N., et al., *Human rhinovirus infection during naturally occurring COPD exacerbations.* Eur Respir J, 2014. **44**(1): p. 87-96.

140. Mallia, P., et al., *Rhinovirus infection induces degradation of antimicrobial peptides and secondary bacterial infection in chronic obstructive pulmonary disease.* Am J Respir Crit Care Med, 2012. **186**(11): p. 1117-24.

141. Molyneaux, P.L., et al., *Outgrowth of the bacterial airway microbiome after rhinovirus exacerbation of chronic obstructive pulmonary disease.* Am J Respir Crit Care Med, 2013. **188**(10): p. 1224-31.

142. Planet, P.J., et al., *Lambda Interferon Restructures the Nasal Microbiome and Increases Susceptibility to Staphylococcus aureus Superinfection.* MBio, 2016. **7**(1): p. e01939-15.

143. Smith, C.M., et al., *Ciliary dyskinesia is an early feature of respiratory syncytial virus infection.* Eur Respir J, 2014. **43**(2): p. 485-96.

144. Chilvers, M.A., et al., *The effects of coronavirus on human nasal ciliated respiratory epithelium.* Eur Respir J, 2001. **18**(6): p. 965-70.

145. Liesman, R.M., et al., *RSV-encoded NS2 promotes epithelial cell shedding and distal airway obstruction.* J Clin Invest, 2014. **124**(5): p. 2219-33.

146. Plotkowski, M.C., et al., *Adherence of type I Streptococcus pneumoniae to tracheal epithelium of mice infected with influenza A/PR8 virus.* Am Rev Respir Dis, 1986. **134**(5): p. 1040-4.

147. Meng, F., et al., *Dynamic Virus-Bacterium Interactions in a Porcine Precision-Cut Lung Slice Coinfection Model: Swine Influenza Virus Paves the Way for Streptococcus suis Infection in a Two-Step Process.* Infect Immun, 2015. **83**(7): p. 2806-15.

148. Avadhanula, V., et al., *Respiratory viruses augment the adhesion of bacterial pathogens to respiratory epithelium in a viral species- and cell type-dependent manner.* J Virol, 2006. **80**(4): p. 1629-36.

149. Ishizuka, S., et al., *Effects of rhinovirus infection on the adherence of Streptococcus pneumoniae to cultured human airway epithelial cells.* J Infect Dis, 2003. **188**(12): p. 1928-39.

150. Li, N., et al., *Influenza viral neuraminidase primes bacterial coinfection through TGF-beta-mediated expression of host cell receptors.* Proc Natl Acad Sci U S A, 2015. **112**(1): p. 238-43.

151. Avadhanula, V., et al., *Nontypeable Haemophilus influenzae and Streptococcus pneumoniae bind respiratory syncytial virus glycoprotein.* J Med Microbiol, 2007. **56**(Pt 9): p. 1133-7.

152. Van Ewijk, B.E., et al., *RSV mediates Pseudomonas aeruginosa binding to cystic fibrosis and normal epithelial cells.* Pediatr Res, 2007. **61**(4): p. 398-403.

153. Hament, J.M., et al., *Direct binding of respiratory syncytial virus to pneumococci: a phenomenon that enhances both pneumococcal adherence to human epithelial cells and pneumococcal invasiveness in a murine model.* Pediatr Res, 2005. **58**(6): p. 1198-203.

154. Smith, C.M., et al., *Respiratory syncytial virus increases the virulence of Streptococcus pneumoniae by binding to penicillin binding protein 1a. A new paradigm in respiratory infection.* Am J Respir Crit Care Med, 2014. **190**(2): p. 196-207.

155. Novotny, L.A. and L.O. Bakaletz, *Intercellular adhesion molecule 1 serves as a primary cognate receptor for the Type IV pilus of nontypeable Haemophilus influenzae.* Cell Microbiol, 2016. **18**(8): p. 1043-55.

156. Shahangian, A., et al., *Type I IFNs mediate development of postinfluenza bacterial pneumonia in mice.* J Clin Invest, 2009. **119**(7): p. 1910-20.

157. Nakamura, S., K.M. Davis, and J.N. Weiser, *Synergistic stimulation of type I interferons during influenza virus coinfection promotes Streptococcus pneumoniae colonization in mice.* J Clin Invest, 2011. **121**(9): p. 3657-65.

158. Kudva, A., et al., *Influenza A inhibits Th17-mediated host defense against bacterial pneumonia in mice.* J Immunol, 2011. **186**(3): p. 1666-74.

159. Lee, B., et al., *Influenza-induced type I interferon enhances susceptibility to gram-negative and gram-positive bacterial pneumonia in mice.* Am J Physiol Lung Cell Mol Physiol, 2015. **309**(2): p. L158-67.

160. Robinson, K.M., et al., *Influenza A virus exacerbates Staphylococcus aureus pneumonia in mice by attenuating antimicrobial peptide production.* J Infect Dis, 2014. **209**(6): p. 865-75.

161. McGillivary, G., et al., *Respiratory syncytial virus-induced dysregulation of expression of a mucosal beta-defensin augments colonization of the upper airway by non-typeable Haemophilus influenzae.* Cell Microbiol, 2009. **11**(9): p. 1399-408.

162. Tian, X., et al., *Poly I:C enhances susceptibility to secondary pulmonary infections by gram-positive bacteria.* PLoS One, 2012. **7**(9): p. e41879.

163. Thompson, A.J. and S.A. Locarnini, *Toll-like receptors, RIG-I-like RNA helicases and the antiviral innate immune response.* Immunol Cell Biol, 2007. **85**(6): p. 435-45.

164. Yoon, J.S., et al., *Cytokine induction by respiratory syncytial virus and adenovirus in bronchial epithelial cells.* Pediatr Pulmonol, 2007. **42**(3): p. 277-82.

165. Piper, S.C., et al., *The role of interleukin-1 and interleukin-18 in pro-inflammatory and anti-viral responses to rhinovirus in primary bronchial epithelial cells.* PLoS One, 2013. **8**(5): p. e63365.

166. Didierlaurent, A., et al., *Sustained desensitization to bacterial Toll-like receptor ligands after resolution of respiratory influenza infection.* J Exp Med, 2008. **205**(2): p. 323-9.

167. LeVine, A.M., V. Koeningsknecht, and J.M. Stark, *Decreased pulmonary clearance of S. pneumoniae following influenza A infection in mice.* J Virol Methods, 2001. **94**(1-2): p. 173-86.

168. Stark, J.M., et al., *Decreased bacterial clearance from the lungs of mice following primary respiratory syncytial virus infection.* J Med Virol, 2006. **78**(6): p. 829-38.

169. Oliver, B.G., et al., *Rhinovirus exposure impairs immune responses to bacterial products in human alveolar macrophages.* Thorax, 2008. **63**(6): p. 519-25.

170. van der Sluijs, K.F., et al., *IL-10 is an important mediator of the enhanced susceptibility to pneumococcal pneumonia after influenza infection.* J Immunol, 2004. **172**(12): p. 7603-9.

171. Sajjan, U.S., et al., *H. influenzae potentiates airway epithelial cell responses to rhinovirus by increasing ICAM-1 and TLR3 expression.* FASEB J, 2006. **20**(12): p. 2121-3.

172. Gulraiz, F., et al., *Haemophilus influenzae increases the susceptibility and inflammatory response of airway epithelial cells to viral infections.* FASEB J, 2015. **29**(3): p. 849-58.

173. Bomberger, J.M., et al., *Pseudomonas aeruginosa Cif protein enhances the ubiquitination and proteasomal degradation of the transporter associated with antigen processing (TAP) and reduces major histocompatibility complex (MHC) class I antigen presentation.* J Biol Chem, 2014. **289**(1): p. 152-62.

174. Marks, L.R., et al., *Interkingdom signaling induces Streptococcus pneumoniae biofilm dispersion and transition from asymptomatic colonization to disease.* MBio, 2013. **4**(4).

175. Chattoraj, S.S., et al., *Rhinovirus infection liberates planktonic bacteria from biofilm and increases chemokine responses in cystic fibrosis airway epithelial cells.* Thorax, 2011. **66**(4): p. 333-9.

176. Weinberg, E.D., *Nutritional immunity. Host's attempt to withold iron from microbial invaders.* JAMA, 1975. **231**(1): p. 39-41.

177. Kochan, I., *The role of iron in bacterial infections, with special consideration of host-tubercle bacillus interaction.* Curr Top Microbiol Immunol, 1973. **60**: p. 1-30.

178. Brubaker, R.R., E.D. Beesley, and M.J. Surgalla, *Pasteurella pestis: Role of Pesticin I and Iron in Experimental Plague.* Science, 1965. **149**(3682): p. 422-4.

179. Sword, C.P., *Mechanisms of pathogenesis in Listeria monocytogenes infection. I. Influence of iron.* J Bacteriol, 1966. **92**(3): p. 536-42.

180. Bullen, J.J., L.C. Leigh, and H.J. Rogers, *The effect of iron compounds on the virulence of Escherichia coli for guinea-pigs.* Immunology, 1968. **15**(4): p. 581-8.

181. Forsberg, C.M. and J.J. Bullen, *The effect of passage and iron on the virulence of Pseudomonas aeruginosa.* J Clin Pathol, 1972. **25**(1): p. 65-8.

182. Cassat, J.E. and E.P. Skaar, *Iron in infection and immunity.* Cell Host Microbe, 2013. **13**(5): p. 509-19.

183. Nemeth, E., et al., *Hepcidin regulates cellular iron efflux by binding to ferroportin and inducing its internalization.* Science, 2004. **306**(5704): p. 2090-3.

184. Hentze, M.W., et al., *Two to tango: regulation of Mammalian iron metabolism.* Cell, 2010. **142**(1): p. 24-38.

185. Delaby, C., et al., *Presence of the iron exporter ferroportin at the plasma membrane of macrophages is enhanced by iron loading and down-regulated by hepcidin.* Blood, 2005. **106**(12): p. 3979-84.

186. Peyssonnaux, C., et al., *TLR4-dependent hepcidin expression by myeloid cells in response to bacterial pathogens.* Blood, 2006. **107**(9): p. 3727-32.

187. Hood, M.I. and E.P. Skaar, *Nutritional immunity: transition metals at the pathogen-host interface.* Nat Rev Microbiol, 2012. **10**(8): p. 525-37.

188. O'Connor T, M., et al., *Subclinical anaemia of chronic disease in adult patients with cystic fibrosis.* J Cyst Fibros, 2002. **1**(1): p. 31-4.

189. Schade, A.L. and L. Caroline, *An Iron-binding Component in Human Blood Plasma.* Science, 1946. **104**(2702): p. 340-1.

190. Garcia-Montoya, I.A., et al., *Lactoferrin a multiple bioactive protein: an overview.* Biochim Biophys Acta, 2012. **1820**(3): p. 226-36.

191. Bellamy, W., et al., *Identification of the bactericidal domain of lactoferrin.* Biochim Biophys Acta, 1992. **1121**(1-2): p. 130-6.

192. van der Kraan, M.I., et al., *Lactoferrampin: a novel antimicrobial peptide in the N1-domain of bovine lactoferrin.* Peptides, 2004. **25**(2): p. 177-83.

193. Schade, A.L. and L. Caroline, *Raw Hen Egg White and the Role of Iron in Growth Inhibition of Shigella Dysenteriae, Staphylococcus Aureus, Escherichia Coli and Saccharomyces Cerevisiae.* Science, 1944. **100**(2584): p. 14-5.

194. Aisen, P. and I. Listowsky, *Iron transport and storage proteins.* Annu Rev Biochem, 1980. **49**: p. 357-93.

195. Makey, D.G. and U.S. Seal, *The detection of four molecular forms of human transferrin during the iron binding process.* Biochim Biophys Acta, 1976. **453**(1): p. 250-6.

196. Luck, A.N. and A.B. Mason, *Transferrin-mediated cellular iron delivery.* Curr Top Membr, 2012. **69**: p. 3-35.

197. Mickelsen, P.A. and P.F. Sparling, *Ability of Neisseria gonorrhoeae, Neisseria meningitidis, and commensal Neisseria species to obtain iron from transferrin and iron compounds.* Infect Immun, 1981. **33**(2): p. 555-64.

198. Herrington, D.A. and P.F. Sparling, *Haemophilus influenzae can use human transferrin as a sole source for required iron.* Infect Immun, 1985. **48**(1): p. 248-51.

199. Senkovich, O., et al., *Unique host iron utilization mechanisms of Helicobacter pylori revealed with iron-deficient chemically defined media.* Infect Immun, 2010. **78**(5): p. 1841-9.

200. Ankenbauer, R., S. Sriyosachati, and C.D. Cox, *Effects of siderophores on the growth of Pseudomonas aeruginosa in human serum and transferrin.* Infect Immun, 1985. **49**(1): p. 132-40.

201. Schryvers, A.B. and L.J. Morris, *Identification and characterization of the transferrin receptor from Neisseria meningitidis.* Mol Microbiol, 1988. **2**(2): p. 281-8.

202. Barber, M.F. and N.C. Elde, *Nutritional immunity. Escape from bacterial iron piracy through rapid evolution of transferrin.* Science, 2014. **346**(6215): p. 1362-6.

203. Tan, S., et al., *Helicobacter pylori perturbs iron trafficking in the epithelium to grow on the cell surface.* PLoS Pathog, 2011. **7**(5): p. e1002050.

204. Banin, E., M.L. Vasil, and E.P. Greenberg, *Iron and Pseudomonas aeruginosa biofilm formation.* Proc Natl Acad Sci U S A, 2005. **102**(31): p. 11076-81.

205. Cornelis, P. and J. Dingemans, *Pseudomonas aeruginosa adapts its iron uptake strategies in function of the type of infections.* Front Cell Infect Microbiol, 2013. **3**: p. 75.

206. Sriyosachati, S. and C.D. Cox, *Siderophore-mediated iron acquisition from transferrin by Pseudomonas aeruginosa.* Infect Immun, 1986. **52**(3): p. 885-91.

207. Reinhart, A.A. and A.G. Oglesby-Sherrouse, *Regulation of Pseudomonas aeruginosa Virulence by Distinct Iron Sources.* Genes (Basel), 2016. **7**(12).

208. Wilderman, P.J., et al., *Characterization of an endoprotease (PrpL) encoded by a PvdS-regulated gene in Pseudomonas aeruginosa.* Infect Immun, 2001. **69**(9): p. 5385-94.

209. Shigematsu, T., et al., *Iron-Mediated regulation of alkaline proteinase production in Pseudomonas aeruginosa.* Microbiol Immunol, 2001. **45**(8): p. 579-90.

210. Britigan, B.E., et al., *Transferrin and lactoferrin undergo proteolytic cleavage in the Pseudomonas aeruginosa-infected lungs of patients with cystic fibrosis.* Infect Immun, 1993. **61**(12): p. 5049-55.

211. Wolz, C., et al., *Iron release from transferrin by pyoverdin and elastase from Pseudomonas aeruginosa.* Infect Immun, 1994. **62**(9): p. 4021-7.

212. Nguyen, A.T., et al., *Adaptation of iron homeostasis pathways by a Pseudomonas aeruginosa pyoverdine mutant in the cystic fibrosis lung.* J Bacteriol, 2014. **196**(12): p. 2265-76.

213. Marvig, R.L., et al., *Within-host evolution of Pseudomonas aeruginosa reveals adaptation toward iron acquisition from hemoglobin.* MBio, 2014. **5**(3): p. e00966-14.

214. Hunter, R.C., et al., *Phenazine content in the cystic fibrosis respiratory tract negatively correlates with lung function and microbial complexity.* Am J Respir Cell Mol Biol, 2012. **47**(6): p. 738-45.

215. Wang, Y., et al., *Phenazine-1-carboxylic acid promotes bacterial biofilm development via ferrous iron acquisition.* J Bacteriol, 2011. **193**(14): p. 3606-17.

216. Li, J., et al., *Exosomes mediate the cell-to-cell transmission of IFN-alpha-induced antiviral activity.* Nat Immunol, 2013. **14**(8): p. 793-803.

217. Raab-Traub, N. and D.P. Dittmer, *Viral effects on the content and function of extracellular vesicles.* Nat Rev Microbiol, 2017. **15**(9): p. 559-572.

218. Valadi, H., et al., *Exosome-mediated transfer of mRNAs and microRNAs is a novel mechanism of genetic exchange between cells.* Nat Cell Biol, 2007. **9**(6): p. 654-9.

219. Skog, J., et al., *Glioblastoma microvesicles transport RNA and proteins that promote tumour growth and provide diagnostic biomarkers.* Nat Cell Biol, 2008. **10**(12): p. 1470-6.

220. Subra, C., et al., *Exosomes account for vesicle-mediated transcellular transport of activatable phospholipases and prostaglandins.* J Lipid Res, 2010. **51**(8): p. 2105-20.

221. Deng, Z.B., et al., *Exosome-like nanoparticles from intestinal mucosal cells carry prostaglandin E2 and suppress activation of liver NKT cells.* J Immunol, 2013. **190**(7): p. 3579-89.

222. Jan, A.T., *Outer Membrane Vesicles (OMVs) of Gram-negative Bacteria: A Perspective Update.* Front Microbiol, 2017. **8**: p. 1053.

223. Brown, L., et al., *Through the wall: extracellular vesicles in Gram-positive bacteria, mycobacteria and fungi.* Nat Rev Microbiol, 2015. **13**(10): p. 620-30.

224. Szempruch, A.J., et al., *Sending a message: extracellular vesicles of pathogenic protozoan parasites.* Nat Rev Microbiol, 2016. **14**(11): p. 669-675.

225. Mantel, P.Y. and M. Marti, *The role of extracellular vesicles in Plasmodium and other protozoan parasites.* Cell Microbiol, 2014. **16**(3): p. 344-54.

226. Nolte-'t Hoen, E., et al., *Extracellular vesicles and viruses: Are they close relatives?* Proc Natl Acad Sci U S A, 2016. **113**(33): p. 9155-61.

227. Harding, C., J. Heuser, and P. Stahl, *Receptor-mediated endocytosis of transferrin and recycling of the transferrin receptor in rat reticulocytes.* J Cell Biol, 1983. **97**(2): p. 329-39.

228. Pan, B.T. and R.M. Johnstone, *Fate of the transferrin receptor during maturation of sheep reticulocytes in vitro: selective externalization of the receptor.* Cell, 1983. **33**(3): p. 967-78.

229. Johnstone, R.M., et al., *Vesicle formation during reticulocyte maturation. Association of plasma membrane activities with released vesicles (exosomes).* J Biol Chem, 1987. **262**(19): p. 9412-20.

230. Raposo, G., et al., *B lymphocytes secrete antigen-presenting vesicles.* J Exp Med, 1996. **183**(3): p. 1161-72.

231. Zitvogel, L., et al., *Eradication of established murine tumors using a novel cell-free vaccine: dendritic cell-derived exosomes.* Nat Med, 1998. **4**(5): p. 594-600.

232. Satta, N., et al., *Monocyte vesiculation is a possible mechanism for dissemination of membrane-associated procoagulant activities and adhesion molecules after stimulation by lipopolysaccharide.* J Immunol, 1994. **153**(7): p. 3245-55.

233. Mesri, M. and D.C. Altieri, *Endothelial cell activation by leukocyte microparticles.* J Immunol, 1998. **161**(8): p. 4382-7.

234. Gasser, O. and J.A. Schifferli, *Activated polymorphonuclear neutrophils disseminate anti-inflammatory microparticles by ectocytosis.* Blood, 2004. **104**(8): p. 2543-8.

235. Barry, O.P., et al., *Transcellular activation of platelets and endothelial cells by bioactive lipids in platelet microparticles.* J Clin Invest, 1997. **99**(9): p. 2118-27.

236. Nabhan, J.F., et al., *Formation and release of arrestin domain-containing protein 1-mediated microvesicles (ARMMs) at plasma membrane by recruitment of TSG101 protein.* Proc Natl Acad Sci U S A, 2012. **109**(11): p. 4146-51.

237. Raposo, G. and W. Stoorvogel, *Extracellular vesicles: exosomes, microvesicles, and friends.* J Cell Biol, 2013. **200**(4): p. 373-83.

238. S, E.L.A., et al., *Extracellular vesicles: biology and emerging therapeutic opportunities.* Nat Rev Drug Discov, 2013. **12**(5): p. 347-57.

239. Samanta, S., et al., *Exosomes: new molecular targets of diseases.* Acta Pharmacol Sin, 2017.

240. Colombo, M., G. Raposo, and C. Thery, *Biogenesis, secretion, and intercellular interactions of exosomes and other extracellular vesicles.* Annu Rev Cell Dev Biol, 2014. **30**: p. 255-89.

241. Maas, S.L., X.O. Breakefield, and A.M. Weaver, *Extracellular Vesicles: Unique Intercellular Delivery Vehicles.* Trends Cell Biol, 2017. **27**(3): p. 172-188.

242. Huotari, J. and A. Helenius, *Endosome maturation.* EMBO J, 2011. **30**(17): p. 3481-500.

243. Colombo, M., et al., *Analysis of ESCRT functions in exosome biogenesis, composition and secretion highlights the heterogeneity of extracellular vesicles.* J Cell Sci, 2013. **126**(Pt 24): p. 5553-65.

244. Trajkovic, K., et al., *Ceramide triggers budding of exosome vesicles into multivesicular endosomes.* Science, 2008. **319**(5867): p. 1244-7.

245. Verweij, F.J., et al., *LMP1 association with CD63 in endosomes and secretion via exosomes limits constitutive NF-kappaB activation.* EMBO J, 2011. **30**(11): p. 2115-29.

246. Savina, A., M. Vidal, and M.I. Colombo, *The exosome pathway in K562 cells is regulated by Rab11.* J Cell Sci, 2002. **115**(Pt 12): p. 2505-15.

247. Ostrowski, M., et al., *Rab27a and Rab27b control different steps of the exosome secretion pathway.* Nat Cell Biol, 2010. **12**(1): p. 19-30; sup pp 1-13.

248. Hsu, C., et al., *Regulation of exosome secretion by Rab35 and its GTPase-activating proteins TBC1D10A-C.* J Cell Biol, 2010. **189**(2): p. 223-32.

249. Baietti, M.F., et al., *Syndecan-syntenin-ALIX regulates the biogenesis of exosomes.* Nat Cell Biol, 2012. **14**(7): p. 677-85.

250. Fu, Y., et al., *Exosome-mediated miR-146a transfer suppresses type I interferon response and facilitates EV71 infection.* PLoS Pathog, 2017. **13**(9): p. e1006611.

251. Ramakrishnaiah, V., et al., *Exosome-mediated transmission of hepatitis C virus between human hepatoma Huh7.5 cells.* Proc Natl Acad Sci U S A, 2013. **110**(32): p. 13109-13.

252. Bukong, T.N., et al., *Exosomes from hepatitis C infected patients transmit HCV infection and contain replication competent viral RNA in complex with Ago2-miR122-HSP90.* PLoS Pathog, 2014. **10**(10): p. e1004424.

253. Brimacombe, C.L., et al., *Neutralizing antibody-resistant hepatitis C virus cell-to-cell transmission.* J Virol, 2011. **85**(1): p. 596-605.

254. Xiao, F., et al., *Hepatitis C virus cell-cell transmission and resistance to direct-acting antiviral agents.* PLoS Pathog, 2014. **10**(5): p. e1004128.

255. Huynh, M.L., V.A. Fadok, and P.M. Henson, *Phosphatidylserine-dependent ingestion of apoptotic cells promotes TGF-beta1 secretion and the resolution of inflammation.* J Clin Invest, 2002. **109**(1): p. 41-50.

256. Szondy, Z., et al., *Anti-inflammatory Mechanisms Triggered by Apoptotic Cells during Their Clearance.* Front Immunol, 2017. **8**: p. 909.

257. Altan-Bonnet, N., *Extracellular vesicles are the Trojan horses of viral infection.* Curr Opin Microbiol, 2016. **32**: p. 77-81.

258. Gutierrez, M.J., et al., *Airway Secretory microRNAome Changes during Rhinovirus Infection in Early Childhood.* PLoS One, 2016. **11**(9): p. e0162244.

259. Zhao, Y., et al., *Systematic Analysis of Cell-Type Differences in the Epithelial Secretome Reveals Insights into the Pathogenesis of Respiratory Syncytial Virus-Induced Lower Respiratory Tract Infections.* J Immunol, 2017. **198**(8): p. 3345-3364.

260. Dreux, M., et al., *Short-range exosomal transfer of viral RNA from infected cells to plasmacytoid dendritic cells triggers innate immunity.* Cell Host Microbe, 2012. **12**(4): p. 558-70.

261. Baglio, S.R., et al., *Sensing of latent EBV infection through exosomal transfer of 5'pppRNA.* Proc Natl Acad Sci U S A, 2016. **113**(5): p. E587-96.

262. Bernard, M.A., et al., *Novel HIV-1 miRNAs stimulate TNFalpha release in human macrophages via TLR8 signaling pathway.* PLoS One, 2014. **9**(9): p. e106006.

263. Kouwaki, T., et al., *Extracellular Vesicles Including Exosomes Regulate Innate Immune Responses to Hepatitis B Virus Infection.* Front Immunol, 2016. **7**: p. 335.

264. Bauer, S., et al., *Activation of NK cells and T cells by NKG2D, a receptor for stress-inducible MICA.* Science, 1999. **285**(5428): p. 727-9.

265. Kloss, M., et al., *Interaction of monocytes with NK cells upon Toll-like receptor-induced expression of the NKG2D ligand MICA.* J Immunol, 2008. **181**(10): p. 6711-9.

266. Delorme-Axford, E., et al., *Human placental trophoblasts confer viral resistance to recipient cells.* Proc Natl Acad Sci U S A, 2013. **110**(29): p. 12048-53.

267. Beatty, W.L., et al., *Trafficking and release of mycobacterial lipids from infected macrophages.* Traffic, 2000. **1**(3): p. 235-47.

268. Beatty, W.L. and D.G. Russell, *Identification of mycobacterial surface proteins released into subcellular compartments of infected macrophages.* Infect Immun, 2000. **68**(12): p. 6997-7002.

269. Kruh-Garcia, N.A., et al., *Detection of Mycobacterium tuberculosis peptides in the exosomes of patients with active and latent M. tuberculosis infection using MRM-MS.* PLoS One, 2014. **9**(7): p. e103811.

270. Bhatnagar, S., et al., *Exosomes released from macrophages infected with intracellular pathogens stimulate a proinflammatory response in vitro and in vivo.* Blood, 2007. **110**(9): p. 3234-44.

271. Sibley, L.D., et al., *Mycobacterial lipoarabinomannan inhibits gamma interferon-mediated activation of macrophages.* Infect Immun, 1988. **56**(5): p. 1232-6.

272. Brightbill, H.D., et al., *Host defense mechanisms triggered by microbial lipoproteins through toll-like receptors.* Science, 1999. **285**(5428): p. 732-6.

273. Nigou, J., et al., *Mannosylated lipoarabinomannans inhibit IL-12 production by human dendritic cells: evidence for a negative signal delivered through the mannose receptor.* J Immunol, 2001. **166**(12): p. 7477-85.

274. Briken, V., et al., *Mycobacterial lipoarabinomannan and related lipoglycans: from biogenesis to modulation of the immune response.* Mol Microbiol, 2004. **53**(2): p. 391-403.

275. Vergne, I., M. Gilleron, and J. Nigou, *Manipulation of the endocytic pathway and phagocyte functions by Mycobacterium tuberculosis lipoarabinomannan.* Front Cell Infect Microbiol, 2014. **4**: p. 187.

276. Yonekawa, A., et al., *Dectin-2 is a direct receptor for mannose-capped lipoarabinomannan of mycobacteria.* Immunity, 2014. **41**(3): p. 402-413.

277. Singh, P.P., et al., *Exosomes isolated from mycobacteria-infected mice or cultured macrophages can recruit and activate immune cells in vitro and in vivo.* J Immunol, 2012. **189**(2): p. 777-85.

278. Schorey, J.S. and S. Bhatnagar, *Exosome function: from tumor immunology to pathogen biology.* Traffic, 2008. **9**(6): p. 871-81.

279. Giri, P.K., et al., *Proteomic analysis identifies highly antigenic proteins in exosomes from M. tuberculosis-infected and culture filtrate protein-treated macrophages.* Proteomics, 2010. **10**(17): p. 3190-202.

280. Diaz, G., et al., *Changes in the Membrane-Associated Proteins of Exosomes Released from Human Macrophages after Mycobacterium tuberculosis Infection.* Sci Rep, 2016. **6**: p. 37975.

281. Athman, J.J., et al., *Bacterial Membrane Vesicles Mediate the Release of Mycobacterium tuberculosis Lipoglycans and Lipoproteins from Infected Macrophages.* J Immunol, 2015. **195**(3): p. 1044-53.

282. Cheng, Y. and J.S. Schorey, *Exosomes carrying mycobacterial antigens can protect mice against Mycobacterium tuberculosis infection.* Eur J Immunol, 2013. **43**(12): p. 3279-90.

283. Athman, J.J., et al., *Mycobacterium tuberculosis Membrane Vesicles Inhibit T Cell Activation.* J Immunol, 2017. **198**(5): p. 2028-2037.

284. Smith, V.L., et al., *Exosomes function in antigen presentation during an in vivo Mycobacterium tuberculosis infection.* Sci Rep, 2017. **7**: p. 43578.

285. Nudel, K., P. Massari, and C.A. Genco, *Neisseria gonorrhoeae Modulates Cell Death in Human Endocervical Epithelial Cells through Export of Exosome-Associated cIAP2.* Infect Immun, 2015. **83**(9): p. 3410-7.

286. Peltzer, N., M. Darding, and H. Walczak, *Holding RIPK1 on the Ubiquitin Leash in TNFR1 Signaling.* Trends Cell Biol, 2016. **26**(6): p. 445-61.

287. Vasilikos, L., et al., *Regulating the balance between necroptosis, apoptosis and inflammation by inhibitors of apoptosis proteins.* Immunol Cell Biol, 2017. **95**(2): p. 160-165.

288. Rajalingam, K., et al., *IAP-IAP complexes required for apoptosis resistance of C. trachomatis-infected cells.* PLoS Pathog, 2006. **2**(10): p. e114.

289. Rodrigue-Gervais, I.G., et al., *Cellular inhibitor of apoptosis protein cIAP2 protects against pulmonary tissue necrosis during influenza virus infection to promote host survival.* Cell Host Microbe, 2014. **15**(1): p. 23-35.

290. Jung, A.L., et al., *Legionella pneumophila infection activates bystander cells differentially by bacterial and host cell vesicles.* Sci Rep, 2017. **7**(1): p. 6301.

291. Duesbery, N.S., et al., *Proteolytic inactivation of MAP-kinase-kinase by anthrax lethal factor.* Science, 1998. **280**(5364): p. 734-7.

292. Abrami, L., et al., *Membrane insertion of anthrax protective antigen and cytoplasmic delivery of lethal factor occur at different stages of the endocytic pathway.* J Cell Biol, 2004. **166**(5): p. 645-51.

293. Abrami, L., et al., *Hijacking multivesicular bodies enables long-term and exosome-mediated long-distance action of anthrax toxin.* Cell Rep, 2013. **5**(4): p. 986-96.

294. Shrestha, A., et al., *Bystander Host Cell Killing Effects of Clostridium perfringens Enterotoxin.* MBio, 2016. **7**(6).

295. Husmann, M., et al., *Elimination of a bacterial pore-forming toxin by sequential endocytosis and exocytosis.* FEBS Lett, 2009. **583**(2): p. 337-44.

296. Bomberger, J.M., et al., *Long-distance delivery of bacterial virulence factors by Pseudomonas aeruginosa outer membrane vesicles.* PLoS Pathog, 2009. **5**(4): p. e1000382.

297. Bomberger, J.M., et al., *A Pseudomonas aeruginosa toxin that hijacks the host ubiquitin proteolytic system.* PLoS Pathog, 2011. **7**(3): p. e1001325.

298. Prados-Rosales, R., et al., *Role for Mycobacterium tuberculosis membrane vesicles in iron acquisition.* J Bacteriol, 2014. **196**(6): p. 1250-6.

299. Lin, J., et al., *A Pseudomonas T6SS effector recruits PQS-containing outer membrane vesicles for iron acquisition.* Nat Commun, 2017. **8**: p. 14888.

300. Manning, A.J. and M.J. Kuehn, *Contribution of bacterial outer membrane vesicles to innate bacterial defense.* BMC Microbiol, 2011. **11**: p. 258.

301. Gitiban, N., et al., *Chinchilla and murine models of upper respiratory tract infections with respiratory syncytial virus.* J Virol, 2005. **79**(10): p. 6035-42.

302. Johnson, T.R., et al., *Role for innate IFNs in determining respiratory syncytial virus immunopathology.* J Immunol, 2005. **174**(11): p. 7234-41.

303. Williams, J.V., et al., *The cotton rat (Sigmodon hispidus) is a permissive small animal model of human metapneumovirus infection, pathogenesis, and protective immunity.* J Virol, 2005. **79**(17): p. 10944-51.

304. Moreau-Marquis, S., et al., *Co-culture models of Pseudomonas aeruginosa biofilms grown on live human airway cells.* J Vis Exp, 2010(44).

305. Zemke, A.C., et al., *Nitrite modulates bacterial antibiotic susceptibility and biofilm formation in association with airway epithelial cells.* Free Radic Biol Med, 2014. **77**: p. 307-16.

306. Jett, B.D., et al., *Simplified agar plate method for quantifying viable bacteria.* Biotechniques, 1997. **23**(4): p. 648-50.

307. Thomas, P., et al., *Optimization of single plate-serial dilution spotting (SP-SDS) with sample anchoring as an assured method for bacterial and yeast cfu enumeration and single colony isolation from diverse samples.* Biotechnol Rep (Amst), 2015. **8**: p. 45-55.

308. Thery, C., et al., *Isolation and characterization of exosomes from cell culture supernatants and biological fluids.* Curr Protoc Cell Biol, 2006. **Chapter 3**: p. Unit 3 22.

309. Bobrie, A., et al., *Diverse subpopulations of vesicles secreted by different intracellular mechanisms are present in exosome preparations obtained by differential ultracentrifugation.* J Extracell Vesicles, 2012. **1**.

310. Kowal, J., et al., *Proteomic comparison defines novel markers to characterize heterogeneous populations of extracellular vesicle subtypes.* Proc Natl Acad Sci U S A, 2016. **113**(8): p. E968-77.

311. Liu, S., et al., *Horizontal Transmission of Cytosolic Sup35 Prions by Extracellular Vesicles.* MBio, 2016. **7**(4).

312. O'Toole, G.A. and R. Kolter, *Initiation of biofilm formation in Pseudomonas fluorescens WCS365 proceeds via multiple, convergent signalling pathways: a genetic analysis.* Mol Microbiol, 1998. **28**(3): p. 449-61.

313. O'Toole, G.A., *Microtiter dish biofilm formation assay.* J Vis Exp, 2011(47).

314. Ducharme, N.A., et al., *Rab11-FIP2 regulates differentiable steps in transcytosis.* Am J Physiol Cell Physiol, 2007. **293**(3): p. C1059-72.

315. Empey, K.M., et al., *Stimulation of immature lung macrophages with intranasal interferon gamma in a novel neonatal mouse model of respiratory syncytial virus infection.* PLoS One, 2012. **7**(7): p. e40499.

316. Graham, B.S., et al., *Primary respiratory syncytial virus infection in mice.* J Med Virol, 1988. **26**(2): p. 153-62.

317. Moore, M.L., et al., *A chimeric A2 strain of respiratory syncytial virus (RSV) with the fusion protein of RSV strain line 19 exhibits enhanced viral load, mucus, and airway dysfunction.* J Virol, 2009. **83**(9): p. 4185-94.

318. Tang, A.C., et al., *Current concepts: host-pathogen interactions in cystic fibrosis airways disease.* Eur Respir Rev, 2014. **23**(133): p. 320-32.

319. Suarez-Arrabal, M.C., et al., *Nasopharyngeal bacterial burden and antibiotics: Influence on inflammatory markers and disease severity in infants with respiratory syncytial virus bronchiolitis.* J Infect, 2015.

320. Varkey, J.B. and B. Varkey, *Viral infections in patients with chronic obstructive pulmonary disease.* Curr Opin Pulm Med, 2008. **14**(2): p. 89-94.

321. Brownlee, J.W. and R.B. Turner, *New developments in the epidemiology and clinical spectrum of rhinovirus infections.* Curr Opin Pediatr, 2008. **20**(1): p. 67-71.

322. Costerton, J.W., *Cystic fibrosis pathogenesis and the role of biofilms in persistent infection.* Trends Microbiol, 2001. **9**(2): p. 50-2.

323. Gifford, A.H., et al., *Iron homeostasis during cystic fibrosis pulmonary exacerbation.* Clin Transl Sci, 2012. **5**(4): p. 368-73.

324. Murphy, T.F., *Pseudomonas aeruginosa in adults with chronic obstructive pulmonary disease.* Curr Opin Pulm Med, 2009. **15**(2): p. 138-42.

325. Cohen, T.S. and A. Prince, *Cystic fibrosis: a mucosal immunodeficiency syndrome.* Nat Med, 2012. **18**(4): p. 509-19.

326. Scagnolari, C., et al., *Gene expression of nucleic acid-sensing pattern recognition receptors in children hospitalized for respiratory syncytial virus-associated acute bronchiolitis.* Clin Vaccine Immunol, 2009. **16**(6): p. 816-23.

327. Hall, C.B., et al., *Interferon production in children with respiratory syncytial, influenza, and parainfluenza virus infections.* J Pediatr, 1978. **93**(1): p. 28-32.

328. Sheppard, P., et al., *IL-28, IL-29 and their class II cytokine receptor IL-28R.* Nat Immunol, 2003. **4**(1): p. 63-8.

329. Hamming, O.J., et al., *Interferon lambda 4 signals via the IFNlambda receptor to regulate antiviral activity against HCV and coronaviruses.* EMBO J, 2013. **32**(23): p. 3055-65.

330. Wark, P.A., et al., *Viral infections trigger exacerbations of cystic fibrosis in adults and children.* Eur Respir J, 2012. **40**(2): p. 510-2.

331. Hament, J.M., et al., *Enhanced adherence of Streptococcus pneumoniae to human epithelial cells infected with respiratory syncytial virus.* Pediatr Res, 2004. **55**(6): p. 972-8.

332. Durbin, R.K., S.V. Kotenko, and J.E. Durbin, *Interferon induction and function at the mucosal surface.* Immunol Rev, 2013. **255**(1): p. 25-39.

333. Chua, S.L., et al., *Dispersed cells represent a distinct stage in the transition from bacterial biofilm to planktonic lifestyles.* Nat Commun, 2014. **5**: p. 4462.

334. Kaneko, Y., et al., *The transition metal gallium disrupts Pseudomonas aeruginosa iron metabolism and has antimicrobial and antibiofilm activity.* J Clin Invest, 2007. **117**(4): p. 877-88.

335. Banin, E., et al., *The potential of desferrioxamine-gallium as an anti-Pseudomonas therapeutic agent.* Proc Natl Acad Sci U S A, 2008. **105**(43): p. 16761-6.

336. Martin, L.W., et al., *Pseudomonas siderophores in the sputum of patients with cystic fibrosis.* Biometals, 2011. **24**(6): p. 1059-67.

337. Lo Cicero, A., P.D. Stahl, and G. Raposo, *Extracellular vesicles shuffling intercellular messages: for good or for bad.* Curr Opin Cell Biol, 2015. **35**: p. 69-77.

338. Admyre, C., et al., *Exosomes with major histocompatibility complex class II and co-stimulatory molecules are present in human BAL fluid.* Eur Respir J, 2003. **22**(4): p. 578-83.

339. Kesimer, M., et al., *Characterization of exosome-like vesicles released from human tracheobronchial ciliated epithelium: a possible role in innate defense.* FASEB J, 2009. **23**(6): p. 1858-68.

340. Torregrosa Paredes, P., et al., *Bronchoalveolar lavage fluid exosomes contribute to cytokine and leukotriene production in allergic asthma.* Allergy, 2012. **67**(7): p. 911-9.

341. Moon, H.G., et al., *CCN1 secretion and cleavage regulate the lung epithelial cell functions after cigarette smoke.* Am J Physiol Lung Cell Mol Physiol, 2014. **307**(4): p. L326-37.

342. Szul, T., et al., *Toll-Like Receptor 4 Engagement Mediates Prolyl Endopeptidase Release from Airway Epithelia via Exosomes.* Am J Respir Cell Mol Biol, 2016. **54**(3): p. 359-69.

343. Fujita, Y., et al., *Extracellular vesicles in lung microenvironment and pathogenesis.* Trends Mol Med, 2015. **21**(9): p. 533-42.

344. Bhagirath, A.Y., et al., *Cystic fibrosis lung environment and Pseudomonas aeruginosa infection.* BMC Pulm Med, 2016. **16**(1): p. 174.

345. Bellingham, S.A., B. Guo, and A.F. Hill, *The secret life of extracellular vesicles in metal homeostasis and neurodegeneration.* Biol Cell, 2015. **107**(11): p. 389-418.

346. Hendricks, M.R., et al., *Respiratory syncytial virus infection enhances Pseudomonas aeruginosa biofilm growth through dysregulation of nutritional immunity.* Proc Natl Acad Sci U S A, 2016. **113**(6): p. 1642-7.

347. Marguerettaz, M., et al., *Sputum containing zinc enhances carbapenem resistance, biofilm formation and virulence of Pseudomonas aeruginosa.* Microb Pathog, 2014. **77**: p. 36-41.

348. Smith, D.J., et al., *Elevated metal concentrations in the CF airway correlate with cellular injury and disease severity.* J Cyst Fibros, 2014. **13**(3): p. 289-95.

349. Hurwitz, S.N., et al., *CD63 Regulates Epstein-Barr Virus LMP1 Exosomal Packaging, Enhancement of Vesicle Production, and Noncanonical NF-kappaB Signaling.* J Virol, 2017. **91**(5).

350. Ramachandra, L., et al., *Mycobacterium tuberculosis synergizes with ATP to induce release of microvesicles and exosomes containing major histocompatibility complex class II molecules capable of antigen presentation.* Infect Immun, 2010. **78**(12): p. 5116-25.

351. Hu, G., et al., *Release of luminal exosomes contributes to TLR4-mediated epithelial antimicrobial defense.* PLoS Pathog, 2013. **9**(4): p. e1003261.

352. Melvin, J.A. and J.M. Bomberger, *Compromised Defenses: Exploitation of Epithelial Responses During Viral-Bacterial Co-Infection of the Respiratory Tract.* PLoS Pathog, 2016. **12**(9): p. e1005797.

353. Siegel, S.J., A.M. Roche, and J.N. Weiser, *Influenza promotes pneumococcal growth during coinfection by providing host sialylated substrates as a nutrient source.* Cell Host Microbe, 2014. **16**(1): p. 55-67.

354. Moreau-Marquis, S., B. Coutermarsh, and B.A. Stanton, *Combination of hypothiocyanite and lactoferrin (ALX-109) enhances the ability of tobramycin and aztreonam to eliminate Pseudomonas aeruginosa biofilms growing on cystic fibrosis airway epithelial cells.* J Antimicrob Chemother, 2015. **70**(1): p. 160-6.

355. Cestari, I., et al., *Trypanosoma cruzi immune evasion mediated by host cell-derived microvesicles.* J Immunol, 2012. **188**(4): p. 1942-52.

356. Rogan, M.P., et al., *Loss of microbicidal activity and increased formation of biofilm due to decreased lactoferrin activity in patients with cystic fibrosis.* J Infect Dis, 2004. **190**(7): p. 1245-53.

357. Chitambar, C.R., *Gallium and its competing roles with iron in biological systems.* Biochim Biophys Acta, 2016. **1863**(8): p. 2044-53.

358. Groves, H.E., et al., *Efficacy and long-term outcomes of palivizumab prophylaxis to prevent respiratory syncytial virus infection in infants with cystic fibrosis in Northern Ireland.* Pediatr Pulmonol, 2016. **51**(4): p. 379-85.

359. Giebels, K., et al., *Prophylaxis against respiratory syncytial virus in young children with cystic fibrosis.* Pediatr Pulmonol, 2008. **43**(2): p. 169-74.

360. Buchs, C., et al., *Palivizumab prophylaxis in infants with cystic fibrosis does not delay first isolation of Pseudomonas aeruginosa or Staphylococcus aureus.* Eur J Pediatr, 2017. **176**(7): p. 891-897.

361. Melvin, J.A., et al., *Simultaneous Antibiofilm and Antiviral Activities of an Engineered Antimicrobial Peptide during Virus-Bacterium Coinfection.* mSphere, 2016. **1**(3).

362. Bakaletz, L.O., *Viral-bacterial co-infections in the respiratory tract.* Curr Opin Microbiol, 2017. **35**: p. 30-35.

363. Goetz, D.H., et al., *The neutrophil lipocalin NGAL is a bacteriostatic agent that interferes with siderophore-mediated iron acquisition.* Mol Cell, 2002. **10**(5): p. 1033-43.

364. Kuss, S.K., et al., *Intestinal microbiota promote enteric virus replication and systemic pathogenesis.* Science, 2011. **334**(6053): p. 249-52.

365. Perez Bay, A.E., et al., *The kinesin KIF16B mediates apical transcytosis of transferrin receptor in AP-1B-deficient epithelia.* EMBO J, 2013. **32**(15): p. 2125-39.

366. Perez Bay, A.E., et al., *Galectin-4-mediated transcytosis of transferrin receptor.* J Cell Sci, 2014. **127**(Pt 20): p. 4457-69.

367. Pfeiffer, J.K. and H.W. Virgin, *Viral immunity. Transkingdom control of viral infection and immunity in the mammalian intestine.* Science, 2016. **351**(6270).

368. Schoggins, J.W., et al., *A diverse range of gene products are effectors of the type I interferon antiviral response.* Nature, 2011. **472**(7344): p. 481-5.